DISSERTATION

GENE REGULATION BY LET-7 MICRORNAS DURING HUMAN AND SHEEP PLACENTAL DEVELOPMENT

Submitted by

Asghar Ali

Department of Biomedical Sciences

In partial fulfillment of the requirements

For the Degree of Doctor of Philosophy

Colorado State University

Fort Collins, Colorado

Spring 2020

Doctoral Committee:

Advisor: Quinton A Winger
Co-Advisor: Gerrit J Bouma

Adam Chicco
Deborah Garrity

ABSTRACT

GENE REGULATION BY LET-7 MICRORNAS DURING HUMAN AND SHEEP PLACENTAL DEVELOPMENT

Intrauterine growth restriction (IUGR) is a major cause of perinatal morbidity and mortality and affects more than 30 million infants every year across the world. Its occurrence is 5–15% of all pregnancies in the United States and 10-55% in developing countries. Most common etiology of IUGR is impaired placental development. Structural and functional abnormalities in placenta can also lead to preeclampsia (PE), still birth and spontaneous abortion. Conditions like IUGR and PE are usually not detected until later stages of gestation. Hence, there is a need to better understand the placental development and function to improve diagnosis and treatment of placenta-associated disorders. In this study, we investigated genetic pathways regulated by *let-7* miRNAs and their potential role in pathogenesis of malformed placenta. *Let-7* miRNAs are markers of cell differentiation and reduce the expression of several genes by translational repression. Biogenesis of *let-7* miRNAs is suppressed by LIN28 which is an RNA binding oncofetal protein with two paralogs, LIN28A and LIN28B. LIN28 is high and *let-7* miRNAs are low in proliferating stem cells whereas LIN28 is low and *let-7* miRNAs are high in differentiated cells. LIN28-*let-7* axis determines fate of cells by regulating the expression of genes associated with cell proliferation and differentiation. In human placenta, LIN28 is mainly found in trophoblast cells and the fetal portion of placenta comprises mainly of trophoblast cells. We found that in term human placentas from IUGR pregnancies, LIN28 is low and *let-7* miRNAs are high compared to placentas from control placentas. We further saw a reduction in the expression of AT-Rich

Interaction Domain 3A (ARID3A) and AT-Rich Interaction Domain 3B (ARID3B). ARID3A and ARID3B promote cell proliferation by transcriptional regulation of stemness genes. In immortalized first trimester human trophoblast (ACH-3P) cells, ARID3A and ARID3B complex with lysine demethylase 4C (KDM4C) to make the ARID3B-complex. This complex binds the promoter regions of proliferation-associated genes such as high mobility group AT-hook 1 (*HMGA1*), transcriptional regulator Myc-like (*c-MYC*), vascular endothelial growth factor A (*VEGF-A*) and Wnt family member 1 (*WNT1*). These genes are also targeted by *let-7* miRNAs. LIN28 knockout ACH-3P cells have significantly increased *let-7* miRNAs and significantly reduced HMGA1, c-MYC, VEGF-A and WNT1. We also saw significant reduction in ARID3A and ARID3B in LIN28 knockout ACH-3P cells. ACH-3P cells with ARID3B knockout also showed significant reduction in HMGA1, c-MYC, VEGF-A and WNT1. Both LIN28 knockout and ARID3B knockout in ACH-3P cells resulted in reduced cell proliferation compared to control. These results suggest that proliferation-associated genes in trophoblast cells are regulated through LIN28-*let-7*-ARID3B pathway. Trophectoderm (TE) specific knockdown of LIN28 in sheep led to reduced conceptus elongation at day 16 of gestation. Furthermore, LIN28 knockdown day 16 TE had significantly increased *let-7* miRNAs and significantly reduced expression of proliferation factors including insulin like growth factor 2 mRNA binding proteins (*IGF2BPs), HMGA1*, *ARID3B* and *c-MYC.* From these findings, we interpret that LIN28-*let-7*-ARID3B pathways regulates proliferation of trophoblast cells and is potentially associated with etiology of IUGR.

ACKNOWLEDGMENTS

Foremost, I would like to express my sincere gratitude to my advisor Dr. Quinton Winger. Dear Dr. Winger, I could have never completed this milestone without the unconditional and continuous support and guidance you have provided me over the last few years. You provided me the freedom to design my research projects without any objection. You have your own way of training your students which I found to be the best way. In our discussions about our research projects, you used to ask me questions which would lead me to the answer. It helped me to critically think about my research and become an independent researcher. Thank you so much for teaching me the embryo work. I also thank you for sponsoring me to attend research meetings which broadened my scientific concepts and understanding. Your support was not limited to lab work, but you also supported and guided me in all tough situations of my life. For that, I will forever be thankful and indebted to you. We had a great relationship and it has been a blessing to have you as my advisor.

I am also grateful to my co-advisor Dr. Gerrit Bouma, for guiding me in my research work. Dr. Bouma, you always found a way to appreciate and encourage me. I always felt motivated after talking to you about my research. Thank you for always being accessible and happy to help whenever needed. During my prelim exams and committee meetings I used to spend a lot of time studying to prepare for answering your questions. That helped me not only to improve my scientific knowledge, but also in designing my research projects.

My special thanks to Dr. Russell Anthony, for continuous and unconditional support during my PhD research. Dr. Anthony, I first saw you in 2014 in the surgery room at ARBL. At that time, I had no idea that one day I will be trained by you. I am grateful to you for teaching me the surgical

embryo transfer in sheep and being patient during my learning period. During all these years, I talked to you many times to seek guidance and share my research ideas. You always listened to my ideas and spent a lot of time showing me the previous data related to my research project. Your insightful input helped me a lot to design my research.

I would also express my gratitude to my committee members, Dr. Adam Chicco and Dr. Deborah Garrity, for their sincere and valuable guidance and encouragement extended to me.

I am thankful to Dr. Kimberly Jeckel for her help and training me when she was a lab scientist in Dr. Anthony's lab. Kimberly, you are a great person and a very valuable friend. You were like a family to me at ARBL and I will always be thankful for that.

I also want to express my sincere gratitude to Dr. Hans Mayan. He was a wonderful human being and a great friend to me. At many instances, I was able to do my work just because he was around to help me fix things. He was a special person and will always be missed.

I would like to thank all ARBL faculty, staff and students. My special thanks to Rick, Greg and Joel. Thank you for all the hard work you do to make our sheep projects successful.

I am very grateful to the United States Education Foundation in Pakistan (USEFP) and Institute of International Education (IIE) for sponsoring my studies through Foreign Fulbright Scholarship Program.

Last but not least, I am thankful to my family. Thank you for loving me so much. I am happy that technology (Skype and WhatsApp) made it possible for me to see you and talk to you almost every day. I love you all. My special thanks to my brother Akbar Ali. You are the nicest and most honest person I have ever seen in my life. Thank you for being a great friend.

DEDICATION

I dedicate this dissertation to my parents; Manzoor Hussain and Aziza Bano, and my brother Naseem Abbas. Dear mother and father, you have, and you will always be a role model for me. You taught me determination, truthfulness and honesty. You are not just important thing to me; you are everything to me. I am sad that I was away from you and was not able to spend time with you when you really needed. Thank you for loving me so much. You are the best parents in the world. Dear brother, you are the person behind my success. After I graduated as DVM, you didn't let me do any job but told me "get us a PhD, because you can do it". That was the turning point of my career. I will always be indebted to you for everything you did for me.

TABLE OF CONTENTS

LIST OF TABLES

LIST OF FIGURES

CHAPTER I: REVIEW OF LITERATURE[1]

Synopsis

The placental disorders are a major cause of pregnancy loss in humans, and 40-60% of embryos are lost between fertilization and birth. Successful embryo implantation and placental development requires rapid proliferation, invasion and migration of trophoblast cells. In recent years, microRNAs (miRNAs) have emerged as key regulators of molecular pathways involved in trophoblast function. A miRNA binds its target mRNA in 3′-untranslated region (3′-UTR), causing its degradation or translational repression. Lethal-7 (let-7) miRNAs induce cell differentiation and reduce cell proliferation by targeting proliferation-associated genes. Biogenesis of let-7 miRNAs is repressed by the oncoprotein LIN28 which has two paralogs; LIN28A and LIN28B. Proliferating cells have high LIN28 and low let-7 miRNAs, whereas differentiating cells have low LIN28 and high let-7 miRNAs. In placenta, low LIN28 and high let-7 miRNAs reduce the proliferation of trophoblast cells, resulting in abnormal placental development. In trophoblast cells, let-7s miRNAs reduce the expression of proliferation factors either directly by binding their mRNA in 3′-UTR or indirectly by targeting the AT-rich interaction domain (ARID)3B-complex, a transcription-activating complex comprised of ARID3A, ARID3B and histone demethylase 4C (KDM4C). In this review, we discuss regulation of trophoblast function by miRNAs, focusing on the role of LIN28-let-7-ARID3B pathway in placental development.

[1] This chapter has been written as a review paper which will be submitted in International Journal of Animal Sciences (IJMS).

1. Introduction

Every year, more than 15 million babies are born preterm in the world. A healthy placenta is required for successful establishment of pregnancy and optimal pregnancy outcome. The placenta plays a crucial role in exchange of nutrients and gases between mother and fetus, thermoregulation and waste elimination [1,2]. Human placental development starts with the attachment of hatched blastocyst to the uterine luminal epithelium, followed by invasion of the blastocyst in maternal decidua and remodeling of spiral arteries. Humans have hemochorial placenta in which placental villi are bathed in maternal blood are the functional unit of placenta [3]. Structural transformation and dynamic growth of placental villi is critical for proper functioning of placenta. Most structural and functional development of placenta occurs during the first trimester of pregnancy which requires rapid proliferation, invasion and migration of trophoblast cells [4]. Improper trophoblast proliferation, invasion or migration can result in placental dysfunction and severe pregnancy-related disorders including miscarriage, pre-term labor, stillbirth, pre-eclampsia (PE) and intrauterine growth restriction (IUGR) [5,6]. Other than perinatal complications, abnormal placental development can cause long-term postnatal complication in mother and fetus [7,8]. Placental abnormalities can also lead to impaired developmental programming of the fetus, predisposing the offspring to different adult diseases [9].

The process of rapid trophoblast proliferation and dynamic transformation in placental structure is poorly understood. Previous studies have shown the role of non-coding miRNAs in regulation of cell proliferation, invasion and migration. *Let-7* miRNAs are one of the most studied family of miRNAs and have a well-established role in cell proliferation, invasion, migration, differentiation and metabolism [10,11]. *Let-7* miRNAs reduce cell proliferation by downregulating the proliferation-associated genes. In highly proliferative cells, the RNA binding protein LIN28

represses the production of mature *let-7* miRNAs [12,13]. During early placental development, high *let-7* miRNAs can lead to reduced proliferation of trophoblast cells and contribute to etiology of placental abnormalities. This review focuses on the role of different miRNAs in trophoblast function, with *let-7* miRNAs being the center of discussion.

2. Early placental development and trophoblast cells

The human blastocyst is formed at day 4-5 after fertilization and contains an outer most layer of zona pellucida, a single layer of mononuclear trophectoderm or trophoblast (TE), a blastocoel cavity and an inner cell mass (ICM) or embryoblast. The blastocyst sheds the zona pellucida at day 7, exposing the TE [14]. Humans have interstitial implantation which starts at day 7 and comprises a set of events including orientation, apposition, attachment and adhesion of the blastocyst to the endometrium. The hatched blastocyst invades the decidualized uterine stroma and nidates into the uterine wall where it undergoes growth and development throughout the gestation [15,16]. Apposition refers to the first loose connection between the blastocyst and the uterine epithelium [17] which is mediated by cytokines and chemokines [18]. Compared to apposition, adhesion is a stronger attachment of the blastocyst to the endometrium. The trophoblast cells express αv and β3 integrins at the site of their contact with endometrium which play a major role in adhesion [19,20]. The trophectoderm that initially adheres to the endometrial epithelium (adjacent to ICM) is called polar trophectoderm. The remainder of the trophectoderm is called mural trophectoderm which is different from polar trophectoderm in a variety of ways including gene expression [21]. The process of adhesion activates the polar trophoblast cells, which start proliferating and give rise to different lineages of trophoblast cells (Figure 1). There are two prominent pathways for generation of trophoblast lineages; syncytial pathway and invasive pathway.

2.1.Syncytial pathway

At the site of attachment, the polar trophoblast cells transform into rapidly proliferating phenotype of trophoblast cells called cytotrophoblasts (CTBs). CTBs undergo rapid proliferation and make a second layer of CTBs overlying the polar trophectoderm. The newly formed CTBs fuse with each other to form multinucleated syncytiotrophoblast (STB), a process called syncytial fusion. The underlying CTBs keep proliferating, while some CTBs fuse with STB layer, a process called cyto-syncytial fusion. CTBs are the progenitor stem cells which proliferate to maintain their population and also differentiate into other lineages of trophoblast cells [22]. Within a few hours, STB expands and surrounds the whole blastocyst and mediates the invasion of blastocyst in the decidualized uterine stroma [23]. Build-up and turnover of STB is a two-phase process [24,25]. In the first phase, CTBs fuse with syncytium called pre-apoptotic phase [26]. The expansion of STB depends upon rapid proliferation and fusion of CTBs [27,28]. In the second phase, the extra mass of STB is removed by shedding the aging nuclei and organelles in maternal circulation in the form of membrane bound vesicles called syncytial knots [29,30]. The exact events that are involved in trophoblast turnover remain to be determined.

By day 8 post conception, fluid filled spaces called lacunae develop in the center of STB, separated by STB pillars called trabeculae [23]. By day 13 post conception, the CTBs invade the trabeculae, which results in growth and branching of trabeculae. The branches of trabeculae filled with CTBs are called primary villi. By day 14, mesenchymal cells start migrating and by day 15-20 they make a core in the primary villi, which are now called secondary villi [31]. Within a few hours after their first appearance in villi, some mesenchymal cells differentiate into hematopoietic and angiogenic precursor cells. These cells form blood capillaries in the secondary villi by day 21 resulting in the formation of tertiary villi which are the functional units of placenta [32,33]. Soon

after formation of tertiary villi, blood vessels originating from allantois also reach the villi. By week 5 after conception, the fetoplacental circulation is fully established.

2.2 Invasive pathway

Numerous daughter villi arise from tertiary villi, some of which remain free and project in the intervillous space hence called free or floating villi whereas some extend to the maternal tissue and serve to anchor the placenta to the uterine wall, called anchoring or stem villi [34–36]. The anchoring sites can be established as early as second week of gestation [34]. At proximal ends of anchoring villi, some highly proliferating CTBs break the overlying STB layer and invade into maternal endometrium and myometrium. This results in formation of the junctional zone which is a mixture of maternal and fetal tissues and ranges from implantation site to superficial third of myometrium [36]. As soon as the detached CTBs make a contact with decidual extracellular matrix, they differentiate into interstitial extravillous trophoblast cells (iEVTs) [37]. The iEVTs are either large polygonal shaped iEVTs or they can be small spindle shaped. The large iEVTs remain around the placental–decidua transition, while small iEVTs have upregulated collagen IV and integrin α1β1, helping them in deep invasion into the decidua [38,39].

One of the major functions of iEVTs is remodeling of maternal spiral arteries to ensure sufficient flow of blood to placenta and growing fetus. There are two routes through which iEVTs can reach and remodel the spiral arteries – intravasation and extravasation. During intravasation, the iEVTs in superficial decidua enter the vascular lumen [40]. During extravasation, enEVTs from an unknown source travel through the lumen of spiral arteries, make enEVTs plugs in the vascular lumen [41]. Once inside the lumen of spiral arteries, the iEVTs differentiate into endovascular trophoblast cells (enEVTs) which transform from an epithelial to an endothelial phenotype and replace the vascular endothelial cells [42,43].

The remodeling of spiral arteries includes loss of endothelial and smooth muscle cells from arterial walls and their replacement by invasive enEVTs, loss of elasticity, dilation of the arterial lumen and the loss of maternal vasomotor control on the remodeled blood vessels [27,41]. Spiral artery remodeling is crucial for normal placental development and enough supply of nutrients to the fetus (Figure 2). Inadequate remodeling of the spiral arteries is associated with conditions such as preeclampsia (PE), intrauterine growth restriction (IUGR)/fetal growth restriction (FGR), and recurrent miscarriage, that are harmful for both mother and the fetus. The proliferation and differentiation of trophoblast cells continues throughout gestation. However, unlike cancerous tissues, the proliferation of trophoblast cells is strictly regulated by complex molecular pathways [44,45]. In recent studies, microRNAs (miRNAs) have been shown to play vital role in trophoblast proliferation and early placental development.

3. Biogenesis of microRNAs

Although 80% of the human genome is transcribed in RNA, most of this RNA does not have the potential to be translated and is referred as "non-coding RNA" (ncRNA) [46]. The ncRNA greater than 200 nucleotide length are called "long non-coding RNAs" (lncRNAs) and the ones smaller than 200 nucleotides are referred as "short non-coding RNAs" (sncRNAs) [47,48]. The sncRNAs include transfer RNAs (t-RNAs), ribosomal RNAs (r-RNAs), P-element-induced wimpy testes (PIWI) interacting RNAs (piRNAs), small interfering RNAs (siRNAs) and microRNAs (miRNAs) [47–49]. MicroRNAs are 20-25 nucleotide long single stranded RNAs involved in post-transcriptional gene silencing through RNA interference [48] and were first identified in *C. elegans* in 1993 [50,51]. Until today, the miRNAs have been found in almost all eukaryotic species and in some viruses as well.

In cells, miRNAs are produced by miRNA coding genes which are transcribed by RNA polymerase II. MicroRNA genes are transcribed either as individual or as a cluster of few to hundreds of miRNAs which are later processed into individual miRNAs [52–54]. The first product of miRNA coding gene transcription is primary miRNA (pri-miRNA) with a 5′-cap and 3′-polyadenylated tail [52]. Pri-miRNAs are in the form of a sequence of hairpin stem-loops with about 33 bp long stems. The 20-25 nucleotide sequence of mature miRNA is a part of the stem [52]. The pri-miRNAs are processed into individual hairpins called precursor miRNAs (pre-miRNAs) by the microprocessor complex. The microprocessor complex is a nuclear protein complex comprised of double-stranded RNA (dsRNA)-binding protein (dsRBP) DiGeorge critical region 8 (DGCR8), RNase III enzyme Drosha, DEAD box RNA helicase p72 (DDX17) and DEAD box RNA helicase p68 (DDX5) [53–56]. The pre-miRNAs are exported to the cytoplasm by GTP-dependent membrane associated transporter exportin 5 (Exp5) [57–59]. In the cytoplasm, 20-25 nucleotide long double stranded RNA is generated from the stem of pre-miRNA by the action of RNase III enzyme Dicer and dsRBP trans-activation-responsive RNA-binding protein (TRBP) [60,61]. Finally, Argonaute (AGO) proteins (AGO1-4) receive the double stranded RNA and selects one strand as miRNA or guide strand while the other strand is discarded as passenger strand. AGO-miRNA duplex becomes a part of miRNA induced silencing complex (miRISC) [62].

The miRNA in the miRISC identifies the complementary nucleotide sequence in the target mRNAs, known as miRNA response elements (MREs) which is usually a part of 3′-untranslated region (3′-UTR) of the target mRNA. If the miRNA is a complete complement to the MRE, the AGO2 protein acts as an endonuclease and cleaves the target mRNA [63]. Most of MREs in animals have mismatches in the central region and the interaction between MREs and miRNAs occurs only at the nucleotide 2 to 8 at 5′ end of miRNA. This sequence of 7 nucleotides is referred

as seed sequence. The incomplete pairing of miRNA with MRE inhibits the endonuclease activity of AGO2 and degradation of target mRNA occurs through a different mechanism [64,65]. In such circumstances, the miRISC complexes with proteins such as poly(A)-deadenylases (PAN2-PAN3 and CCR4-NOT), decapping protein 2 (DCP2) and exoribonuclease 1 (XRN1). PAN2-PAN3 and CCR4-NOT cause poly(A)-deadenylation of the target mRNA, which is later decapped by DCP2 and degraded by XRN1 [66–68].

4. Functional analysis of microRNAs in trophoblast cells

MicroRNAs have been shown to play important role in deciding the fate of trophoblast cells [69]. Since their discovery, miRNAs have been the center of biomedical research due to their role in regulating genes involved in vital cellular processes. Until now, 1000 human genes have been identified which encode for miRNAs, more than 50% of which are associated with important biological processes including development, growth and metabolism [70,71]. Proliferation, invasion and migration of trophoblast cells is a critical step during early human placental development. With increasing evidence for role of miRNAs in regulation of genes associated with cell proliferation, invasion and migration, several studies have been conducted to investigate the role of miRNAs in placental development and pathogenesis of placenta-associated disorders.

miRNAs impose their effect by regulating the expression of different genes and the effect of a specific miRNA on the phenotype of a cell or tissue depends upon the role of genes targeted by that miRNA. Hence, depending upon the function of their target genes in trophoblast cells, some miRNAs support successful placental development by promoting trophoblast cell proliferation, invasion and migration, and inhibiting the apoptosis of trophoblast cells, whereas some miRNAs can lead to abnormal placental development by reducing cell proliferation, invasion and migration, and increasing apoptosis of trophoblast cells. Table 1 describes the genes regulated

by miRNAs and their effect on functionality of trophoblast cells as described in some recent studies. All gene symbols used in table 1 are according to HUGO Gene Nomenclature.

5. *Let-7* miRNAs

The lethal-7 (*let-7)* family of miRNAs was first discovered in 2002 as development regulator in *C. elegans* [126]. The expression of *let-7* miRNAs is low in undifferentiated cells and increases gradually as the cells differentiate during development [127], therefore *let-7* miRNAs are also referred to as differentiation-inducing miRNAs. The *let-7* mutated *C. elegans* larvae do not mature to adult stage but keep proliferating and eventually die, earning the name "*lethal-7* (*let-7*)" to this family of miRNAs [126]. *Let-7* miRNAs are highly conserved in various animal species [128], suggesting that *let-7* miRNAs regulate same molecular pathways and biological process in different organisms. In humans, *let-7* miRNAs family comprises of 12 members including *let-7a, let-7b, let-7c, let-7d, let-7e, let-7f, let-7g, let-7i* and *miR-98* [129], which are originated from 8 different genomic loci [130]. Some *let-7* miRNAs produced from different genomic loci at different chromosomes have same sequence. For examples, in humans, *let-7a-1, let-7a-2* and *let-7a-3* have same sequence but encoded by loci on chromosomes 9, 11 and 12 respectively. Similarly, *let-7f-1* and *let-7f-2* are encoded by different genomic loci but have same sequence [131]. *Let-7* miRNAs have a common seed sequence of 7 nucleotides "GAGGUAG" from nucleotide 2 to 8 in all species, which plays an important role in recognizing MRE in 3′-UTR of their target mRNA [131]. However, difference in non-seed flanking sequence of *let-7* miRNAs affects the target specificity [132,133]. Presence of similar seed sequence in all *let-7* miRNAs across different species suggests that *let-7* miRNAs have same mechanism for target recognition and might have overlapping targets.

Let-7 miRNAs play profound role in several biological processes including embryo development, glucose metabolism, cell pluripotency and differentiation, tumorigenesis, tissue regeneration, age of onset of puberty and menopause in humans, and organ growth [134,135]. Various studies have shown that *let-7* miRNAs induce cell differentiation and act as fundamental tumor suppressors by downregulating oncogenes [136–139]. At early stages of cancer development, *let-7* miRNAs are downregulated and *let-7* targeted oncofetal genes (LOG) are re-expressed [140]. Comparative bioinformatics analysis shows that *let-7* miRNAs targets several oncofetal genes including HMGA2, insulin like growth factor 2 mRNA binding protein 1 (IMP1), IMP2, IMP3 and malignancy marker nucleosome assembly protein 1 like 1 (NAP1L1) [140]. In hematopoietic stem cell, *let-7* miRNAs inhibit transforming growth factor β (TGFβ) pathway and high mobility group AT-hook 2 (HMGA2) and decide the fate of these cells, regulate cell proliferation, self-renewal and differentiation [141,142].

Let-7 miRNAs are synthesized following the same general mechanism for miRNAs synthesis. The *let-7* loci are transcribed as pri-*let-7* miRNA, then processed into 67-80 nucleotide long pre-*let-7* miRNA by microprocessor complex [130]. Based on the mechanism of further processing, pre-*let-7* miRNAs are divided in two groups. Group I pre-*let-7* miRNAs (pre-*let-7a-2, 7c* and *7e*) are processed in cytoplasm *by* direct action of Dicer, whereas group II pre-*let-7* miRNAs (all remaining *let-7s*) are mono-uridylated prior to processing by Dicer [143]. Action of Dicer produces 22 nucleotide long mature *let-7* miRNAs, called *let-7-5p*. As a part of miRISC, *let-7* miRNAs suppress a wide range of genes involved in development, cell proliferation, metabolism and other important physiological processes [144]. There is no significant difference in expression of pri-*let-7* and pre-*let-7* miRNAs between undifferentiated and differentiated cells, however mature *let-7* miRNAs are high in differentiated cells compared to undifferentiated cells [145].

Mature *let-7* miRNA is a part of hairpin structure in pri- and pre-*let-7* miRNA. This hairpin structure contains mature *let-7* miRNA (*let-7-5p)* in the stem and a partially complimentary strand of nucleotides called *let-7-3p* miRNA, connected by terminal loop region of different lengths called pre-element (preE) [146]. The process of generation of mature *let-7* miRNAs is more precisely regulated compared to the synthesis of other miRNAs. Different proteins regulate posttranscriptional biogenesis of mature *let-7* miRNA by binding the preE region of pri- and pre-*let-7* miRNAs [147]. One of the most prominent mechanism for regulation of *let-7* miRNAs biogenesis is through LIN28 [148].

6. Suppression of *let-7* miRNAs by LIN28

LIN28 is a highly conserved RNA binding protein with two paralogues, 209 amino acids LIN28A and 250 amino acids LIN28B. Both LIN28A and LIN28B have a cold-shock domain (CSD) at N-terminal and two zinc knuckle domains (ZKD) at C-terminal [149]. LIN28 promotes cell proliferation and inhibits cell differentiation [150]. LIN28 is also involved in reprogramming of differentiated somatic cells into tumor or stem cells, hence known as oncoprotein [151,152]. Reduced expression of LIN28 in embryos results in reduced prenatal growth and development and long-term metabolic abnormalities [153]. Knockout of LIN28A in mice leads to perinatal lethality while LIN28B knockout results in postnatal growth abnormalities in males. Knockout of both LIN28A and LIN28B in mice is embryonic lethal at around E13. Conditional knockout of LIN28A and LIN28B in mice at 6 weeks of age does not produce any evident phenotype [154]. Collectively, these findings show that LIN28 has more profound role during prenatal development and organogenesis.

LIN28 regulates expression of several genes either directly binding to the mRNA of target genes or by repressing the production of mature *let-7* miRNAs, later being more prevalent

mechanism [154,155]. There are conflicting theories about their localization of LIN28A and LIN28B in the cells. LIN28A is predominantly localized in the cytoplasm but can be found in nucleus as well [156,157], however according to another study LIN28A is exclusively localized in the cytoplasm [158]. LIN28B has nucleolar and nuclear localization signal, while some others found it predominantly in cytoplasm with a possibility to shuttle to the nucleus [149,155,159]. LIN28A and LIN28B selectively repress the expression and maturation of *let-7* miRNAs by distinct mechanisms, without directly affecting the expression of other miRNAs [160]. LIN28A CSD binds GNGAY motif while ZKDs bind GGAG motif in the stem loop pre-*let-7* miRNA in the cytoplasm. After binding to pre-*let-7* miRNA, LIN28A recruits TUTase Zcchc11 (also referred as TUT4). TUT4 causes polyuridylation of pre-*let-7* miRNA which blocks the cleavage of pre-*let-7* miRNA by Dicer and hence inhibits the production of mature *let-7* miRNAs [160–162]. Polyuridylated pre-*let-7* miRNA is recognized and degraded by exonuclease Dis3L2 [163]. The mechanism of *let-7* miRNA suppression by LIN28B remains controversial and there are four different theories about it. First, LIN28B inhibits maturation of *let-7* miRNAs by TUT4 independent mechanism. In the nucleus, LIN28B binds the pri-*let-7* miRNA by its CSD and ZKDs and inhibits its processing by microprocessor [164]. Second, in the cytoplasm, LIN28B binds to pre-*let-7* miRNA and inhibits its processing by Dicer [165]. Third, in the cytoplasm, LIN28B binds to pre-*let-7* miRNA and leads to it polyuridylation by recruiting an unknown TUTase, leading to its degradation [166]. Fourth, in the nucleolus, LIN28B has the ability to sequester pri-*let-7* miRNAs and hence inhibits further processing to mature pre-*let-7* miRNAs [167].

In 2018, Ustianenko et al. demonstrated that LIN28 selectively regulates a subclass of *let-7* miRNAs [168]. Using single nucleotide resolution, they identified –(U)GAU- as the new binding motif of CSD. Some pre-*let-7* miRNAs with both (U)GAU and GGAG motifs in the stem loop

make a stronger and stable interaction with LIN28 and are referred to as CSD^+, while the others which do not contain (U)GAU motif are called CSD^-. The CSD^+ subclass includes pre-*let-7b,* pre-*let-7d,* pre-*let-7f-1,* pre-*let-7g,* pre-*let-7i* and *miR-98.* The CSD^- subclass includes pre-*let-7a-1,* pre-*let-7a-2,* pre-*let-7-3,* pre-*let-7c,* pre-*let-7e* and pre-*let-7f-2* [168,169]. Although all *let-7* miRNAs express ZKD binding GGAG motif, both LIN28A and LIN28B have shown greater binding affinity for CSD^+ pre-*let-7* miRNAs and hence leading to their polyuridylation and repression [168].

7. Gene regulation by LIN28-*let-7* miRNA axis in trophoblast cells

Due to profound role of *let-7* miRNAs as differentiation-inducing miRNAs, the focus of our lab has been to investigate the role of LIN28-*let-7* miRNA axis in trophoblast cells. Both LIN28A and LIN28B have high expression in human placenta and are localized in trophoblast cells [72,170,171]. High throughput genotyping array reveals that LIN28B is paternally imprinted in human placenta [172,173]. Using single cell transcriptome profiling, Liu et al. identified 14 different cell types in human placenta and showed that paternally imprinted LIN28B has high expression in CTBs, EVTs and STB, whereas it has no to low expression in mesenchymal cells, macrophages and blood cells in placenta [174]. They further showed that LIN28B expression in week 24 EVTs was lower compared to week 8 EVTs [174], suggesting that expression of LIN28B in trophoblast cells reduces as the pregnancy progresses. LIN28B is the main paralogue of LIN28 in human placenta and *LIN28B* mRNA is 1300-fold higher compared to *LIN28A* mRNA in term human placental tissue [175]. Immunohistochemical analysis of term human placenta shows that LIN28B expression in CTBs and STB is higher compared to placental decidual cells [175]. In 2013, Gu el al., compared the expression of miRNAs between first and third trimester human placentas [176]. They reported that along with many other miRNAs, *let-7a, let-7c, let-7d, let-7f,*

let-7g and *let-7i* are upregulated in third trimester compared to first trimester human placenta [176]. We measured *LIN28A* and *LIN28B* mRNA in first trimester (11 week) *vs* term human placentas and found that *LIN28A* mRNA is nearly 700-fold higher and *LIN28B* mRNA is nearly 300-fold higher in first trimester compared to term human placenta (Figure 3). Based on these results, we suggest that increased expression of *let-7* miRNAs in term human placentas, reported in Gu et al. study, are due to reduced expression of *LIN28A* and *LIN28B*. Low LIN28 and higher level of *let-7* miRNAs in term placenta compared to first trimester placenta suggests that proliferation rate of trophoblast cells is higher during first trimester and decreases with the advancement in gestational age. As LIN28-*let-7* miRNA axis regulates expression of several genes, it would not surprising to see a difference in gene expression in first trimester *vs* third trimester human placenta.

In IUGR pregnancies, the size of placenta is significantly smaller compared to normal pregnancies [177], which suggests the role of reduced trophoblast proliferation in etiology of IUGR. In a recently published study, we showed that term human placentas from IUGR pregnancies have low LIN28A and LIN28B, and high *let-7* miRNAs compared to term human placentas from normal pregnancies [72]. Canfield et al, reported that term human placentas from preeclamptic pregnancies have reduced LIN28B but no change in LIN28A compared to normal term placentas [175]. They further demonstrated that in first trimester human placenta, LIN28B is higher in extravillous cytotrophoblasts compared to villous trophoblast cells, indicating their role in trophoblast cell invasion [175]. Low LIN28 and high *let-7* miRNAs during first trimester of pregnancy can lead to reduced trophoblast proliferation and invasion leading to pregnancy related disorders.

Due to limitation that humans cannot be used as experimental models, most studies investigating molecular mechanisms involved in human placental development are conducted using placental cell lines. Commonly used human trophoblast-derived cell lines include BeWo, ACH-3P, Jeg-3, JAR, Sw.71 and HTR-8/SVneo. LIN28A knockdown in immortalized first trimester human trophoblast (ACH-3P) cells drives these cells towards syncytial differentiation and increases the expression of syncytiotrophoblast markers including *hCG, LGALS13* and *ERVW-1* [178]. Moreover, knockdown of LIN28A increases the expression of *let-7* miRNAs including *let-7a, let-7c, let-7d, let-7e, let-7g* and *let-7i* [178], suggesting that differentiation of cells might be due to increased levels of *let-7* miRNAs. Overexpression of LIN28B in HTR8 cells increases cell proliferation, invasion and migration, whereas knockdown of LIN28B in JEG3 cells reduces cell proliferation [175]. In a recently published study, we further investigated the correlation between LIN28 and *let-7* miRNAs in trophoblast cells using first trimester human trophoblast-derived ACH-3P and Sw.71 cells. ACH-3P cells were generated by fusing first trimester human trophoblast cells with human choriocarcinoma cells, whereas Sw.71 cells were generated by overexpressing h-TERT in first trimester human trophoblast cells [179,180]. These cell lines have contrasting levels of LIN28 and *let-7* miRNAs [72]. ACH-3P cells have high expression of LIN28A and LIN28B whereas these proteins are not detectable in Sw.71 cells [72]. The expression of all *let-7* miRNAs is 50-500-fold higher in Sw.71 cells compared to ACH-3P cells, potentially due to depleted LIN28A and LIN28B in Sw.71 cells which are major suppressors of *let-7* miRNAs [72]. The contrasting levels of LIN28 and *let-7* miRNAs between ACH-3P and Sw.71 cells are potentially due to difference of methodology used to generate these cell lines. LIN28A knockout in ACH-3P cells increases *let-7a, let-7b, let-7c, let-7d* and *let-7e*, whereas LIN28B knockout in ACH-3P cells increases *let-7a, let-7b, let-7c, let-7d, let-7e* and *let-7i.* Double knockout of LIN28A

and LIN28B in ACH-3P cells results in increased expression of all *let-7* miRNAs compared to knockout of either LIN28A or LIN28B. Similarly, LIN28A overexpression Sw.71cells decreases *let-7d* and *let-7i*, whereas LIN28B overexpression causes reduction in all *let-7* miRNAs. However, overexpression of both LIN28A and LIN28B in Sw.71 cells results in decreased expression of all *let-7* miRNAs compared to overexpression of either LIN28A or LIN28B [72]. These results suggest that, LIN28A and LIN28B work in coordination to suppress *let-7* miRNAs and manipulating one paralogue of LIN28 in human trophoblast cells might not induce a similar phenotype compared to if both paralogues are changed.

Majority of *let-7*-regulated genes are associated with cell proliferation, migration and invasion - the processes which are crucial during early human placental development. We recently demonstrated that double knockout of LIN28A and LIN28B in ACH-3P cells increases in *let-7* miRNAs and leads to reduction in expression of proliferation-associated genes including high-mobility group AT-hook 1 (*HMGA1*), MYC protooncogene (*c-MYC*), vascular endothelial growth factor A (*VEGF-A*), and Wnt family member 1 (*WNT1*). LIN28A/B knockout reduces trophoblast cell proliferation and drives them towards differentiating to syncytiotrophoblast [72,170]. Similarly, double knockin of LIN28A/B in Sw.71 cells leads to reduction in *let-7* miRNAs and increases the expression of *HMGA1*, *c-MYC*, *VEGF-A*, and *WNT1* [72]. Other than its role in cell proliferation, VEGF-A is required at all steps of angiogenesis during placental development [181]. Reduced expression of VEGF-A due high *let-7* miRNAs can lead to serious pregnancy complications due to impaired angiogenesis in placenta.

Androgen receptor (AR) is also a *let-7* target gene and promotes cancer cell proliferation [182–186]. AR plays a role in placental angiogenesis by regulating VEGF-A expression [187]. In term human placenta, AR is localized in cytotrophoblasts, syncytiotrophoblast and villous stromal

cells [188,189], suggesting its role in regulating trophoblast function. Another study showed that, in first trimester human placenta, AR is localized in cytotrophoblasts and stromal cells but not in syncytiotrophoblast [182]. Knockdown of LIN28B in ACH-3P cells increases *let-7c* miRNA and reduces AR expression [182]. ACH-3P cells treated with *let-7c* mimic have reduced AR whereas *let-7e* and *let-7f* mimics do not affect AR expression, suggesting that AR is targeted specifically by *let-7c* in human trophoblast cells. Moreover, reduced AR expression in response to *let-7c* mimic drives cells towards syncytialization [182].

Several studies have demonstrated that *let-7* miRNAs bind the 3′-UTR of HMGA2 and reduces its expression in cancer cells [190–192]. However, in a recent study, we found a different mechanism of HMGA2 regulation in human trophoblast cells. Double knockout of LIN28A/B in ACH-3P cells increases *let-7* miRNAs but does not change HMGA2 expression [170]. Along with increased *let-7* miRNAs, LIN28A/B double knockout also increases miR-182. The exact mechanism behind increase in miR-182 in LIN28A/B double knockout ACH-3P cells is not clear. We further showed that HMGA2 expression in trophoblast cells is regulated by a transcription-repressing complex comprised of breast cancer susceptibility gene 1 (BRCA1), CtBP-interacting protein (CtIP) and zinc finger protein 350 (ZNF350). This complex, also called BRCA1 repressor complex, binds the promoter region of HMGA2 and inhibits its transcription [170]. In LIN28A/B double knockout ACH-3P cells, high miR-182 targets BRCA1 leading to inhibition of BRCA1 repressor complex and hence increases HMGA2 expression [170]. Therefore, the expected decrease in HMGA2 due to high *let-7* miRNAs is rescued by inhibition of BRCA1 repressor complex. These findings indicate that all genetic pathways demonstrated in the cancer cells might not be applicable in trophoblast cells. It further suggests that rapid proliferation of trophoblast cells during early placental development is more precisely regulated compared to cancer cells.

Although *in vitro* studies demonstrate the vital role of LIN28-*let-7* miRNA axis in trophoblast function, its role in placental development *in vivo* is not well understood. Using sheep as experimental model, we investigated the role of LIN28-*let-7* miRNA axis in trophoblast proliferation *in vivo*. In sheep, the hatched blastocyst undergoes a phase of trophectoderm elongation before attachment to the uterine epithelium. The conceptus elongation is accomplished by rapid proliferation of trophoblast cells. Trophoblast proliferation is a critical process in early placental development both in humans and sheep. Trophoblast specific knockdown of LIN28A or LIN28B in sheep leads to reduced conceptus elongation due to reduced proliferation of trophoblast cells [193] suggesting that both LIN28A and LIN28B are equally important for in early placental development. Knockdown of LIN28A and LIN28B leads to increase in *let-7* miRNAs and decrease in expression of proliferation-associated genes including insulin like growth factor 2 mRNA binding proteins (IGF2BP1-3), high mobility group AT-hook 1 (*HMGA1*), AT-rich interaction domain 3B (ARID3B) and MYC protooncogene (*c-MYC*) [193]. Additionally, overexpression of LIN28A or LIN28B in immortalized ovine trophoblast cells (iOTR) reduces *let-7* miRNAs, increases the expression of proliferation associated genes and increases cell proliferation [193]. These findings further strengthen the data from *in vitro* studies about the role of LIN28-*let-7* miRNA axis in proliferation of human trophoblast cells.

8. LIN28-*let-7*-ARID3B pathway in trophoblast cells

AT-rich interactive domain (ARID) proteins, first recognized in 1997, are a family of 15 proteins which bind to AT-rich regions of DNA [194,195]. ARID proteins play an important role in cell proliferation, differentiation and development, and are upregulated in tumorous tissues [196]. The subfamilies of ARID proteins include ARID1, ARID2, ARID3, ARID4, ARID5, JARID1and JARID2. The ARID3 subfamily has 3 members including ARID3A, ARID3B and

ARID3C. Although most of the ARID proteins act as tumor suppressors, ARID3A and ARID3B promote tumorigenesis [195]. ARID3A inhibits cell differentiation, promotes cell proliferation and increases survival potential of cells [196,197], whereas ARID3B promotes proliferation, invasion and migration of cancer cells [198–200]. However, Moreover, ARID3B is more widely expressed in different tissues compared to ARID3A, suggesting more involvement of ARID3B in biological functions [201]. ARID3A and ARID3B are structurally similar and bind the similar region of DNA. Both ARID3A and ARID3B have extended central ARID domain and two conserved amino acid domains at the C-terminal, termed REKLES α and REKLES β. Only members of ARID3 subfamily have REKLES domains [202].

In contrast to ARID3B which is exclusively localized in the nucleus, ARID3A shuttle between nucleus and cytoplasm. Once in the nucleus, ARID3A interacts with ARID3B through REKLES β domain. Therefore, localization of ARID3A in the nucleus is dependent on its interaction with ARID3B in the nucleus, suggesting the dominant role ARID3B [202,203]. In cancer cells, ARID3A and ARID3B recruit histone demethylase 4C (KDM4C) to make a tri-protein complex, called the ARID3B-complex [204]. The ARID3B-complex binds in the promoter areas of stemness genes and *let-7* target genes, leading to histone demethylation by KDM4C and increased gene expression by initiation of transcription [204]. Therefore, genes regulated by the ARID3B-complex also include *let-7* miRNA target genes. Liao et al., further demonstrated that both ARID3A and ARID3B are targeted by *let-7* miRNAs. Hence, other than directly targeting the mRNAs of target genes, *let-7* miRNA can indirectly regulate their target genes by targeting and reducing the expression of *ARID3A* and *ARID3B* (Figure 4) [72,204].

Both ARID3A and ARID3B have high expression in human trophoblast cells [205,206]. ARID3A knockout mice have severe structural defects in placenta [207]. In ACH-3P cells

ARID3A, ARID3B and KDM4C make the tri-protein ARID3B complex [72]. In term human placentas from IUGR pregnancies, LIN28A and LIN28B are low, *let-7* miRNAs are high, and ARID3A and ARID3B are low which suggests a correlation between LIN28-*let-7* miRNA axis and the ARID3B complex [72]. Due to the well-established pathway of regulation of *let-7* target genes through ARID3B complex and their role in cell proliferation, it is important to understand this phenomenon in early placental development. We have recently shown the correlation between LIN28-*let-7* miRNA axis and the ARID3B complex using ACH-3P and Sw.71 cell. Double knockout of LIN28A and LIN28B in ACH-3P cells increases *let-7* miRNAs and decreases the expression ARID3A, ARID3B and KDM4C. Similarly, double knockin of LIN28A and LIN28B in Sw.71 cells decreases *let-7* miRNAs and increases expression of ARID3A, ARID3B and KDM4C [72]. In trophoblast cells, the ARID3B-complex binds to the promoter areas of proliferation-associated *let-7* target genes including *HMGA1, c-MYC, VEGF-A* and *WNT1,* facilitating their transcription via KDM4C mediated histone demethylation. ARID3B knockout ACH-3P cells, KDM4C cannot be recruited in the promoter regions of *HMGA1, c-MYC, VEGF-A* and *WNT1* and expression of these genes is also significantly reduced [73]. Moreover, ARID3B knockout ACH-3P cells have reduced proliferation rate compared to control cells [72]. Knockdown of LIN28A or LIN28B in sheep trophectoderm increases *let-7* miRNAs and reduces the expression of ARID3A and ARID3B [193], showing the regulation of the ARID3B-complex by LIN28-*let-7* miRNA axis *in vivo.* Collectively these findings show that *let-7* miRNAs target the ARID3B-complex in trophoblast cells, and the ARID3B-complex regulates genes with known importance in placental development.

9. Conclusion

For a long time, transcription activating proteins were thought to be the main regulators of gene expression in cells. However, in recent years microRNAs have emerged as "regulators of the regulators". miRNAs regulate important processes in trophoblast cells including cell proliferation, differentiation, invasion and migration. LIN28-*let-7*-ARID3B pathway regulates trophoblast cell proliferation by modulating the expression of proliferation associated genes *in vitro* and *in vivo.* The trophoblast cells with low LIN28 will have high *let-7* miRNAs and low ARID3B. There are two possible pathways of regulation of proliferation-associated genes by *let-7* miRNAs in trophoblast cells (Figure 5). On pathway involves binding of *let-7* miRNAs in 3′-UTR of their target mRNA leading to mRNA degradation or translational repression. Secondly, *let-7* miRNAs target ARID3A, ARID3B and KDM4C to inhibit or reduce transcriptional activation of proliferation-associated genes by the ARID3B-complex. Therefore, trophoblast cells with high *let-7* miRNAs will have reduced expression of proliferation factors and more tendency to differentiate. High *let-7* miRNAs during early placental development reduce cell proliferation, invasion and migration of trophoblast cells, leading to placental abnormalities. *Let-7* miRNAs might be the major players in pathogenesis of placenta-associated disorders. miRNAs can be readily measured in peripheral blood, tissue biopsies, saliva, cerebrospinal fluid, urine and other biological samples. High *let-7* miRNAs are upregulated in IUGR and preeclamptic placentas, suggesting that *let-7* miRNAs can be potential biomarkers for early diagnosis of PE and IUGR. It remains to be explored if early stage placentas from compromised pregnancies will have high *let-7* miRNAs and will the increase in *let-7* miRNAs in placenta be reflected in maternal blood. Animal models of IUGR can be used to answer these questions.

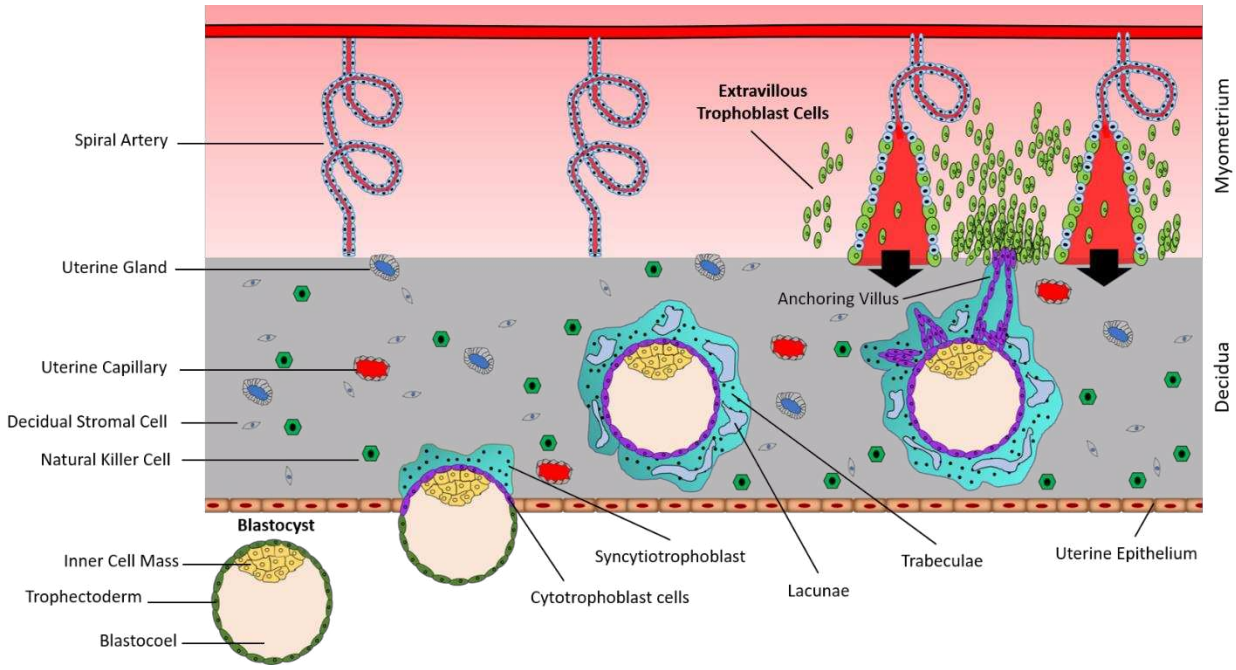

Figure 1. Early placental development and spiral artery remodeling. Human placental development starts with interaction between hatched blastocyst and uterine epithelium. The trophoblast cells that contact with the uterine epithelium transform into highly proliferative cytotrophoblasts (CTBs). Cytotrophoblasts undergo rapid proliferation and some of them fuse to form multinucleated syncytiotrophoblast (STB). Within few hours, STB expands and covers whole blastocyst and helps in blastocyst invasion into the uterine decidua. Continuous proliferation of CTBs results in formation of villi. Some CTBs from the tip of anchoring villi break the STB cover, invade in the uterine stroma and myometrium and transform into EVTs. EVTs remodel the spiral arteries to ensure sufficient flow of blood to the placenta.

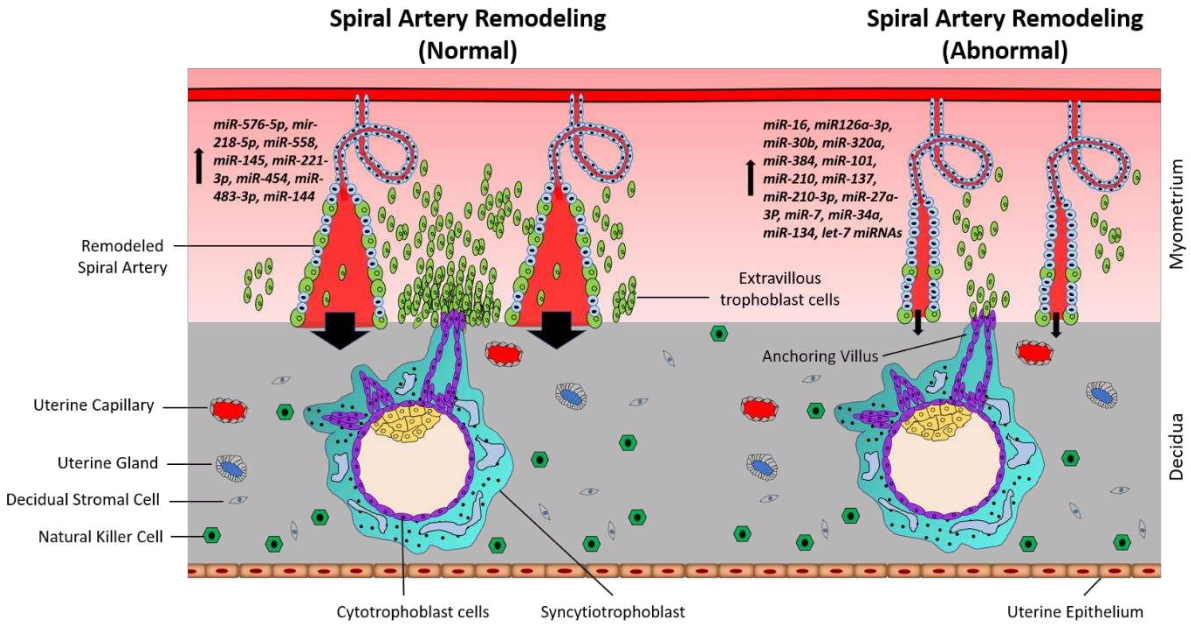

Figure 2. Normal *vs* abnormal spiral artery remodeling. CTBs from anchoring villi break out of SCT layer and enter uterine stroma where they differentiate into extravillous trophoblasts (EVTs). Spiral artery remodeling is accomplished by invasion and migration of EVTs. EVTs replace the vascular endothelial cells, remodel the spiral arteries and ensures sufficient flow of blood to placenta. In placenta-associated disorders like preeclampsia, reduced proliferation of CTBs results in less availability of EVTs. This leads to insufficient remodeling of spiral arteries and reduced blood flow to the placenta. Based on different studies listed in table 1, a different set of miRNAs is upregulated in trophoblast cells during normal *vs* preeclamptic pregnancies.

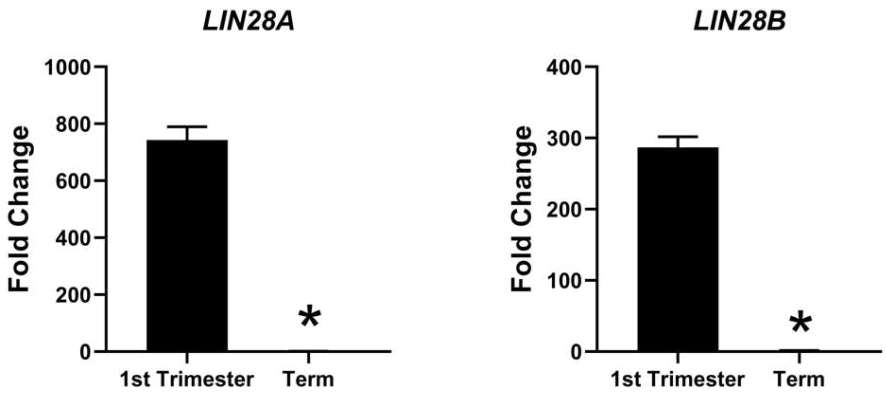

Figure 3. LIN28 mRNA in human placenta. mRNA was extracted from first trimester (week 11) and term human placentas and *LIN28A* and *LIN28B* mRNA levels were measured using real-time RT-PCR, where *$p<0.05$.

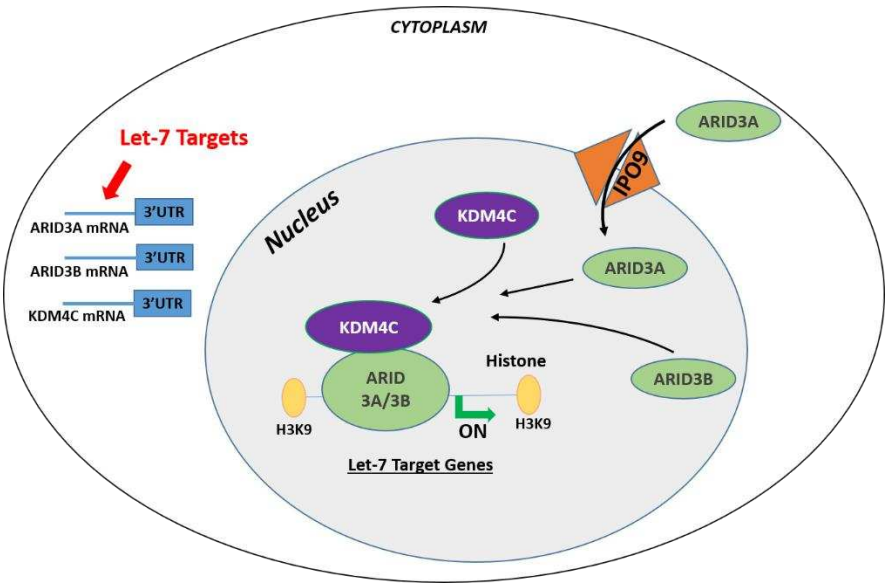

Figure 4. Gene regulation by the ARID3B-complex. ARID3A is imported in nucleus by IPO9, where it binds ARID3B and KDM4C to form the ARID3B-complex. The ARID3B-complex binds in the promoter regions and activates transcription of *let-7* target genes. Other than directly binding the mRNA of their target genes, *let-7* miRNAs also target the ARID3B-complex and reduce its expression, ultimately leading to reduced expression of *let-7* target genes.

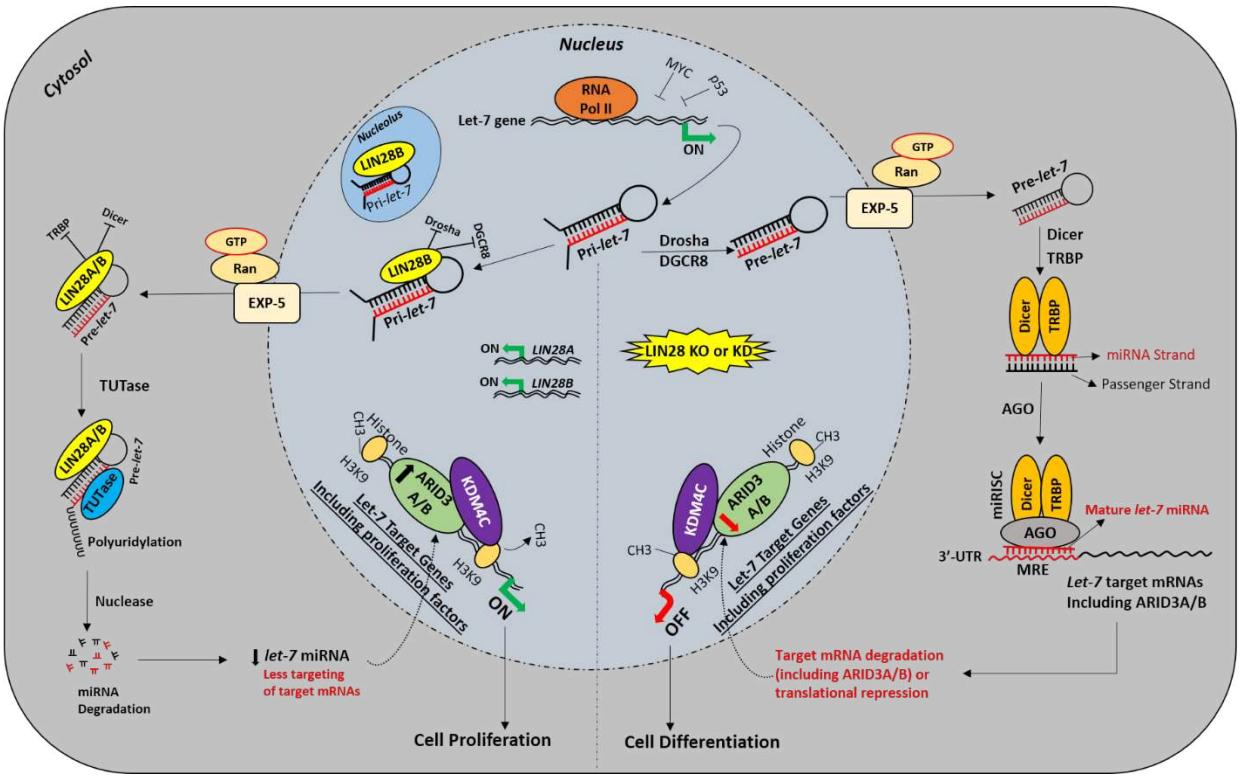

Figure 5. Proposed mechanism for gene regulation in trophoblast cells. Left panel of figure: LIN28 represses the biogenesis of mature *let-7* miRNAs by binding pri-*let-7* and pre-*let-7* miRNAs and inhibiting their processing. Due to low level of mature *let-7* miRNAs in the cells, there will be less targeting of proliferation-associated genes. Moreover, the ARID3B-complex will initiate the transcription of proliferation-associated genes and increase their expression. Increased expression of proliferation-associated genes will lead to increased cell proliferation. Right panel of figure: If LIN28 is knocked-out or knocked-down, there will be no suppression of *let-7* miRNA biogenesis. High *let-7* miRNAs will target and reduce the expression of proliferation associated genes and the ARDI3B-complex, driving the cells towards differentiation.

Table 1. Gene regulation by miRNAs in trophoblast cells

miRNA	Target Genes	Effect of higher miRNA expression	Reference
let-7	*ARID3A, ARID3B, HMGA1, cMYC*	Reduce proliferation of trophoblast cells	[72]
miR-200c	*Wnt/β-catenin*	Increases apoptosis of trophoblast cells	[73]
miR-16	*Notch2*	Inhibits proliferation, migration, and invasion, and facilitates the apoptosis of trophoblast cells	[74]
miR-576-5p	*TFAP2A*	Enhances invasion ability of trophoblast cells	[75]
miR-126a-3p	*ADAM9*	Induces proliferation, migration and invasion of trophoblast cells	[76]
miR-210	*CPEB2*	Inhibits trophoblast syncytialization	[77]
miR-218-5p	*TGFB2*	Promotes enEVTs and spiral artery remodeling	[78]
miR-133	*Rho/ROCK*	Increases apoptosis of trophoblast cells	[79]
miR-30b	*MXRA5*	Inhibits invasion of trophoblast cells	[80]
miR-106a	*hCYP19A1, hGCM1*	Inhibits trophoblast syncytialization	[81]
miR-320a	*IL-4*	Inhibits growth and invasion of trophoblasts	[82]
miR-384	*STAT3*	Reduces the proliferation and invasion of trophoblast cells	[83]
miR-182	*BRCA1*	Increases apoptosis of trophoblast cells	[84]
miR-155	*HIF-1α*	Increases apoptosis of trophoblast cells	[85]
miR-101	*CXCL6*	Inhibits migration and invasion of trophoblasts	[86]
miR-152	*Bax, Bcl-2*	Promotes apoptosis of trophoblast cells	[87]
miR-210	*Notch1*	Inhibit proliferation, invasion and migration of trophoblast cells	[88]
miR-137	*FNDC5*	Reduces viability and migration of trophoblasts	[89]
miR-210-3p	*FGF1*	Reduces proliferation and invasiveness of trophoblast cells	[90]
miR-27a-3p	*USP25*	Inhibits migration and invasion of trophoblasts	[91]
miR-558	*TIMP4*	Increases invasion of trophoblast	[92]
miR-184	*WIG1*	Promotes apoptosis of trophoblast cells	[93]
miR-371a	*XIAP*	Promotes apoptosis of trophoblast cells	[94]
miR-7	*EMT-related TFs*	Reduces invasion of trophoblast cells	[95]
miR-125a	*MCL1*	Increases apoptosis of trophoblast cells	[96]
miR-34a-5p	*Smad4*	Inhibits migration and invasion of trophoblasts	[97]
miR-145	*MUC1*	Increases proliferation and invasion, and reduces apoptosis of trophoblast cells	([98]
miR-221-3p	*THBS2*	Promotes growth, invasion and migration of trophoblast cells	[99]
miR-454	*ALK7*	Promotes proliferation and invasion, and reduces apoptosis of trophoblast cells	[100]
miR-34a	*Notch*	Suppresses trophoblast cells invasion	[101]

miR-101-3p	*mTOR*	Increases apoptosis and reduce migration of trophoblast cells	[102]
miR-96-5p	*mTOR, Bcl-2*	Increases apoptosis and reduce migration of trophoblast cells	[102]
miR-431	*ZEB1*	Inhibits invasion and migration of trophoblasts	[103]
miR-320a	*ERRγ*	Induces apoptosis while inhibits proliferation, migration, and invasion of trophoblast cells	[104]
miR-145-5p	*Cyr61*	Suppresses invasion of trophoblast cells	[105]
miR-483-3p	*RB1CC1*	Increases proliferation of trophoblast cells	[106]
miR-134	*ITGB1*	Inhibits invasion of trophoblast cells	[107]
miR-362-3p	*Pax3*	Inhibits invasion and migration of trophoblasts	[108]
miR-518b	*Rap1b*	Increases proliferation of trophoblast cells	[109]
miR-203	*VEGFA*	Inhibits proliferation, migration and invasion of trophoblast cells	[110]
miR-181a-5p	*IGF2BP2*	Suppresses invasion and migration of trophoblast cells	[111]
miR-30a-3p	*IGF1*	Reduces invasion and increases apoptosis of trophoblast cells	[112]
miR-299	*HDAc2*	Suppresses invasion and migration of trophoblast cells	[113]
miR-18b	*HIF-1α*	Reduces invasion, migration and viability of trophoblast cells	[114]
miR-34a	*BCL-2*	Increases apoptosis of trophoblast cells	[115]
miR-18a	*ER1*	Increases apoptosis of trophoblast cells	[116]
miR-23a	*XIAP*	Induces apoptosis of trophoblast cells	[117]
miR-144	*PTEN*	Increases proliferation, migration and invasion of trophoblast cells	[118]
miR-106b	*MMP-2*	Inhibits proliferation and invasion of trophoblast cells	[119]
miR-520g	*MMP-2*	Inhibits migration and invasion of trophoblasts	[120]
miR-218	*SOX4*	Inhibits migration and invasion of trophoblasts	[121]
miR-520	*PARP1*	Promotes apoptosis of trophoblast cells	[122]
miR-193b	*TGF-β2*	Reduces migration and invasion of trophoblasts	[123]
miR-34a	*MYC*	Inhibits invasion of trophoblast cells	[124]
miR-519d	*MMP-2*	Inhibits invasion and migration of trophoblasts	[125]

REFERENCES

1. Carter, A.M. Evolution of placental function in mammals: the molecular basis of gas and nutrient transfer, hormone secretion, and immune responses. *Physiol. Rev.* 2012, *92*, 1543–1576.
2. Gude, N.M.; Roberts, C.T.; Kalionis, B.; King, R.G. Growth and function of the normal human placenta. *Thromb. Res.* 2004, *114*, 397–407.
3. Burton, G.J.; Charnock-Jones, D.S.; Jauniaux, E. Regulation of vascular growth and function in the human placenta. *Reprod. Camb. Engl.* 2009, *138*, 895–902.
4. Hamilton, W.J.; Boyd, J.D. Development of the human placenta in the first three months of gestation. *J. Anat.* 1960, *94*, 297–328.
5. Crocker, I.P.; Cooper, S.; Ong, S.C.; Baker, P.N. Differences in apoptotic susceptibility of cytotrophoblasts and syncytiotrophoblasts in normal pregnancy to those complicated with preeclampsia and intrauterine growth restriction. *Am. J. Pathol.* 2003, *162*, 637–643.
6. Longtine, M.S.; Chen, B.; Odibo, A.O.; Zhong, Y.; Nelson, D.M. Villous trophoblast apoptosis is elevated and restricted to cytotrophoblasts in pregnancies complicated by preeclampsia, IUGR, or preeclampsia with IUGR. *Placenta* 2012, *33*, 352–359.
7. Barker, D.J.P. The developmental origins of well-being. *Philos. Trans. R. Soc. Lond. B. Biol. Sci.* 2004, *359*, 1359–1366.
8. Barker, D.J.P. The developmental origins of chronic adult disease. *Acta Paediatr. Oslo Nor. 1992 Suppl.* 2004, *93*, 26–33.
9. Burton, G.J.; Fowden, A.L.; Thornburg, K.L. Placental Origins of Chronic Disease. *Physiol. Rev.* 2016, *96*, 1509–1565.

10. Jiang, S. A Regulator of Metabolic Reprogramming: MicroRNA Let-7. *Transl. Oncol.* 2019, *12*, 1005–1013.

11. Boyerinas, B.; Park, S.M.; Hau, A.; Murmann, A.E.; Peter, M.E. The role of let-7 in cell differentiation and cancer. *Endocr. Relat. Cancer* 2010, *17*, F19–F36.

12. Hunter, S.E.; Finnegan, E.F.; Zisoulis, D.G.; Lovci, M.T.; Melnik-Martinez, K.V.; Yeo, G.W.; Pasquinelli, A.E. Functional genomic analysis of the let-7 regulatory network in Caenorhabditis elegans. *PLoS Genet.* 2013, *9*, e1003353.

13. Wang, X.; Cao, L.; Wang, Y.; Wang, X.; Liu, N.; You, Y. Regulation of let-7 and its target oncogenes (Review). *Oncol. Lett.* 2012, *3*, 955–960.

14. Bazer, F.W.; Spencer, T.E.; Johnson, G.A.; Burghardt, R.C.; Wu, G. Comparative aspects of implantation. *Reprod. Camb. Engl.* 2009, *138*, 195–209.

15. Mclaren, A. Embryo research Available online: https://www.nature.com/articles/320570b0 (accessed on Apr 6, 2018).

16. Wimsatt, W.A. Some comparative aspects of implantation. *Biol. Reprod.* 1975, *12*, 1–40.

17. Boron, W.F. *Medical Physiology: A Cellular and Molecular Approach*; W.B. Saunders, 2003; ISBN 978-0-7216-3256-8.

18. Bentin-Ley, U. Relevance of endometrial pinopodes for human blastocyst implantation. *Hum. Reprod. Oxf. Engl.* 2000, *15 Suppl 6*, 67–73.

19. Bloor, D.J.; Metcalfe, A.D.; Rutherford, A.; Brison, D.R.; Kimber, S.J. Expression of cell adhesion molecules during human preimplantation embryo development. *Mol. Hum. Reprod.* 2002, *8*, 237–245.

20. Campbell, S.; Swann, H.R.; Seif, M.W.; Kimber, S.J.; Aplin, J.D. Cell adhesion molecules on the oocyte and preimplantation human embryo. *Hum. Reprod. Oxf. Engl.* 1995, *10*, 1571–1578.

21. Herzog Maximilian A contribution to our knowledge of the earliest known stages of placentation and embryonic development in man. *Am. J. Anat.* 2005, *9*, 361–400.

22. Pötgens, A.J.G.; Schmitz, U.; Bose, P.; Versmold, A.; Kaufmann, P.; Frank, H.-G. Mechanisms of syncytial fusion: a review. *Placenta* 2002, *23 Suppl A*, S107-113.

23. Enders, A.C. Trophoblast differentiation during the transition from trophoblastic plate to lacunar stage of implantation in the rhesus monkey and human. *Am. J. Anat.* 1989, *186*, 85–98.

24. Nelson, D.M. Apoptotic changes occur in syncytiotrophoblast of human placental villi where fibrin type fibrinoid is deposited at discontinuities in the villous trophoblast. *Placenta* 1996, *17*, 387–391.

25. Yasuda, M.; Umemura, S.; Osamura, R.Y.; Kenjo, T.; Tsutsumi, Y. Apoptotic cells in the human endometrium and placental villi: pitfalls in applying the TUNEL method. *Arch. Histol. Cytol.* 1995, *58*, 185–190.

26. Huppertz, B.; Frank, H.G.; Reister, F.; Kingdom, J.; Korr, H.; Kaufmann, P. Apoptosis cascade progresses during turnover of human trophoblast: analysis of villous cytotrophoblast and syncytial fragments in vitro. *Lab. Investig. J. Tech. Methods Pathol.* 1999, *79*, 1687–1702.

27. Benirschke, K.; Burton, G.J.; Baergen, R.N. *Pathology of the Human Placenta*; 6th ed.; Springer-Verlag: Berlin Heidelberg, 2012; ISBN 978-3-642-23940-3.

28. Frank, H.-G. 10 - Placental Development. In *Fetal and Neonatal Physiology (Fifth Edition)*; Polin, R.A., Abman, S.H., Rowitch, D.H., Benitz, W.E., Fox, W.W., Eds.; Elsevier, 2017; pp. 101–113 ISBN 978-0-323-35214-7.

29. Mayhew, T.M.; Leach, L.; McGee, R.; Ismail, W.W.; Myklebust, R.; Lammiman, M.J. Proliferation, differentiation and apoptosis in villous trophoblast at 13-41 weeks of gestation (including observations on annulate lamellae and nuclear pore complexes). *Placenta* 1999, *20*, 407–422.

30. Huppertz, B.; Kaufmann, P. The apoptosis cascade in human villous trophoblast: A review. *Placenta* 1999, *20*, 215–242.

31. Benirschke, K.; Burton, G.J.; Baergen, R.N. *Pathology of the Human Placenta*; 6th ed.; Springer-Verlag: Berlin Heidelberg, 2012; ISBN 978-3-642-23940-3.

32. Demir, R.; Kaufmann, P.; Castellucci, M.; Erbengi, T.; Kotowski, A. Fetal vasculogenesis and angiogenesis in human placental villi. *Acta Anat. (Basel)* 1989, *136*, 190–203.

33. Dempsey, E.W. The development of capillaries in the villi of early human placentas. *Am. J. Anat.* 1972, *134*, 221–237.

34. Vićovac, L.; Jones, C.J.; Aplin, J.D. Trophoblast differentiation during formation of anchoring villi in a model of the early human placenta in vitro. *Placenta* 1995, *16*, 41–56.

35. Damsky, C.H.; Fitzgerald, M.L.; Fisher, S.J. Distribution patterns of extracellular matrix components and adhesion receptors are intricately modulated during first trimester cytotrophoblast differentiation along the invasive pathway, in vivo. *J. Clin. Invest.* 1992, *89*, 210–222.

36. Prakobphol, A.; Genbacev, O.; Gormley, M.; Kapidzic, M.; Fisher, S.J. A role for the L-selectin adhesion system in mediating cytotrophoblast emigration from the placenta. *Dev. Biol.* 2006, *298*, 107–117.

37. Kemp, B.; Kertschanska, S.; Kadyrov, M.; Rath, W.; Kaufmann, P.; Huppertz, B. Invasive depth of extravillous trophoblast correlates with cellular phenotype: a comparison of intra- and extrauterine implantation sites. *Histochem. Cell Biol.* 2002, *117*, 401–414.

38. Damsky, C.H.; Fisher, S.J. Trophoblast pseudo-vasculogenesis: faking it with endothelial adhesion receptors. *Curr. Opin. Cell Biol.* 1998, *10*, 660–666.

39. Huppertz, B. The feto-maternal interface: setting the stage for potential immune interactions. *Semin. Immunopathol.* 2007, *29*, 83–94.

40. Pijnenborg, R.; Dixon, G.; Robertson, W.B.; Brosens, I. Trophoblastic invasion of human decidua from 8 to 18 weeks of pregnancy. *Placenta* 1980, *1*, 3–19.

41. Anin, S.A.; Vince, G.; Quenby, S. Trophoblast invasion. *Hum. Fertil. Camb. Engl.* 2004, *7*, 169–174.

42. Pijnenborg, R.; Vercruysse, L.; Hanssens, M. The uterine spiral arteries in human pregnancy: facts and controversies. *Placenta* 2006, *27*, 939–958.

43. Lyall, F. Mechanisms regulating cytotrophoblast invasion in normal pregnancy and pre-eclampsia. *Aust. N. Z. J. Obstet. Gynaecol.* 2006, *46*, 266–273.

44. Red-Horse, K.; Zhou, Y.; Genbacev, O.; Prakobphol, A.; Foulk, R.; McMaster, M.; Fisher, S.J. Trophoblast differentiation during embryo implantation and formation of the maternal-fetal interface. *J. Clin. Invest.* 2004, *114*, 744–754.

45. Reynolds, L.P.; Redmer, D.A. Angiogenesis in the placenta. *Biol. Reprod.* 2001, *64*, 1033–1040.

46. Srijyothi, L.; Ponne, S.; Prathama, T.; Ashok, C.; Baluchamy, S. Roles of Non-Coding RNAs in Transcriptional Regulation. *Transcr. Post-Transcr. Regul.* 2018.

47. Winter, J.; Jung, S.; Keller, S.; Gregory, R.I.; Diederichs, S. Many roads to maturity: microRNA biogenesis pathways and their regulation. *Nat. Cell Biol.* 2009, *11*, 228–234.

48. Bartel, D.P. MicroRNAs: Genomics, Biogenesis, Mechanism, and Function. *Cell* 2004, *116*, 281–297.

49. Siomi, M.C.; Sato, K.; Pezic, D.; Aravin, A.A. PIWI-interacting small RNAs: the vanguard of genome defence. *Nat. Rev. Mol. Cell Biol.* 2011, *12*, 246–258.

50. Lee, R.C.; Feinbaum, R.L.; Ambros, V. The C. elegans heterochronic gene lin-4 encodes small RNAs with antisense complementarity to lin-14. *Cell* 1993, *75*, 843–854.

51. Wightman, B.; Ha, I.; Ruvkun, G. Posttranscriptional regulation of the heterochronic gene lin-14 by lin-4 mediates temporal pattern formation in C. elegans. *Cell* 1993, *75*, 855–862.

52. Lee, Y.; Kim, M.; Han, J.; Yeom, K.-H.; Lee, S.; Baek, S.H.; Kim, V.N. MicroRNA genes are transcribed by RNA polymerase II. *EMBO J.* 2004, *23*, 4051–4060.

53. Landthaler, M.; Yalcin, A.; Tuschl, T. The human DiGeorge syndrome critical region gene 8 and Its D. melanogaster homolog are required for miRNA biogenesis. *Curr. Biol. CB* 2004, *14*, 2162–2167.

54. Han, J.; Lee, Y.; Yeom, K.-H.; Kim, Y.-K.; Jin, H.; Kim, V.N. The Drosha-DGCR8 complex in primary microRNA processing. *Genes Dev.* 2004, *18*, 3016–3027.

55. Denli, A.M.; Tops, B.B.J.; Plasterk, R.H.A.; Ketting, R.F.; Hannon, G.J. Processing of primary microRNAs by the Microprocessor complex. *Nature* 2004, *432*, 231–235.

56. Gregory, R.I.; Yan, K.-P.; Amuthan, G.; Chendrimada, T.; Doratotaj, B.; Cooch, N.; Shiekhattar, R. The Microprocessor complex mediates the genesis of microRNAs. *Nature* 2004, *432*, 235–240.

57. Yi, R.; Qin, Y.; Macara, I.G.; Cullen, B.R. Exportin-5 mediates the nuclear export of pre-microRNAs and short hairpin RNAs. *Genes Dev.* 2003, *17*, 3011–3016.

58. Bohnsack, M.T.; Czaplinski, K.; Gorlich, D. Exportin 5 is a RanGTP-dependent dsRNA-binding protein that mediates nuclear export of pre-miRNAs. *RNA N. Y. N* 2004, *10*, 185–191.

59. Lund, E.; Güttinger, S.; Calado, A.; Dahlberg, J.E.; Kutay, U. Nuclear export of microRNA precursors. *Science* 2004, *303*, 95–98.

60. Vazquez, F.; Gasciolli, V.; Crété, P.; Vaucheret, H. The nuclear dsRNA binding protein HYL1 is required for microRNA accumulation and plant development, but not posttranscriptional transgene silencing. *Curr. Biol. CB* 2004, *14*, 346–351.

61. Han, M.-H.; Goud, S.; Song, L.; Fedoroff, N. The Arabidopsis double-stranded RNA-binding protein HYL1 plays a role in microRNA-mediated gene regulation. *Proc. Natl. Acad. Sci. U. S. A.* 2004, *101*, 1093–1098.

62. Kobayashi, H.; Tomari, Y. RISC assembly: Coordination between small RNAs and Argonaute proteins. *Biochim. Biophys. Acta* 2016, *1859*, 71–81.

63. Jo, M.H.; Shin, S.; Jung, S.-R.; Kim, E.; Song, J.-J.; Hohng, S. Human Argonaute 2 Has Diverse Reaction Pathways on Target RNAs. *Mol. Cell* 2015, *59*, 117–124.

64. Ellwanger, D.C.; Büttner, F.A.; Mewes, H.-W.; Stümpflen, V. The sufficient minimal set of miRNA seed types. *Bioinforma. Oxf. Engl.* 2011, *27*, 1346–1350.

65. Xu, W.; San Lucas, A.; Wang, Z.; Liu, Y. Identifying microRNA targets in different gene regions. *BMC Bioinformatics* 2014, *15 Suppl 7*, S4.

66. Braun, J.E.; Truffault, V.; Boland, A.; Huntzinger, E.; Chang, C.-T.; Haas, G.; Weichenrieder, O.; Coles, M.; Izaurralde, E. A direct interaction between DCP1 and XRN1 couples mRNA decapping to 5' exonucleolytic degradation. *Nat. Struct. Mol. Biol.* 2012, *19*, 1324–1331.

67. Christie, M.; Boland, A.; Huntzinger, E.; Weichenrieder, O.; Izaurralde, E. Structure of the PAN3 pseudokinase reveals the basis for interactions with the PAN2 deadenylase and the GW182 proteins. *Mol. Cell* 2013, *51*, 360–373.

68. Behm-Ansmant, I.; Rehwinkel, J.; Doerks, T.; Stark, A.; Bork, P.; Izaurralde, E. mRNA degradation by miRNAs and GW182 requires both CCR4:NOT deadenylase and DCP1:DCP2 decapping complexes. *Genes Dev.* 2006, *20*, 1885–1898.

69. Doridot, L.; Miralles, F.; Barbaux, S.; Vaiman, D. Trophoblasts, invasion, and microRNA. *Front. Genet.* 2013, *4*.

70. Nizyaeva, N.V.; Kulikova, G.V.; Shchyogolev, A.I.; Zemskov, V.M. The role of microRNA in regulation of the body's immune responses. *Biol. Bull. Rev.* 2016, *6*, 473–482.

71. Ardekani, A.M.; Naeini, M.M. The Role of MicroRNAs in Human Diseases. *Avicenna J. Med. Biotechnol.* 2010, *2*, 161–179.

72. Ali, A.; Anthony, R.V.; Bouma, G.J.; Winger, Q.A. LIN28-let-7 axis regulates genes in immortalized human trophoblast cells by targeting the ARID3B-complex. *FASEB J. Off. Publ. Fed. Am. Soc. Exp. Biol.* 2019, *33*, 12348–12363.

73. Zhang, X.; Ge, Y.-W.; Wang, Z.-X.; Xu, Q.-L.; Guo, R.; Xu, H.-Y. MiR-200c regulates apoptosis of placental trophoblasts in preeclampsia rats through Wnt/β-catenin signaling pathway. *Eur. Rev. Med. Pharmacol. Sci.* 2019, *23*, 7209–7216.

74. Yuan, Y.; Wang, X.; Sun, Q.; Dai, X.; Cai, Y. MicroRNA-16 is involved in the pathogenesis of pre-eclampsia via regulation of Notch2. *J. Cell. Physiol.* 2019.

75. Wang, X.; Peng, S.; Cui, K.; Hou, F.; Ding, J.; Li, A.; Wang, M.; Geng, L. MicroRNA-576-5p enhances the invasion ability of trophoblast cells in preeclampsia by targeting TFAP2A. *Mol. Genet. Genomic Med.* 2019, e1025.

76. Zhao, S.; Wang, J.; Cao, Z.; Gao, L.; Zheng, Y.; Wang, J.; Liu, X. miR-126a-3p induces proliferation, migration and invasion of trophoblast cells in pre-eclampsia-like rats by inhibiting A Disintegrin and Metalloprotease 9. *Biosci. Rep.* 2019, *39*.

77. Wang, H.; Zhao, Y.; Luo, R.; Bian, X.; Wang, Y.; Shao, X.; Li, Y.-X.; Liu, M.; Wang, Y.-L. A positive feedback self-regulatory loop between miR-210 and HIF-1α mediated by CPEB2 is involved in trophoblast syncytiolization: implication of trophoblast malfunction in preeclampsia. *Biol. Reprod.* 2019.

78. Brkić, J.; Dunk, C.; O'Brien, J.; Fu, G.; Nadeem, L.; Wang, Y.; Rosman, D.; Salem, M.; Shynlova, O.; Yougbaré, I.; et al. MicroRNA-218-5p Promotes Endovascular Trophoblast Differentiation and Spiral Artery Remodeling. *Mol. Ther.* 2018, *26*, 2189–2205.

79. Zhang, W.-M.; Cao, P.; Xin, L.; Zhang, Y.; Liu, Z.; Yao, N.; Ma, Y.-Y. Effect of miR-133 on apoptosis of trophoblasts in human placenta tissues via Rho/ROCK signaling pathway. *Eur. Rev. Med. Pharmacol. Sci.* 2019, *23*, 10600–10608.

80. Qian, S.; Liu, R. miR-30b facilitates preeclampsia through targeting MXRA5 to inhibit the viability, invasion and apoptosis of placental trophoblast cells. *Int. J. Clin. Exp. Pathol.* 2019, *12*, 4057–4065.

81. Kumar, P.; Luo, Y.; Tudela, C.; Alexander, J.M.; Mendelson, C.R. The c-Myc-regulated microRNA-17~92 (miR-17~92) and miR-106a~363 clusters target hCYP19A1 and hGCM1 to inhibit human trophoblast differentiation. *Mol. Cell. Biol.* 2013, *33*, 1782–1796.

82. Xie, N.; Jia, Z.; Li, L. miR-320a upregulation contributes to the development of preeclampsia by inhibiting the growth and invasion of trophoblast cells by targeting interleukin 4. *Mol. Med. Rep.* 2019, *20*, 3256–3264.

83. Zhou, W.; Wang, H.; Yang, J.; Long, W.; Zhang, B.; Liu, J.; Yu, B. Down-regulated circPAPPA suppresses the proliferation and invasion of trophoblast cells via the miR-384/STAT3 pathway. *Biosci. Rep.* 2019, *39*.

84. West, R.C.; Russ, J.E.; Bouma, G.J.; Winger, Q.A. BRCA1 regulates HMGA2 levels in the Swan71 trophoblast cell line. *Mol. Reprod. Dev.* 2019, *86*, 1663–1670.

85. Li, X.; Lu, J.; Dong, L.; Lv, F.; Liu, W.; Liu, G.; Zhu, W.; Diao, X. Effects of MiR-155 on trophoblast apoptosis in placental tissues of preeclampsia rats through HIF-1α signaling pathway. *Panminerva Med.* 2019.

86. Zhang, S.; Wang, Y.; Li, J.; Zhong, Q.; Li, Y. MiR-101 inhibits migration and invasion of trophoblast HTR-8/SVneo cells by targeting CXCL6 in preeclampsia. *Minerva Med.* 2019.

87. Zhang, L.; Yuan, J.-M.; Zhao, R.-H.; Wang, L.-M.; Tu, Z.-B. Correlation of MiR-152 expression with VEGF expression in placental tissue of preeclampsia rat and its influence on apoptosis of trophoblast cells. *Eur. Rev. Med. Pharmacol. Sci.* 2019, *23*, 3553–3560.

88. Wang, R.; Liu, W.; Liu, X.; Liu, X.; Tao, H.; Wu, D.; Zhao, Y.; Zou, L. MicroRNA-210 regulates human trophoblast cell line HTR-8/SVneo function by attenuating Notch1 expression: Implications for the role of microRNA-210 in pre-eclampsia. *Mol. Reprod. Dev.* 2019, *86*, 896–907.

89. Peng, H.-Y.; Li, M.-Q.; Li, H.-P. MiR-137 Restricts the Viability and Migration of HTR-8/SVneo Cells by Downregulating FNDC5 in Gestational Diabetes Mellitus. *Curr. Mol. Med.* 2019, *19*, 494–505.

90. Li, L.; Huang, X.; He, Z.; Xiong, Y.; Fang, Q. miRNA-210-3p regulates trophoblast proliferation and invasiveness through fibroblast growth factor 1 in selective intrauterine growth restriction. *J. Cell. Mol. Med.* 2019, *23*, 4422–4433.

91. Ding, J.; Cheng, Y.; Zhang, Y.; Liao, S.; Yin, T.; Yang, J. The miR-27a-3p/USP25 axis participates in the pathogenesis of recurrent miscarriage by inhibiting trophoblast migration and invasion. *J. Cell. Physiol.* 2019, *234*, 19951–19963.

92. Cheng, D.; Jiang, S.; Chen, J.; Li, J.; Ao, L.; Zhang, Y. Upregulated long noncoding RNA Linc00261 in pre-eclampsia and its effect on trophoblast invasion and migration via regulating miR-558/TIMP4 signaling pathway. *J. Cell. Biochem.* 2019, *120*, 13243–13253.

93. Zhang, Y.; Zhou, J.; Li, M.-Q.; Xu, J.; Zhang, J.-P.; Jin, L.-P. MicroRNA-184 promotes apoptosis of trophoblast cells via targeting WIG1 and induces early spontaneous abortion. *Cell Death Dis.* 2019, *10*, 223.

94. Du, E.; Cao, Y.; Feng, C.; Lu, J.; Yang, H.; Zhang, Y. The Possible Involvement of miR-371a-5p Regulating XIAP in the Pathogenesis of Recurrent Pregnancy Loss. *Reprod. Sci. Thousand Oaks Calif* 2019, *26*, 1468–1475.

95. Shih, J.-C.; Lin, H.-H.; Hsiao, A.-C.; Su, Y.-T.; Tsai, S.; Chien, C.-L.; Kung, H.-N. Unveiling the role of microRNA-7 in linking TGF-β-Smad-mediated epithelial-mesenchymal transition with negative regulation of trophoblast invasion. *FASEB J. Off. Publ. Fed. Am. Soc. Exp. Biol.* 2019, *33*, 6281–6295.

96. Gu, Y.; Meng, J.; Zuo, C.; Wang, S.; Li, H.; Zhao, S.; Huang, T.; Wang, X.; Yan, J. Downregulation of MicroRNA-125a in Placenta Accreta Spectrum Disorders Contributes Antiapoptosis of Implantation Site Intermediate Trophoblasts by Targeting MCL1. *Reprod. Sci. Thousand Oaks Calif* 2019, *26*, 1582–1589.

97. Xue, F.; Yang, J.; Li, Q.; Zhou, H. Down-regulation of microRNA-34a-5p promotes trophoblast cell migration and invasion via targetting Smad4. *Biosci. Rep.* 2019, *39*.

98. Chi, Z.; Zhang, M. Exploration of the regulation and control mechanisms of miR-145 in trophoblast cell proliferation and invasion. *Exp. Ther. Med.* 2018, *16*, 5298–5304.

99. Yang, Y.; Li, H.; Ma, Y.; Zhu, X.; Zhang, S.; Li, J. MiR-221-3p is down-regulated in preeclampsia and affects trophoblast growth, invasion and migration partly via targeting thrombospondin 2. *Biomed. Pharmacother. Biomedecine Pharmacother.* 2019, *109*, 127–134.

100. Shi, Z.; She, K.; Li, H.; Yuan, X.; Han, X.; Wang, Y. MicroRNA-454 contributes to sustaining the proliferation and invasion of trophoblast cells through inhibiting Nodal/ALK7 signaling in pre-eclampsia. *Chem. Biol. Interact.* 2019, *298*, 8–14.

101. Liu, J.-J.; Zhang, L.; Zhang, F.-F.; Luan, T.; Yin, Z.-M.; Rui, C.; Ding, H.-J. Influence of miR-34a on preeclampsia through the Notch signaling pathway. *Eur. Rev. Med. Pharmacol. Sci.* 2019, *23*, 923–931.

102. Mao, Z.; Yao, M.; Li, Y.; Fu, Z.; Li, S.; Zhang, L.; Zhou, Z.; Tang, Q.; Han, X.; Xia, Y. miR-96-5p and miR-101-3p as potential intervention targets to rescue TiO2 NP-induced autophagy and migration impairment of human trophoblastic cells. *Biomater. Sci.* 2018, *6*, 3273–3283.

103. Yang, X.; Meng, T. MicroRNA-431 affects trophoblast migration and invasion by targeting ZEB1 in preeclampsia. *Gene* 2019, *683*, 225–232.

104. Liu, R.-H.; Meng, Q.; Shi, Y.-P.; Xu, H.-S. Regulatory role of microRNA-320a in the proliferation, migration, invasion, and apoptosis of trophoblasts and endothelial cells by targeting estrogen-related receptor γ. *J. Cell. Physiol.* 2018, *234*, 682–691.

105. Wen, Z.; Chen, Y.; Long, Y.; Yu, J.; Li, M. Tumor necrosis factor-alpha suppresses the invasion of HTR-8/SVneo trophoblast cells through microRNA-145-5p-mediated downregulation of Cyr61. *Life Sci.* 2018, *209*, 132–139.

106. Li, J.; Fu, Z.; Jiang, H.; Chen, L.; Wu, X.; Ding, H.; Xia, Y.; Wang, X.; Tang, Q.; Wu, W. IGF2-derived miR-483-3p contributes to macrosomia through regulating trophoblast proliferation by targeting RB1CC1. *Mol. Hum. Reprod.* 2018, *24*, 444–452.

107. Zou, A.-X.; Chen, B.; Li, Q.-X.; Liang, Y.-C. MiR-134 inhibits infiltration of trophoblast cells in placenta of patients with preeclampsia by decreasing ITGB1 expression. *Eur. Rev. Med. Pharmacol. Sci.* 2018, *22*, 2199–2206.

108. Wang, N.; Feng, Y.; Xu, J.; Zou, J.; Chen, M.; He, Y.; Liu, H.; Xue, M.; Gu, Y. miR-362-3p regulates cell proliferation, migration and invasion of trophoblastic cells under hypoxia through targeting Pax3. *Biomed. Pharmacother. Biomedecine Pharmacother.* 2018, *99*, 462–468.

109. Liu, M.; Wang, Y.; Lu, H.; Wang, H.; Shi, X.; Shao, X.; Li, Y.-X.; Zhao, Y.; Wang, Y.-L. miR-518b Enhances Human Trophoblast Cell Proliferation Through Targeting Rap1b and Activating Ras-MAPK Signal. *Front. Endocrinol.* 2018, *9*, 100.

110. Liu, F.; Wu, K.; Wu, W.; Chen, Y.; Wu, H.; Wang, H.; Zhang, W. miR-203 contributes to pre-eclampsia via inhibition of VEGFA expression. *Mol. Med. Rep.* 2018, *17*, 5627–5634.

111. Wu, L.; Song, W.-Y.; Xie, Y.; Hu, L.-L.; Hou, X.-M.; Wang, R.; Gao, Y.; Zhang, J.-N.; Zhang, L.; Li, W.-W.; et al. miR-181a-5p suppresses invasion and migration of HTR-8/SVneo cells by directly targeting IGF2BP2. *Cell Death Dis.* 2018, *9*, 16.

112. Niu, Z.-R.; Han, T.; Sun, X.-L.; Luan, L.-X.; Gou, W.-L.; Zhu, X.-M. MicroRNA-30a-3p is overexpressed in the placentas of patients with preeclampsia and affects trophoblast invasion and apoptosis by its effects on IGF-1. *Am. J. Obstet. Gynecol.* 2018, *218*, 249.e1-249.e12.

113. Gao, Y.; She, R.; Wang, Q.; Li, Y.; Zhang, H. Up-regulation of miR-299 suppressed the invasion and migration of HTR-8/SVneo trophoblast cells partly via targeting HDAC2 in pre-eclampsia. *Biomed. Pharmacother. Biomedecine Pharmacother.* 2018, *97*, 1222–1228.

114. Wang, S.; Wang, X.; Weng, Z.; Zhang, S.; Ning, H.; Li, B. Expression and role of microRNA 18b and hypoxia inducible factor-1α in placental tissues of preeclampsia patients. *Exp. Ther. Med.* 2017, *14*, 4554–4560.

115. Guo, M.; Zhao, X.; Yuan, X.; Li, P. Elevated microRNA-34a contributes to trophoblast cell apoptosis in preeclampsia by targeting BCL-2. *J. Hum. Hypertens.* 2017, *31*, 815–820.

116. Yang, Y.; Zhang, S.; Li, Y.; Han, B.; Ma, Y. [Inhibition of miR-18a increases expression of estrogen receptor 1 and promotes apoptosis in human HTR8 trophoblasts]. *Xi Bao Yu Fen Zi Mian Yi Xue Za Zhi Chin. J. Cell. Mol. Immunol.* 2017, *33*, 1102–1107.

117. Li, L.; Hou, A.; Gao, X.; Zhang, J.; Zhang, L.; Wang, J.; Li, H.; Song, Y. Lentivirus-mediated miR-23a overexpression induces trophoblast cell apoptosis through inhibiting X-linked inhibitor of apoptosis. *Biomed. Pharmacother. Biomedecine Pharmacother.* 2017, *94*, 412–417.

118. Xiao, J.; Tao, T.; Yin, Y.; Zhao, L.; Yang, L.; Hu, L. miR-144 may regulate the proliferation, migration and invasion of trophoblastic cells through targeting PTEN in preeclampsia. *Biomed. Pharmacother. Biomedecine Pharmacother.* 2017, *94*, 341–353.

119. Li, J.; Wang, J.M.; Liu, Y.H.; Zhang, Z.; Han, N.; Wang, J.Y.; Xue, S.H.; Wang, P. [Effect of microRNA-106b on the invasion and proliferation of trophoblasts through targeting MMP-2]. *Zhonghua Fu Chan Ke Za Zhi* 2017, *52*, 327–332.

120. Jiang, L.; Long, A.; Tan, L.; Hong, M.; Wu, J.; Cai, L.; Li, Q. Elevated microRNA-520g in pre-eclampsia inhibits migration and invasion of trophoblasts. *Placenta* 2017, *51*, 70–75.

121. Chen, Y.-J.; Wu, P.-Y.; Gao, R.-Q. [MiR-218 inhibits HTR-8 cells migration and invasion by targeting SOX4]. *Zhongguo Ying Yong Sheng Li Xue Za Zhi Zhongguo Yingyong Shenglixue Zazhi Chin. J. Appl. Physiol.* 2017, *33*, 169–173.

122. Dong, X.; Yang, L.; Wang, H. miR-520 promotes DNA-damage-induced trophoblast cell apoptosis by targeting PARP1 in recurrent spontaneous abortion (RSA). *Gynecol. Endocrinol. Off. J. Int. Soc. Gynecol. Endocrinol.* 2017, *33*, 274–278.

123. Zhou, X.; Li, Q.; Xu, J.; Zhang, X.; Zhang, H.; Xiang, Y.; Fang, C.; Wang, T.; Xia, S.; Zhang, Q.; et al. The aberrantly expressed miR-193b-3p contributes to preeclampsia through regulating transforming growth factor-β signaling. *Sci. Rep.* 2016, *6*, 19910.

124. Sun, M.; Chen, H.; Liu, J.; Tong, C.; Meng, T. MicroRNA-34a inhibits human trophoblast cell invasion by targeting MYC. *BMC Cell Biol.* 2015, *16*.

125. Ding, J.; Huang, F.; Wu, G.; Han, T.; Xu, F.; Weng, D.; Wu, C.; Zhang, X.; Yao, Y.; Zhu, X. MiR-519d-3p Suppresses Invasion and Migration of Trophoblast Cells via Targeting MMP-2. *PLoS ONE* 2015, *10*.

126. Reinhart, B.J.; Slack, F.J.; Basson, M.; Pasquinelli, A.E.; Bettinger, J.C.; Rougvie, A.E.; Horvitz, H.R.; Ruvkun, G. The 21-nucleotide let-7 RNA regulates developmental timing in Caenorhabditis elegans. *Nature* 2000, *403*, 901–906.

127. Liu, S.; Xia, Q.; Zhao, P.; Cheng, T.; Hong, K.; Xiang, Z. Characterization and expression patterns of let-7 microRNA in the silkworm (Bombyx mori). *BMC Dev. Biol.* 2007, *7*, 88.

128. Pasquinelli, A.E.; Reinhart, B.J.; Slack, F.; Martindale, M.Q.; Kuroda, M.I.; Maller, B.; Hayward, D.C.; Ball, E.E.; Degnan, B.; Müller, P.; et al. Conservation of the sequence and temporal expression of let-7 heterochronic regulatory RNA. *Nature* 2000, *408*, 86–89.

129. Landgraf, P.; Rusu, M.; Sheridan, R.; Sewer, A.; Iovino, N.; Aravin, A.; Pfeffer, S.; Rice, A.; Kamphorst, A.O.; Landthaler, M.; et al. A mammalian microRNA expression atlas based on small RNA library sequencing. *Cell* 2007, *129*, 1401–1414.

130. Roush, S.; Slack, F.J. The let-7 family of microRNAs. *Trends Cell Biol.* 2008, *18*, 505–516.

131. Lee, H.; Han, S.; Kwon, C.S.; Lee, D. Biogenesis and regulation of the let-7 miRNAs and their functional implications. *Protein Cell* 2016, *7*, 100–113.

132. Zhang, H.; Artiles, K.L.; Fire, A.Z. Functional relevance of “seed” and “non-seed” sequences in microRNA-mediated promotion of C. elegans developmental progression. *RNA* 2015, *21*, 1980–1992.

133. Kehl, T.; Backes, C.; Kern, F.; Fehlmann, T.; Ludwig, N.; Meese, E.; Lenhof, H.-P.; Keller, A. About miRNAs, miRNA seeds, target genes and target pathways. *Oncotarget* 2017, *8*, 107167–107175.

134. Shyh-Chang, N.; Zhu, H.; Yvanka de Soysa, T.; Shinoda, G.; Seligson, M.T.; Tsanov, K.M.; Nguyen, L.; Asara, J.M.; Cantley, L.C.; Daley, G.Q. Lin28 enhances tissue repair by reprogramming cellular metabolism. *Cell* 2013, *155*, 778–792.

135. Shyh-Chang, N.; Daley, G.Q. Lin28: primal regulator of growth and metabolism in stem cells. *Cell Stem Cell* 2013, *12*, 395–406.

136. Caygill, E.E.; Johnston, L.A. Temporal regulation of metamorphic processes in Drosophila by the let-7 and miR-125 heterochronic microRNAs. *Curr. Biol. CB* 2008, *18*, 943–950.

137. Wang, X.; Cao, L.; Wang, Y.; Wang, X.; Liu, N.; You, Y. Regulation of let-7 and its target oncogenes (Review). *Oncol. Lett.* 2012, *3*, 955–960.

138. Wagner, S.; Ngezahayo, A.; Murua Escobar, H.; Nolte, I. Role of miRNA let-7 and its major targets in prostate cancer. *BioMed Res. Int.* 2014, *2014*, 376326.

139. Takamizawa, J.; Konishi, H.; Yanagisawa, K.; Tomida, S.; Osada, H.; Endoh, H.; Harano, T.; Yatabe, Y.; Nagino, M.; Nimura, Y.; et al. Reduced Expression of the let-7 MicroRNAs in Human Lung Cancers in Association with Shortened Postoperative Survival. *Cancer Res.* 2004, *64*, 3753–3756.

140. Boyerinas, B.; Park, S.-M.; Shomron, N.; Hedegaard, M.M.; Vinther, J.; Andersen, J.S.; Feig, C.; Xu, J.; Burge, C.B.; Peter, M.E. Identification of Let-7–Regulated Oncofetal Genes. *Cancer Res.* 2008, *68*, 2587–2591.

141. Copley, M.R.; Babovic, S.; Benz, C.; Knapp, D.J.H.F.; Beer, P.A.; Kent, D.G.; Wohrer, S.; Treloar, D.Q.; Day, C.; Rowe, K.; et al. The Lin28b-let-7-Hmga2 axis determines the higher self-renewal potential of fetal haematopoietic stem cells. *Nat. Cell Biol.* 2013, *15*, 916–925.

142. Emmrich, S.; Rasche, M.; Schöning, J.; Reimer, C.; Keihani, S.; Maroz, A.; Xie, Y.; Li, Z.; Schambach, A.; Reinhardt, D.; et al. miR-99a/100~125b tricistrons regulate hematopoietic

stem and progenitor cell homeostasis by shifting the balance between TGFβ and Wnt signaling. *Genes Dev.* 2014, *28*, 858–874.

143. Heo, I.; Ha, M.; Lim, J.; Yoon, M.-J.; Park, J.-E.; Kwon, S.C.; Chang, H.; Kim, V.N. Mono-uridylation of pre-microRNA as a key step in the biogenesis of group II let-7 microRNAs. *Cell* 2012, *151*, 521–532.

144. Büssing, I.; Slack, F.J.; Grosshans, H. let-7 microRNAs in development, stem cells and cancer. *Trends Mol. Med.* 2008, *14*, 400–409.

145. Thomson, J.M.; Newman, M.; Parker, J.S.; Morin-Kensicki, E.M.; Wright, T.; Hammond, S.M. Extensive post-transcriptional regulation of microRNAs and its implications for cancer. *Genes Dev.* 2006, *20*, 2202–2207.

146. Nam, Y.; Chen, C.; Gregory, R.I.; Chou, J.J.; Sliz, P. Molecular basis for interaction of let-7 microRNAs with Lin28. *Cell* 2011, *147*, 1080–1091.

147. Zhang, P.; Elabd, S.; Hammer, S.; Solozobova, V.; Yan, H.; Bartel, F.; Inoue, S.; Henrich, T.; Wittbrodt, J.; Loosli, F.; et al. TRIM25 has a dual function in the p53/Mdm2 circuit. *Oncogene* 2015, *34*, 5729–5738.

148. Treiber, T.; Treiber, N.; Meister, G. Regulation of microRNA biogenesis and its crosstalk with other cellular pathways. *Nat. Rev. Mol. Cell Biol.* 2019, *20*, 5–20.

149. Guo, Y.; Chen, Y.; Ito, H.; Watanabe, A.; Ge, X.; Kodama, T.; Aburatani, H. Identification and characterization of lin-28 homolog B (LIN28B) in human hepatocellular carcinoma. *Gene* 2006, *384*, 51–61.

150. Tsialikas, J.; Romer-Seibert, J. LIN28: roles and regulation in development and beyond. *Dev. Camb. Engl.* 2015, *142*, 2397–2404.

151. Yu, J.; Vodyanik, M.A.; Smuga-Otto, K.; Antosiewicz-Bourget, J.; Frane, J.L.; Tian, S.; Nie, J.; Jonsdottir, G.A.; Ruotti, V.; Stewart, R.; et al. Induced pluripotent stem cell lines derived from human somatic cells. *Science* 2007, *318*, 1917–1920.

152. Jiang, S.; Baltimore, D. RNA-binding protein Lin28 in cancer and immunity. *Cancer Lett.* 2016, *375*, 108–113.

153. Shinoda, G.; Shyh-Chang, N.; Soysa, T.Y. de; Zhu, H.; Seligson, M.T.; Shah, S.P.; Abo-Sido, N.; Yabuuchi, A.; Hagan, J.P.; Gregory, R.I.; et al. Fetal deficiency of lin28 programs life-long aberrations in growth and glucose metabolism. *Stem Cells Dayt. Ohio* 2013, *31*, 1563–1573.

154. Mayr, F.; Heinemann, U. Mechanisms of Lin28-Mediated miRNA and mRNA Regulation—A Structural and Functional Perspective. *Int. J. Mol. Sci.* 2013, *14*, 16532–16553.

155. Zhang, J.; Ratanasirintrawoot, S.; Chandrasekaran, S.; Wu, Z.; Ficarro, S.B.; Yu, C.; Ross, C.A.; Cacchiarelli, D.; Xia, Q.; Seligson, M.; et al. LIN28 Regulates Stem Cell Metabolism and Conversion to Primed Pluripotency. *Cell Stem Cell* 2016, *19*, 66–80.

156. Viswanathan, S.R.; Daley, G.Q.; Gregory, R.I. Selective blockade of microRNA processing by Lin-28. *Science* 2008, *320*, 97–100.

157. Heo, I.; Joo, C.; Cho, J.; Ha, M.; Han, J.; Kim, V.N. Lin28 Mediates the Terminal Uridylation of let-7 Precursor MicroRNA. *Mol. Cell* 2008, *32*, 276–284.

158. Piskounova, E.; Polytarchou, C.; Thornton, J.E.; LaPierre, R.J.; Pothoulakis, C.; Hagan, J.P.; Iliopoulos, D.; Gregory, R.I. Lin28A and Lin28B inhibit let-7 microRNA biogenesis by distinct mechanisms. *Cell* 2011, *147*, 1066–1079.

159. Molenaar, J.J.; Domingo-Fernández, R.; Ebus, M.E.; Lindner, S.; Koster, J.; Drabek, K.; Mestdagh, P.; van Sluis, P.; Valentijn, L.J.; van Nes, J.; et al. LIN28B induces neuroblastoma and enhances MYCN levels via let-7 suppression. *Nat. Genet.* 2012, *44*, 1199–1206.

160. Thornton, J.E.; Chang, H.-M.; Piskounova, E.; Gregory, R.I. Lin28-mediated control of let-7 microRNA expression by alternative TUTases Zcchc11 (TUT4) and Zcchc6 (TUT7). *RNA N. Y. N* 2012, *18*, 1875–1885.

161. Heo, I.; Joo, C.; Kim, Y.-K.; Ha, M.; Yoon, M.-J.; Cho, J.; Yeom, K.-H.; Han, J.; Kim, V.N. TUT4 in concert with Lin28 suppresses microRNA biogenesis through pre-microRNA uridylation. *Cell* 2009, *138*, 696–708.

162. Hagan, J.P.; Piskounova, E.; Gregory, R.I. Lin28 recruits the TUTase Zcchc11 to inhibit let-7 maturation in mouse embryonic stem cells. *Nat. Struct. Mol. Biol.* 2009, *16*, 1021–1025.

163. Faehnle, C.R.; Walleshauser, J.; Joshua-Tor, L. Mechanism of Dis3l2 substrate recognition in the Lin28-let-7 pathway. *Nature* 2014, *514*, 252–256.

164. Piskounova, E.; Polytarchou, C.; Thornton, J.E.; LaPierre, R.J.; Pothoulakis, C.; Hagan, J.P.; Iliopoulos, D.; Gregory, R.I. Lin28A and Lin28B inhibit let-7 microRNA biogenesis by distinct mechanisms. *Cell* 2011, *147*, 1066–1079.

165. Rybak, A.; Fuchs, H.; Smirnova, L.; Brandt, C.; Pohl, E.E.; Nitsch, R.; Wulczyn, F.G. A feedback loop comprising lin-28 and let-7 controls pre-let-7 maturation during neural stem-cell commitment. *Nat. Cell Biol.* 2008, *10*, 987–993.

166. Heo, I.; Joo, C.; Cho, J.; Ha, M.; Han, J.; Kim, V.N. Lin28 mediates the terminal uridylation of let-7 precursor MicroRNA. *Mol. Cell* 2008, *32*, 276–284.

167. Piskounova, E.; Polytarchou, C.; Thornton, J.E.; LaPierre, R.J.; Pothoulakis, C.; Hagan, J.P.; Iliopoulos, D.; Gregory, R.I. Lin28A and Lin28B inhibit let-7 microRNA biogenesis by distinct mechanisms. *Cell* 2011, *147*, 1066–1079.

168. Ustianenko, D.; Chiu, H.-S.; Treiber, T.; Weyn-Vanhentenryck, S.M.; Treiber, N.; Meister, G.; Sumazin, P.; Zhang, C. LIN28 selectively modulates a subclass of let-7 microRNAs. *Mol. Cell* 2018, *71*, 271-283.e5.

169. Nam, Y.; Chen, C.; Gregory, R.I.; Chou, J.J.; Sliz, P. Molecular basis for interaction of let-7 microRNAs with Lin28. *Cell* 2011, *147*, 1080–1091.

170. West, R.C.; McWhorter, E.S.; Ali, A.; Goetzman, L.N.; Russ, J.E.; Anthony, R.V.; Bouma, G.J.; Winger, Q.A. HMGA2 is regulated by LIN28 and BRCA1 in human placental cells†. *Biol. Reprod.* 2018.

171. Seabrook, J.L.; Cantlon, J.D.; Cooney, A.J.; McWhorter, E.E.; Fromme, B.A.; Bouma, G.J.; Anthony, R.V.; Winger, Q.A. Role of LIN28A in Mouse and Human Trophoblast Cell Differentiation. *Biol. Reprod.* 2013, *89*, 95.

172. Barbaux, S.; Gascoin-Lachambre, G.; Buffat, C.; Monnier, P.; Mondon, F.; Tonanny, M.-B.; Pinard, A.; Auer, J.; Bessières, B.; Barlier, A.; et al. A genome-wide approach reveals novel imprinted genes expressed in the human placenta. *Epigenetics* 2012, *7*, 1079–1090.

173. Monk, D. Genomic imprinting in the human placenta. *Am. J. Obstet. Gynecol.* 2015, *213*, S152-162.

174. Liu, Y.; Fan, X.; Wang, R.; Lu, X.; Dang, Y.-L.; Wang, H.; Lin, H.-Y.; Zhu, C.; Ge, H.; Cross, J.C.; et al. Single-cell RNA-seq reveals the diversity of trophoblast subtypes and patterns of differentiation in the human placenta. *Cell Res.* 2018, *28*, 819–832.

175. Canfield, J.; Arlier, S.; Mong, E.F.; Lockhart, J.; VanWye, J.; Guzeloglu-Kayisli, O.; Schatz, F.; Magness, R.R.; Lockwood, C.J.; Tsibris, J.C.M.; et al. Decreased LIN28B in preeclampsia impairs human trophoblast differentiation and migration. *FASEB J. Off. Publ. Fed. Am. Soc. Exp. Biol.* 2018, fj201801163R.

176. Gu, Y.; Sun, J.; Groome, L.J.; Wang, Y. Differential miRNA expression profiles between the first and third trimester human placentas. *Am. J. Physiol. Endocrinol. Metab.* 2013, *304*, E836-843.

177. Souza, M.A.; de Lourdes Brizot, M.; Biancolin, S.E.; Schultz, R.; de Carvalho, M.H.B.; Francisco, R.P.V.; Zugaib, M. Placental weight and birth weight to placental weight ratio in monochorionic and dichorionic growth-restricted and non-growth-restricted twins. *Clin. Sao Paulo Braz.* 2017, *72*, 265–271.

178. Seabrook, J.L.; Cantlon, J.D.; Cooney, A.J.; McWhorter, E.E.; Fromme, B.A.; Bouma, G.J.; Anthony, R.V.; Winger, Q.A. Role of LIN28A in Mouse and Human Trophoblast Cell Differentiation. *Biol. Reprod.* 2013, *89*, 95.

179. Hiden, U.; Wadsack, C.; Prutsch, N.; Gauster, M.; Weiss, U.; Frank, H.-G.; Schmitz, U.; Fast-Hirsch, C.; Hengstschläger, M.; Pötgens, A.; et al. The first trimester human trophoblast cell line ACH-3P: a novel tool to study autocrine/paracrine regulatory loops of human trophoblast subpopulations--TNF-alpha stimulates MMP15 expression. *BMC Dev. Biol.* 2007, *7*, 137.

180. Straszewski-Chavez, S.L.; Abrahams, V.M.; Alvero, A.B.; Aldo, P.B.; Ma, Y.; Guller, S.; Romero, R.; Mor, G. The isolation and characterization of a novel telomerase immortalized first trimester trophoblast cell line, Swan 71. *Placenta* 2009, *30*, 939–948.

181. Chen, D.; Zheng, J. Regulation of Placental Angiogenesis. *Microcirc. N. Y. N 1994* 2014, *21*, 15–25.

182. McWhorter, E.S.; West, R.C.; Russ, J.E.; Ali, A.; Winger, Q.A.; Bouma, G.J. LIN28B regulates androgen receptor in human trophoblast cells through Let-7c. *Mol. Reprod. Dev.* 2019, *86*, 1086–1093.

183. Nadiminty, N.; Tummala, R.; Lou, W.; Zhu, Y.; Zhang, J.; Chen, X.; eVere White, R.W.; Kung, H.-J.; Evans, C.P.; Gao, A.C. MicroRNA let-7c suppresses androgen receptor expression and activity via regulation of Myc expression in prostate cancer cells. *J. Biol. Chem.* 2012, *287*, 1527–1537.

184. Ding, M.; Jiang, C.-Y.; Zhang, Y.; Zhao, J.; Han, B.-M.; Xia, S.-J. SIRT7 depletion inhibits cell proliferation and androgen-induced autophagy by suppressing the AR signaling in prostate cancer. *J. Exp. Clin. Cancer Res.* 2020, *39*, 28.

185. Schiewer, M.J.; Augello, M.A.; Knudsen, K.E. The AR dependent cell cycle: Mechanisms and cancer relevance. *Mol. Cell. Endocrinol.* 2012, *352*, 34–45.

186. Guan, Z.; Li, C.; Fan, J.; He, D.; Li, L. Androgen receptor (AR) signaling promotes RCC progression via increased endothelial cell proliferation and recruitment by modulating AKT → NF-κB → CXCL5 signaling. *Sci. Rep.* 2016, *6*, 1–11.

187. Cleys, E.R.; Halleran, J.L.; Enriquez, V.A.; da Silveira, J.C.; West, R.C.; Winger, Q.A.; Anthony, R.V.; Bruemmer, J.E.; Clay, C.M.; Bouma, G.J. Androgen receptor and histone lysine demethylases in ovine placenta. *PloS One* 2015, *10*, e0117472.

188. Horie, K.; Takakura, K.; Imai, K.; Liao, S.; Mori, T. Immunohistochemical localization of androgen receptor in the human endometrium, decidua, placenta and pathological conditions of the endometrium. *Hum. Reprod. Oxf. Engl.* 1992, *7*, 1461–1466.

189. Iwamura, M.; Abrahamsson, P.A.; Benning, C.M.; Cockett, A.T.; di Sant'Agnese, P.A. Androgen receptor immunostaining and its tissue distribution in formalin-fixed, paraffin-embedded sections after microwave treatment. *J. Histochem. Cytochem. Off. J. Histochem. Soc.* 1994, *42*, 783–788.

190. Wagner, S.; Ngezahayo, A.; Murua Escobar, H.; Nolte, I. Role of miRNA Let-7 and Its Major Targets in Prostate Cancer Available online: https://www.hindawi.com/journals/bmri/2014/376326/ (accessed on Apr 3, 2020).

191. Madison, B.B.; Jeganathan, A.N.; Mizuno, R.; Winslow, M.M.; Castells, A.; Cuatrecasas, M.; Rustgi, A.K. Let-7 Represses Carcinogenesis and a Stem Cell Phenotype in the Intestine via Regulation of Hmga2. *PLOS Genet.* 2015, *11*, e1005408.

192. Lee, Y.S.; Dutta, A. The tumor suppressor microRNA let-7 represses the HMGA2 oncogene. *Genes Dev.* 2007, *21*, 1025–1030.

193. Ali, A.; Stenglein, M.D.; Spencer, T.E.; Bouma, G.J.; Anthony, R.V.; Winger, Q.A. Trophectoderm-Specific Knockdown of LIN28 Decreases Expression of Genes Necessary for Cell Proliferation and Reduces Elongation of Sheep Conceptus. *Int. J. Mol. Sci.* 2020, *21*, 2549.

194. Wilsker, D.; Patsialou, A.; Dallas, P.B.; Moran, E. ARID proteins: a diverse family of DNA binding proteins implicated in the control of cell growth, differentiation, and development. *Cell Growth Differ. Mol. Biol. J. Am. Assoc. Cancer Res.* 2002, *13*, 95–106.

195. Lin, C.; Song, W.; Bi, X.; Zhao, J.; Huang, Z.; Li, Z.; Zhou, J.; Cai, J.; Zhao, H. Recent advances in the ARID family: focusing on roles in human cancer. *OncoTargets Ther.* 2014, *7*, 315–324.

196. Fukuyo, Y.; Takahashi, A.; Hara, E.; Horikoshi, N.; Pandita, T.K.; Nakajima, T. E2FBP1 antagonizes the p16(INK4A)-Rb tumor suppressor machinery for growth suppression and cellular senescence by regulating promyelocytic leukemia protein stability. *Int. J. Oral Sci.* 2011, *3*, 200–208.

197. Fukuyo, Y.; Mogi, K.; Tsunematsu, Y.; Nakajima, T. E2FBP1/hDril1 modulates cell growth through downregulation of promyelocytic leukemia bodies. *Cell Death Differ.* 2004, *11*, 747–759.

198. Kobayashi, K.; Jakt, L.M.; Nishikawa, S.-I. Epigenetic regulation of the neuroblastoma genes, Arid3b and Mycn. *Oncogene* 2013, *32*, 2640–2648.

199. Bobbs, A.; Gellerman, K.; Hallas, W.M.; Joseph, S.; Yang, C.; Kurkewich, J.; Cowden Dahl, K.D. ARID3B Directly Regulates Ovarian Cancer Promoting Genes. *PloS One* 2015, *10*, e0131961.

200. Nakahara, S.; Fukushima, S.; Yamashita, J.; Kubo, Y.; Tokuzumi, A.; Miyashita, A.; Harada, M.; Nakamura, K.; Jinnin, M.; Ihn, H. AT-rich Interaction Domain-containing Protein 3B is a New Tumour Marker for Melanoma. *Acta Derm. Venereol.* 2017, *97*, 112–114.

201. Wilsker, D.; Patsialou, A.; Dallas, P.B.; Moran, E. ARID proteins: a diverse family of DNA binding proteins implicated in the control of cell growth, differentiation, and development. *Cell Growth Differ. Mol. Biol. J. Am. Assoc. Cancer Res.* 2002, *13*, 95–106.

202. Kim, D.; Probst, L.; Das, C.; Tucker, P.W. REKLES Is an ARID3-restricted Multifunctional Domain. *J. Biol. Chem.* 2007, *282*, 15768–15777.

203. Webb, C.F.; Bryant, J.; Popowski, M.; Allred, L.; Kim, D.; Harriss, J.; Schmidt, C.; Miner, C.A.; Rose, K.; Cheng, H.-L.; et al. The ARID family transcription factor bright is required

for both hematopoietic stem cell and B lineage development. *Mol. Cell. Biol.* 2011, *31*, 1041–1053.

204. Liao, T.-T.; Hsu, W.-H.; Ho, C.-H.; Hwang, W.-L.; Lan, H.-Y.; Lo, T.; Chang, C.-C.; Tai, S.-K.; Yang, M.-H. let-7 Modulates Chromatin Configuration and Target Gene Repression through Regulation of the ARID3B Complex. *Cell Rep.* 2016, *14*, 520–533.

205. Uhlen, M.; Oksvold, P.; Fagerberg, L.; Lundberg, E.; Jonasson, K.; Forsberg, M.; Zwahlen, M.; Kampf, C.; Wester, K.; Hober, S.; et al. Towards a knowledge-based Human Protein Atlas. *Nat. Biotechnol.* 2010, *28*, 1248–1250.

206. Rhee, C.; Lee, B.-K.; Beck, S.; Anjum, A.; Cook, K.R.; Popowski, M.; Tucker, H.O.; Kim, J. Arid3a is essential to execution of the first cell fate decision via direct embryonic and extraembryonic transcriptional regulation. *Genes Dev.* 2014, *28*, 2219–2232.

207. Rhee, C.; Edwards, M.; Dang, C.; Harris, J.; Brown, M.; Kim, J.; Tucker, H.O. ARID3A is required for mammalian placenta development. *Dev. Biol.* 2017, *422*, 83–91.

CHAPTER II: LIN28-LET-7 AXIS REGULATES GENES IN IMMORTALIZED HUMAN TROPHOBLAST CELLS BY TARGETING THE ARID3B-COMPLEX[2,3]

Synopsis

Abnormal placental development is one of the main etiological factors for intrauterine growth restriction (IUGR). Here, we show that LIN28A and LIN28B are significantly lower and lethal-7 (let-7) microRNAs (miRNAs) significantly higher in term human IUGR vs. normal placentas. We hypothesize that let-7 miRNAs regulate genes with known importance for human placental development [high-mobility group AT-hook 1 (HMGA1), transcriptional regulator Myc-like (c-myc), vascular endothelial growth factor A (VEGF-A), and Wnt family member 1 (WNT1)] by targeting the AT-rich interacting domain (ARID)-3B complex. ACH-3P cells with LIN28A and LIN28B knockout (DKOs) significantly increased let-7miRNAs, leading to significantly decreased ARID3A, ARID3B, and lysine demethylase 4C (KDM4C). Similarly, Sw.71 cells overexpressing LIN28A and LIN28B (DKIs) significantly decreased let-7 miRNAs, leading to significantly increased ARID3A, ARID3B, and KDM4C. In ACH-3P cells, ARID3A, ARID3B, and KDM4C make a triprotein complex [triprotein complex comprising ARID3A, ARID3B, and KDM4C (ARID3B-complex)] that binds the promoter regions of HMGA1, c-MYC, VEGF-A, and WNT1. ARID3B knockout in ACH-3P cells disrupted the ARID3B-complex, leading to a significant decrease in HMGA1, c-MYC, VEGF-A, and WNT1. DKOs had a significant reduction, whereas DKIs had a significant increase in HMGA1, c-MYC, VEGF-A, andWNT1, potentially

[2] This chapter has been published in the FASEB Journal.

[3] List of authors: Asghar Ali, Russell V Anthony, Gerrit J Bouma, Quinton A Winger

due to regulation by theARID3B-complex. This is the first study showing regulation of let-7 targets in immortalized human trophoblast cells by the ARID3B-complex.

1. Introduction

Intrauterine growth restriction (IUGR) is a pregnancy associated condition in which the fetuses cannot reach their maximum growth potential. Every year, about 30 million neonates in the world are born intrauterine growth restricted (1, 2). Although there are many risk factors for development of IUGR, placenta associated conditions such as abnormal uteroplacental vasculature, preeclampsia, avascular villi, single umbilical artery, placental insufficiency, abruptio placenta and placental infections are the most common etiological factors (3–5). In pregnancies compromised by IUGR, the size of the placenta is approximately 24% smaller compared to placenta from normal pregnancies (6). A malfunctioning placenta fails to supply enough nutrients and oxygen to the growing fetus leading to IUGR and other long-term complications in both mother and fetus (7, 8). Hence, healthy and properly functioning placenta is essential for normal fetal growth.

During the first trimester of human pregnancy, fetal derived trophoblast cells proliferate and differentiate into different trophoblast lineages; syncytiotrophoblast and extravillous trophoblast cells (9). The extravillous trophoblast cells invade the maternal uterus and remodel the spiral arteries to ensure proper blood flow to the growing fetus (9). These events are regulated through complex genetic pathways. If any of these steps are compromised, it can result in placental disorders leading to IUGR (10). Therefore, investigating the underlying molecular mechanisms of trophoblast proliferation, invasion and migration, and spiral artery remodeling is necessary to improve diagnosis and treatment of various pregnancy-related disorders.

Oncofetal-placental proteins play a significant role in placental development and maintenance (11). The pluripotency factor LIN28 is a highly conserved oncofetal-placental protein with two paralogs, LIN28A and LIN28B. LIN28 has also been described as a protooncogene due to its ability to regulate and stabilize oncogenes at the post-transcriptional level in tumor cells (12, 13). Another important function of LIN28 is to inhibit the biogenesis of lethal-7 (let-7) miRNAs in mammalian cells by binding pri-let-7 and pre-let-7 (14–19). We have previously shown that in first trimester (11.5 week) human placenta LIN28B is dominant and is localized to cytotrophoblast cells (20). In another study, Canfield (21) showed that in term human placenta LIN28B mRNA is 1300-fold higher than LIN28A mRNA and LIN28B protein level is significantly higher in both cytotrophoblasts and syncytiotrophoblast compared to decidua. Knockdown of LIN28 in mouse and human trophoblast cells increases the level of let-7 miRNAs (20, 22).

Liao (23) demonstrated that let-7 miRNAs modulate their target genes in cancer cells by two distinct mechanisms. Either they follow a pathway of directly binding the mRNAs of target genes, or they follow a chromatin-dependent pathway involving 4 different proteins; AT-Rich Interaction Domain 3A (ARID3A), AT-Rich Interaction Domain 3B (ARID3B), lysine demethylase 4C (KDM4C) and membrane transporter importin-9 (IPO9) (23). ARID3A and ARID3B are members of the highly conserved family of AT-rich Interactive Domain (ARID) proteins which regulate gene expression by binding AT-rich DNA in promoter regions of genes and remodeling the chromatin material (24, 25). These two paralogs share 89.9% amino acid similarity and bind the same DNA regions (26). ARID3A and ARID3B function together and play a vital role in lymphocyte expansion, proliferation of human hematopoietic progenitors, development of colorectal cancer, cell cycle, embryonic development and transcriptional regulation of stemness genes (27–31). Arid3a has also been shown to play an important role in

development of murine placenta. Arid3a knockout results in abnormal placental development and embryonic lethality at day 12.5 (32). Knockout of Arid3b in mice causes developmental abnormalities and is embryonic lethal (32–34). In humans, ARID3B is high in malignant tumor tissues compared to control tissues, suggesting a role in cell proliferation and migration (34). ARID3B is exclusively localized in the nucleus while ARID3A is shuttled between the cytoplasm and nucleus by the membrane transporter IPO9 (23, 36, 37). In the nucleus, ARID3B binds ARID3A by interacting with its REKLES-β domain (23, 37). ARID3A-ARID3B duplex binds KDM4C to make a tri-protein complex, hereafter referred as the ARID3B-complex, which binds the promoter regions of genes and demethylates H3K9me3 and H3K27me3 (23). Histone demethylation caused by KDM4C leads to structural modifications in chromatin, resulting in increased expression of target genes (23). Let-7 miRNAs regulate their target genes in different cancer cell lines by targeting the ARID3B-complex mRNAs (23). However, existence and functionality of this pathway in placenta is yet to be explored.

Many core targets of let-7 miRNAs identified in cancer studies also play a critical role in early human placental development, and are important for rapid proliferation of trophoblast cells, maintaining a population of progenitor cytotrophoblasts, placental angiogenesis and modification of spiral arteries (38–42). High mobility group AT-hook 1 (HMGA1), transcriptional regulator Myc-like (c-MYC), vascular endothelial growth factor A (VEGF-A) and Wnt family member 1 (WNT1) are examples of such genes. HMGA1 promotes the invasion of trophoblast cells and reduced levels of HMGA1 has been linked to pathogenesis of preeclampsia (43, 44). The c-MYC protooncogene has been identified as a proliferation factor in human cytotrophoblast cells. Its amount decreases when cytotrophoblasts differentiate into syncytiotrophoblast (45). VEGF-A plays a critical role in human trophoblast migration and differentiation, spiral artery remodeling

and placental angiogenesis (46–49). Reduced concentration of VEGF-A is one of the factors in the pathogenesis of preeclampsia and IUGR (50). The protooncogene WNT1 is highly expressed in early placenta compared to term placenta. It is important for proliferation of trophoblast cells and reduced WNT1 is also one of the factors in the pathogenesis of preeclampsia (51, 52). Hence, HMGA1, c-MYC, VEGF-A and WNT1 are important for placental development and exploring the mechanisms behind the regulation of these genes will be a step towards diagnosis and management of placenta associated disorders. The objective of this study is to explore the mechanism for regulation of HMGA1, c-MYC, VEGF-A and WNT1 by the ARID3B-complex and its correlation with LIN28-let7 axis in immortalized first trimester human trophoblast cells.

2. Materials and Methods

2.1.Term human placental tissue samples

Term human placental tissue samples and the clinical characteristics of the patients used in this study have been described previously (53). Briefly, term placentas from normal pregnancies (control) and the IUGR pregnancies were collected immediately postpartum. The collected tissue samples were snap frozen in liquid nitrogen and then stored at -80˚C. mRNA, miRNA and protein were extracted from these samples for further analysis.

2.2.Cell lines

Two different first trimester human trophoblast cell lines, ACH-3P and Sw.71, were used in this study. ACH-3P cells are hybrid cells obtained by fusion of primary first trimester human trophoblast cells (week 12 of gestation) with a human choriocarcinoma cell line (AC1-1) (54). Sw.71 are immortalized first trimester human trophoblast cells (week 7 of gestation) produced by infecting primary trophoblast cells with human telomerase reverse transcriptase (hTERT) (55).

Both cell lines were maintained in DMEM/F-12 media supplemented with 10% heat-inactivated fetal bovine serum and 1x penicillin-streptomycin-amphotericin B solution, at 37°C and 5% CO2.

2.3.CRISPR-Cas9

Knockout ACH-3P cells were generated using CRISPR-Cas9 based genome editing technique. Target specific gRNAs for LIN28A, LIN28B and ARID3B were designed using web-based tools (56, 57), and cloned in lentiCRISPR v2 plasmid. The lentiCRISPR v2 plasmids (Addgene, Watertown, MA, USA) with specific gRNAs were used to make 2nd generation lentiviral particles. The lentiviral particles were used to infect the ACH-3P cells at 70-80% confluency in one well of 12-well plate (Corning Inc., Corning, NY, USA). After 48-72 hours, the infected cells were selected using 2-4 ng/µl puromycin. Western blot was performed to confirm gene knockout. To obtain cell lines with complete knockout of the target gene, single cell colonies were selected. Colonies with depletion of protein of interest were used for further experiments. ACH-3P cells with knockout of LIN28A (AKO), LIN28B (BKO), both LIN28A and LIN28B (DKO), and ARID3B (ARID3B KO) were generated. To create DKO ACH-3P cells, AKO ACH-3P cells were infected with lentiviral particles designed for knockout of LIN28B. Single cell colonies were selected and tested by western blot to confirm a double knockout of LIN28A and LIN28B. ACH-3P cells infected with lentiviral particles containing scrambled gRNA were used as control cells (SC). The gRNA sequences used in this study are listed in table 2.

2.4.Overexpression of LIN28A and LIN28B

To overexpress genes in Sw.71 cells, lentiviral gene expression vectors expressing LIN28A (pLV[Exp]-Puro-EF1A>hLIN28A[XM_011542148.1]) or LIN28B (pLV[Exp]-Bsd-EF1A>hLIN28B[NM_001004317.3]) were purchased (VectorBuilder Inc., Shenandoah, TX,

USA). Second generation lentiviral particles were generated using expression vectors. Lentiviral particles were used to infect Sw.71 cells at 70-80% confluency in one well of a 12-well plate (Corning Inc., Corning, NY, USA). After 48-72 hours, the infected cells were selected using appropriate antibiotics (2-4 ng/µl puromycin for LIN28A expressing cells and 4-8 ng/µl blasticidin for LIN28B expressing cells). Successful gene knock-in was confirmed using real-time RT-PCR and western blot analysis. Sw.71 cells with knock-in of LIN28A (AKI), LIN28B (BKI), and both LIN28A and LIN28B (DKI) were generated. To create DKI Sw.71 cells, LIN28A overexpressing cells were infected with LIN28B expression lentiviral particles. Sw.71 cells infected with lentiviral expression particles containing stuffer nucleotide sequence were used to generate an expression vector control (EVC) Sw.71 cells.

2.5.Production of 2nd generation lentiviral particles

To generate 2nd generation lentiviral particles, three vectors were used including transfer vector (lentiCRISPR v2 or expression vector), packaging plasmid (psPAX2 from Addgene, Watertown, MA, USA) and envelope plasmid (pMD2.G from Addgene, Watertown, MA, USA). 293FT cells (Invitrogen, Carlsbad, CA, USA) were cultured in DMEM high-glucose media supplemented with 10% heat-inactivated fetal bovine serum and 1x penicillin-streptomycin-amphotericin B solution, at 37°C and 5% CO2. 8.82 µg transfer vector DNA, 6.66 µg psPAX2 packaging plasmid DNA and 2.70 µg pMD2.G envelope plasmid DNA were used to make viral particles. The plasmid DNA was mixed with 180 µl of polyfect transfection reagent (Qiagen Inc., Germantown, MD, USA) and final volume was brought up to 855 µl using DMEM high-glucose media without any supplements. The plasmids-polyfect mixture was incubated at room temperature for 10 min and then gently mixed in the media on 70-80 % confluent 293FT cells. Cells were incubated for 4–6 h at 37°C and 5% CO2. After incubation time, the transfection media

was replaced by fresh DMEM high glucose media supplemented with 10% heat-inactivated fetal bovine serum and 1x penicillin-streptomycin-amphotericin B solution. After 72 h, the medium containing lentiviral particles was collected and ultra-centrifuged over a 20% sucrose cushion at 22,000 RPM for 2 h at 4°C. The pelleted lentiviral particles were resuspended in 1x PBS, aliquoted and stored at −80°C. The frozen viral aliquot was resuspended in 0.5-1 ml of appropriate media with 8 µg/ml polybrene. The target cells were incubated with lentiviral particles for 24 h, at 37˚C and 5% CO2. After 24 h of incubation, targeted cells were washed, and fresh media was put on the cells. After 72 h of culture, cells were selected with appropriate selection antibiotic as described earlier.

2.6.RNA extraction and real-time RT-PCR

For real-time RT-PCR analysis, mRNA was isolated from human placental tissue and immortalized first trimester human trophoblast cells using RNeasy Mini Kit (Qiagen Inc. Germantown, MD, USA), following the manufacturer's protocol. The mRNA was reverse transcribed to cDNA using iScript cDNA synthesis kit (Bio-Rad Laboratories, Hercules, CA, USA). Real-time RT-PCR reactions were run in triplicate in 384-well plates, using 10µl reaction volume in each well. The reaction volume included 5µl of 2x Light-Cycler 480 SYBR Green I Master (Roche Applied Science, Penzberg, Germany), 50ng cDNA and 1µM of target specific forward and reverse primers. Primer sequences used for real-time RTPCR are listed in table 3. PCR reactions were incubated in the Light-Cycler 480 PCR machine (Roche Applied Science, Penzberg, Germany) at the following cycling conditions: 95˚C for 10 min, 45 cycles of 95˚C for 30 seconds, 55˚C for 1 minute, and 72˚C for 1 min. Relative mRNA levels were normalized using GAPDH. For miRNA profiling, total RNA was extracted using a miRNeasy Mini Kit (Qiagen Inc. Germantown, MD, USA), following the manufacturer's protocol. 300 ng total RNA was reverse

transcribed to cDNA using miScript RT II kit (Qiagen Inc. Germantown, MD, USA). Real-time RT-PCR reactions were run in triplicate in 384-well plates, using 10µl reaction volume in each well. The reaction volume included 5µl of 2x QuantiTech SYBR Green Master Mix (Qiagen Inc. Germantown, MD, USA), 3ng cDNA, 1x miScript universal primer (Qiagen Inc. Germantown, MD, USA) and 1x miScript assay for let-7 miRNA (let-7a, let-7b, let-7c, let-7d, let-7e, let-7f, let-7g, let-7i). These reactions were incubated in the Light-Cycler 480 PCR machine (Roche Applied Science, Penzberg, Germany) at following cycling conditions: 95˚C for 15 minutes, 45 cycles of 94˚C for 15 seconds, 55˚C for 30 seconds, and 70˚C for 30 seconds. Relative miRNA levels were normalized using SNORD-48.

2.7.Protein Extraction and Western Blot

Western blot analysis was performed using whole cell lysate to quantify proteins in cells and tissue samples. For protein extraction, cell pellets were resuspended in 200-400 µl RIPA buffer (20 mM Tris, 137 mM NaCl, 10% glycerol, 1% nonidet P-40, 3.5 mM SDS, 1.2 mM sodium deoxycholate, 1.6 mM EDTA, pH 8) containing 1x protease/phosphate inhibitor cocktail (Sigma-Aldrich, St. Louis, MO, USA). Whole cell lysate was incubated on ice for 5 min and then centrifuged at 14,000 g for 5 min to remove cell debris. To extract protein from human placental tissues, the tissue was dipped in liquid nitrogen and ground using mortar and pestle, and then homogenized in RIPA buffer. Homogenized samples were sonicated using a Bioruptor Sonication System (Diagenode, Denville, NJ, USA) for 5 cycles of 30 seconds “ON” and 30 seconds “OFF”. Sonicated samples were centrifuged at 14,000 g for 5 minutes to remove debris. Protein concentration was measured using the BCA protein assay kit (ThermoFisher, Waltham, MA, USA). Protein was separated in 10% Bis-Tris gels (Bio-Rad Laboratories, Hercules, CA, USA) at 90 volts for 15 min and 125 volts for 60 min, and then transferred to 0.45 µm pore size

nitrocellulose membrane (Bio-Rad Laboratories, Hercules, CA, USA) at 100 volts for 2 hours at 4°C. The membranes were then blocked in 5% non-fat dry milk solution in TBST (50 mM Tris, 150 mM NaCl, 0.05% Tween 20, pH 7.6) for 1 hour at room temperature. After blocking, the membranes were washed 3 times with 1x TBST for 5 min each, and then incubated at 4°C overnight with specific primary antibody. After overnight incubation, the membranes were washed 3 times with 1x TBST for 5 min each. After washing, the membranes were incubated with appropriate secondary antibody conjugated to horseradish peroxidase for 1 hour at room temperature. After removing the secondary antibody, the membranes were washed following the same procedure and developed using Super Signal WestDura Extended Duration Substrate (ThermoFisher, Waltham, MA, USA) and imaged using ChemiDoc XRS+ chemiluminescence system (Bio-Rad Laboratories, Hercules, CA, USA). The images were quantified using Image-Lab software (Bio-Rad Laboratories, Hercules, CA, USA). To normalize protein quantity, β-actin, α-tubulin, or GAPDH were used as loading control. Each experiment was repeated on three replicates. The antibodies used and their dilutions are listed in table 4.

2.8.Co-immunoprecipitation

Proteins were extracted from cells following the same procedure used for western blotting. Protein-G magnetic beads (Bio-Rad Laboratories, Hercules, CA, USA) were used following manufacturer's protocol. Briefly, 100 µl of thoroughly resuspended protein-G magnetic beads were conjugated with 2 µg ARID3A or ARID3B antibody. The antibody conjugated protein-G beads were then incubated with 25-50 µg protein sample. After immunoprecipitation, proteins were eluted using 1x laemmli buffer and used for western blot following the same procedure described earlier. The membranes were probed using ARID3B and KDM4C antibodies to

determine protein-protein interaction. Normal mouse IgG was used as a negative control in this experiment.

2.9.Chromatin Immunoprecipitation

Chromatin immunoprecipitation (ChIP) assay was performed using Magna ChIP G (EMD Millipore Corp., Burlington, MA, USA) following manufacturer's protocol. 70-80% confluent WT ACH-3P cells or ARID3B KO ACH-3P cells were used in this procedure. 550 µl formaldehyde was added in 19 ml media for crosslinking and kept on ice for 10 minutes. Chromatin was extracted from formaldehyde treated cells and sheared to produce 100-1000 bp strands using Bioruptor Sonication System (Diagenode, Denville, NJ, USA). Sonication was done at 4˚C for 20 cycles; 30 seconds "ON" and 30 seconds "OFF". Immunoprecipitation was done using ARID3B or KDM4C antibodies and immunoprecipitated DNA was eluted and used to run end-point PCR for HMGA1, c-MYC, VEGF-A or WNT1 using positive primers designed to amplify the promoter region and negative primers designed to amplify distal enhancer region upstream to the promoter region of specific gene. The primers used in ChIP assay are listed in table 5. ChIP input DNA was used as positive controls for PCR, and sheared chromatin immunoprecipitated by normal Rabbit IgG was used as negative control.

2.10. Cell Proliferation Assay

Cell proliferation was measured using Quick Cell Proliferation Assay Kit (ab65475, Abcam, Cambridge, MA, USA) following manufacturer's protocol. This assay is based on cleavage of tetrazolium salt (WST-1) to formazan by mitochondrial dehydrogenases. SC, LIN28 DKO and ARID3B KO ACH-3P cells were plated to a density of 2500 cells/100 µl in 96-well tissue culture plates, with four replicates of each cell type. After 24 or 48 hours of plating the cells,

10 µl WST-1 reagent was added in each well followed by incubation for 2 hours in standard culture conditions. Absorbance was measured using Cytation 3 Multi-Mode Reader (BioTek Instruments, Inc., VT, USA) at 440 nm with reference wavelength of 650 nm.

2.11. Statistics

All data were analyzed using GraphPad Prism 7 Software. To determine significance of mRNAs and proteins, all values were compared between KI vs ECV Sw.71 cells, KO vs SC ACH-3P cells, and term human placental tissue from IUGR pregnancies vs normal pregnancies using student t-test. Treatment effects on miRNAs expression were determined by analysis of variance followed by Tukey's HSD post-hoc test. P values less than 0.05 were considered statistically significant. The error bars in the figures indicate standard error of the mean (SEM).

3. Results

3.1.LIN28A/B and ARID3A/B in term human placentas from IUGR pregnancies and normal pregnancies

LIN28A and LIN28B were quantified by real-time RT-PCR and western blot in term human placentas from IUGR pregnancies (n=8) and normal pregnancies (n=8). Both LIN28A and LIN28B were significantly reduced in term human placentas from IUGR pregnancies compared to normal pregnancies (Fig. 6A). Densitometric analysis of western blots showed that LIN28A and LIN28B proteins were significantly reduced in term human placentas from IUGR pregnancies compared to normal pregnancies (Fig. 6B). Real-time RT-PCR data showed that let-7 miRNAs (let-7a, let-7b, let-7c, let-7d, let-7e, let-7f, let-7g, let-7i) were significantly higher in term human placentas from IUGR pregnancies compared to normal pregnancies (Fig. 6C). Western blot data showed that ARID3A and ARID3B proteins were also significantly reduced in term human

placentas from IUGR pregnancies compared to normal pregnancies (Fig. 6D). These results suggest that reduced levels of LIN28A and LIN28B in term human placentas from IUGR pregnancies lead to significantly higher levels of let-7 miRNAs which correlates with reduced levels of ARID3A and ARID3B.

3.2.LIN28A, LIN28B, and let-7 miRNAs in immortalized first trimester human trophoblast cell lines

The results from human term placental tissues led us to further investigate the LIN28-let-7 axis and its potential role in early placental development. For this purpose, two first trimester human trophoblast cell lines were used ACH-3P cells and Sw.71 cells. Real-time RT-PCR data showed that LIN28A was about 10,000-fold higher and LIN28B was about 15,000-fold higher in ACH-3P cells compared to Sw.71 cells (Fig. 7A). Western blot data showed prominent bands for both LIN28A and LIN28B in ACH-3P cells and no detectable proteins in Sw.71 cells (Fig. 7B). Real-time RT-PCR analysis revealed that let-7 miRNAs (let-7a, let-7b, let-7c, let-7d, let-7e, let-7f, let-7g, let-7i) were significantly higher in Sw.71 cells compared to ACH-3P cells (Fig. 7C). These results suggest that let-7 miRNAs are low in ACH-3P cells and correspond to high LIN28A and LIN28B, whereas let-7 miRNAs are high in Sw.71 cells and correspond to low LIN28A and LIN28B.

3.3.Knockout of LIN28 in ACH-3P cells

ACH-3P cells had high LIN28A and LIN28B. To see if reduced levels of LIN28A and/or LIN28B would affect let-7 miRNA levels, three knockout cell lines were generated using CRISPR-Cas9 based genome editing; ACH-3P cells with knockout of LIN28A (AKO), ACH-3P cells with knockout of LIN28B (BKO) and ACH-3P cells with knockout of both LIN28A and LIN28B

(DKO). Western blot analysis confirmed that AKO cells had significant depletion of LIN28A, without significant change in LIN28B compared to scramble control (SC) ACH-3P cells (Fig. 8A). BKO cells had significant depletion of LIN28B, without significant change in LIN28A compared to SC (Fig. 8B). In DKO cells, both LIN28A and LIN28B were significantly depleted compared to SC (Fig. 8C). Real-time RT-PCR analysis was done to compare let-7 miRNAs (let-7a, let-7b, let-7c, let-7d, let-7e, let-7f, let-7g, let-7i) between SC, AKO, BKO and DKO ACH-3P cells. AKO ACH-3P cells had significantly higher levels of let-7a, let-7b, let-7c, let-7d and let-7e, and no significant change in levels of let-7d, let-7f and let-7i compared to SC. BKO ACH-3P cells had significantly higher levels of let-7a, let-7b, let-7c, let-7d, let-7e and let-7i, and no change in let-7f and let-7g compared to SC. However, compared to AKO ACH-3P cells, the levels of let-7a, let-7b, let-7c, let-7e and let-7i significantly increased, whereas the levels of let-7d, let-7f and let-7g remained unchanged in BKO ACH-3P cells. DKO ACH-3P cells had significant increase in all let-7 miRNAs (let-7a, let-7b, let-7c, let-7d, let-7e, let-7f, let-7g and let-7i) compared to SC, AKO and BKO ACH-3P cells (Fig. 8D). These results show that knockout of LIN28B affects more let-7 miRNAs than knockout of LIN28A, and DKO ACH-3P cells had the greatest increase in let-7 miRNAs.

3.4.Overexpression of LIN28 in Sw.71 cells

We further assessed the regulation of let-7 miRNAs by LIN28 by overexpressing one or both paralogs of LIN28 in Sw.71 cells which have low expression of LIN28A and LIN28B. For this purpose, three knock-in cell lines were generated; Sw.71 cells overexpressing LIN28A (AKI), Sw.71 cells overexpressing LIN28B (BKI) and Sw.71 cells overexpressing both LIN28A and LIN28B (DKI). Real-time RT-PCR and western blot analysis confirmed that AKI cells had significantly higher LIN28A, and no change in LIN28B compared to expression vector control

(EVC) Sw.71 cells (Fig. 9A). BKI cells had significantly higher LIN28B, and no change in LIN28A compared to EVC (Fig. 9B). DKI cells had significant increase in both LIN28A and LIN28B compared to EVC (Fig. 9C). Real-time RT-PCR analysis was done to compare let-7 miRNAs (let-7a, let-7b, let-7c, let-7d, let-7e, let-7f, let-7g, let-7i) between these cell lines. AKI Sw.71 cells had significant decreased in let-7d and let7i, whereas let-7a, let-7b, let-7c, let-7e, let-7f and let-7g were unchanged compared to EVC. BKI Sw.71 cells had significant decrease in all let-7 miRNAs (let-7a, let-7b, let-7c, let-7d, let-7e, let-7f, let-7g, let-7i) compared to EVC as well as AKI Sw.71 cells. DKI Sw.71 cells had significant reduction in all let-7 miRNAs (let-7a, let-7b, let-7c, let-7d, let-7e, let-7f, let-7g, let-7i) compared to EVC and AKI Sw.71 cells, whereas let-7b, let-7c, let-7d, let-7e, let-7f, let-7g and let-7i significantly increased while let-7a remained unchanged compared to BKI Sw.71 cells (Fig. 9D). These results indicate that overexpression of LIN28B have greater impact on let-7 miRNAs compared to overexpression of LIN28A, whereas overexpression of both LIN28A and LIN28B results in significant reduction in let-7 miRNAs compared to overexpression of LIN28A or LIN28B alone.

3.5.ARID3A, ARID3B and KDM4C in DKO ACH-3P and DKI Sw.71 Cells

To determine if a change in let-7 miRNAs affects the components of chromatin-based gene regulation pathway (ARID3A, ARID3B and KDM4C), the mRNA and protein levels of these genes were analyzed in DKO ACH-3P cells and DKI Sw.71 cells. Real-time RT-PCR and western blot data showed that ARID3A, ARID3B and KDM4C were significantly reduced in DKO ACH-3P cells compared to SC (Fig. 10A-C). These results indicate that elevated let-7 miRNAs correlate with reduced ARID3A, ARID3B and KDM4C in DKO ACH-3P cells. Similarly, real-time RT-PCR and western blot data showed significant increase in ARID3A, ARID3B and KDM4C in DKI

Sw.71 cells compared to EVC (Fig. 11A-C), suggesting that reduced let-7 miRNAs correlate with increased ARID3A, ARID3B and KDM4C in DKI Sw.71 cells.

3.6.ARID3A, ARID3B and KDM4C co-occupy promoter regions in HMGA1, c-MYC, VEGF-A and WNT1

To determine if ARID3A, ARID3B and KDM4C regulate let-7 miRNA target genes with known importance for placental development (HMGA1, c-MYC, VEGF-A and WNT1), co-IP and ChIP assays were performed using ACH-3P cells. Co-IP using ARID3A antibody indicated that ARID3A is complexed with ARID3B and KDM4C in ACH-3P cells (Fig. 12A). Furthermore, co-IP using ARID3B antibody confirmed complex formation between ARID3B and KDM4C in ACH-3P cells (Fig. 12B). These results indicate the existence of ARID3B-complex comprised of ARID3A, ARID3B and KDM4C in ACH-3P cells. ChIP assay confirmed co-occupancy of ARID3B and KDM4C in promoter regions of HMGA1, c-MYC, VEGF-A and WNT1 (Fig. 12C). This data suggests that the ARID3B-complex is involved in regulation of HMGA1, c-MYC, VEGF-A and WNT1 expression by binding their promoter regions in immortalized first trimester human trophoblast cells.

3.7.HMGA1, c-MYC, VEGF-A and WNT1 in ARID3B KO ACH-3P cells

To test the role of ARID3B-complex in regulation of HMGA1, c-MYC, VEGF-A and WNT1 in immortalized first trimester human trophoblast cells, this complex was disrupted by knocking out ARID3B in ACH-3P using CRISPR-Cas9 based genome editing. Western blot analysis confirmed significant depletion of ARID3B in ARID3B KO ACH-3P cells compared to SC (Fig. 13A). ChIP assay performed using KDM4C antibody revealed that KDM4C could not bind to the promoter regions of HMGA1, c-MYC, VEGF-A and WNT1 in ARID3B KO ACH-3P

cells (Fig. 13B). This data confirms that KDM4C binds the promoter regions of HMGA1, c-MYC, VEGF-A and WNT1 only in presence of ARID3B. Because KDM4C could not bind the promoter regions of HMGA1, c-MYC, VEGF-A and WNT1 in ARID3B KO ACH-3P cells, we determined its effect on the expression of these genes. Real-time RT-PCR and western blot analysis showed a significant reduction in HMGA1, c-MYC, VEGF-A and WNT1 in ARID3B KO ACH-3P cells compared to SC (Fig. 14A-D), indicating that the disruption of ARID3B-complex is correlated with reduction in HMGA1, c-MYC, VEGF-A and WNT1 in ACH-3P cells.

3.8.HMGA1, c-MYC, VEGF-A and WNT1 in DKO ACH-3P cells and DKI Sw.71 cells

ARID3B-complex regulates HMGA1, c-MYC, VEGF-A and WNT1, and because levels of ARID3A, ARID3B and KDM4C decreased in LIN28 DKO ACH-3P cells and increased in DKI Sw.71 cells, we measured the levels of HMGA1, c-MYC, VEGF-A and WNT1 in these cells. Real-time RT-PCR and western blot data revealed that HMGA1, c-MYC, VEGF-A and WNT1 were significantly reduced in DKO ACH-3P cells compared to SC (Fig. 15A-D) and significantly increased in DKI Sw.71 cells compared to EVC (Fig. 16A-D). These results suggest that HMGA1, c-MYC, VEGF-A and WNT1 are regulated by the ARID3B-complex and let-7 miRNAs.

3.9.Proliferation of LIN28 DKO and ARID3B KO ACH-3P cells

To determine the effect of LIN28 DKO or ARID3B KO on the functionality of ACH-3P cells, proliferation was measured after 24 h and 48 h. Proliferation of LIN28 DKO and ARID3B KO ACH-3P cells was significantly reduced compared to SC (Fig. 17).

4. Discussion

The pluripotency factors LIN28A and LIN28B have both been detected in human placenta, and potentially regulate trophoblast cell proliferation (20, 21). The LIN28 proteins are known to

inhibit the maturation of let-7 miRNAs, which regulate expression of many genes post-transcriptionally by binding their mRNAs. According to a recent study, LIN28B is the predominant LIN28 paralog and is significantly reduced in term human placentas from pregnancies with preeclampsia without IUGR compared to placentas from normal pregnancies, while there was no change in LIN28A (21). They further reported that there was no change in the level of let-7g miRNAs, which may suggest a compensatory role of LIN28A, however they did not report levels of other let-7 miRNAs (21). In this study, we compared levels of LIN28 and let-7 miRNAs in term human placentas from IUGR pregnancies vs normal pregnancies. The results showed that both LIN28A and LIN28B were significantly reduced and levels of let-7 miRNAs were significantly increased in placentas from IUGR pregnancies. Let-7 miRNAs target genes with known importance for placental development, including ARID3A and ARID3B. Understanding gene regulation by the LIN28-let-7 axis in human placenta during the first trimester of pregnancy can provide more insight about its role in placental growth and placenta associated disorders.

Although both ACH-3P and Sw.71 cells are immortalized first trimester human trophoblast cell lines, they were created using different methods. ACH-3P cells were obtained by fusion of primary first trimester human trophoblast cells (week 12 of gestation) with a human choriocarcinoma cell line (AC1-1) (54). Sw.71 cells are immortalized first trimester human trophoblast cells (week 7 of gestation) produced by expressing human telomerase reverse transcriptase (hTERT) in primary trophoblast cells (55). We compared the expression of LIN28 and let-7 miRNAs in these cell lines. Surprisingly, ACH-3P cells have higher LIN28A and LIN28B, and lower let-7 miRNAs compared to Sw.71 cells. The contrasting level of LIN28 and let-7 miRNAs in these cells is interesting and suggests a potential difference in let-7 gene regulation in these different cell lines. The detection of let-7 miRNA target genes HMGA1, c-

MYC, VEGF-A and WNT1 protein by western blot was lower in Sw.71 compared to ACH-3P cells suggesting targeting of mRNA by let-7 miRNA. Knockout of LIN28 in ACH-3P cells lead to a significant increase in levels of let-7 miRNAs and a significant reduction in HMGA1, c-MYC, VEGF-A and WNT1 compared to SC. Similarly, overexpression of LIN28 in Sw.71 cells lead to a significant decrease in levels of let-7 miRNAs and significant increase in HMGA1, c-MYC, VEGF-A and WNT1 compared to EVC. These results suggest that let-7 miRNAs target genes in immortalized first trimester human trophoblast cells and are important regulators of gene expression during placental development.

In cancer cells the ARID3B-complex binds the promoter regions of genes and regulates their expression through the histone demethylation action of KDM4C (23). Although HMGA1, c-MYC, VEGF-A and WNT1 have been shown as targets of let-7 miRNAs, this is the first study describing regulation of these genes through the ARID3B-complex in immortalized first trimester human trophoblast cell lines. Co-IP data confirmed complex formation between ARID3A, ARID3B and KDM4C in ACH-3P cells, and ChIP assay showed that the ARID3B-complex binds the promoter regions of HMGA1, c-MYC, VEGF-A and WNT1. ChIP using ARID3B knockout ACH-3P cells showed that with the loss of ARID3B, KDM4C could no longer bind the promoter regions of HMGA1, c-MYC, VEGF-A and WNT1 suggesting that ARID3B complex formation is required for binding of KDM4C to the promoter regions of these genes. This inability of KDM4C to bind to the promoter region and produce histone demethylation potentially resulted in the significant reduction in levels of HMGA1, c-MYC, VEGF-A and WNT1 detected in ARID3B KO ACH-3P cells. Although the ARID3B-complex is important for activation of HMGA1, c-MYC, VEGF-A and WNT1, the presence of low levels of HMGA1, c-MYC, VEGF-A and WNT1 in

ARID3B KO ACH-3P cells indicates the potential involvement of other pathways in the regulation of these genes (Fig. 18).

To our knowledge, the LIN28-let-7-ARID3B pathway has not previously been described as a mechanism for gene regulation in immortalized first trimester human trophoblast cells. Knockout of LIN28A and LIN28B in ACH-3P cells not only significantly increased amounts of let-7 miRNAs but also led to significant reduction in ARID3B-complex proteins potentially due to increased targeting by let-7 miRNAs. Hence, significant reduction in HMGA1, c-MYC, VEGF-A and WNT1 in DKO ACH-3P cells can be both due to increased targeting of their mRNAs by let-7 miRNAs and reduced activation of these genes by the ARID3B-complex. Similarly, overexpression of LIN28A and LIN28B in Sw.71 cells not only significantly reduced the levels of let-7 miRNAs but also increased the expression of ARID3B-complex proteins. Significant increase in HMGA1, c-MYC, VEGF-A and WNT1 in DKI Sw.71 cells could be due to less targeting of their mRNAs by let-7 miRNAs and increased activation of these genes by the ARID3B-complex.

During early placental development in humans, a reserve of progenitor cytotrophoblast cells is maintained while these cells differentiate to different lineages. Complex molecular mechanisms are involved in maintaining this balance, many of which are yet to be explored. This study not only extends the understanding of LIN28-let-7 axis in immortalized first trimester human trophoblast cells, but also highlights the importance of the ARID3B-complex in regulation of genes with known roles in placental health and disease. Rapidly proliferating cytotrophoblast cells play a critical role in placental development. Our results showed that knockout of LIN28A/B or ARID3B significantly reduced HMGA1, c-MYC, VEGF-A and WNT1 and decreased proliferation of immortalized first trimester human trophoblast cells. We suggest that decreased expression of LIN28A/B or ARID3A/B in human placenta can result in reduced proliferation of

progenitor cytotrophoblast cells, potentially leading to development of IUGR. Further studies need to be done to explore other genes regulated by let-7 miRNAs and the role of ARID3B-complex in regulation of non-let-7 target genes in placenta.

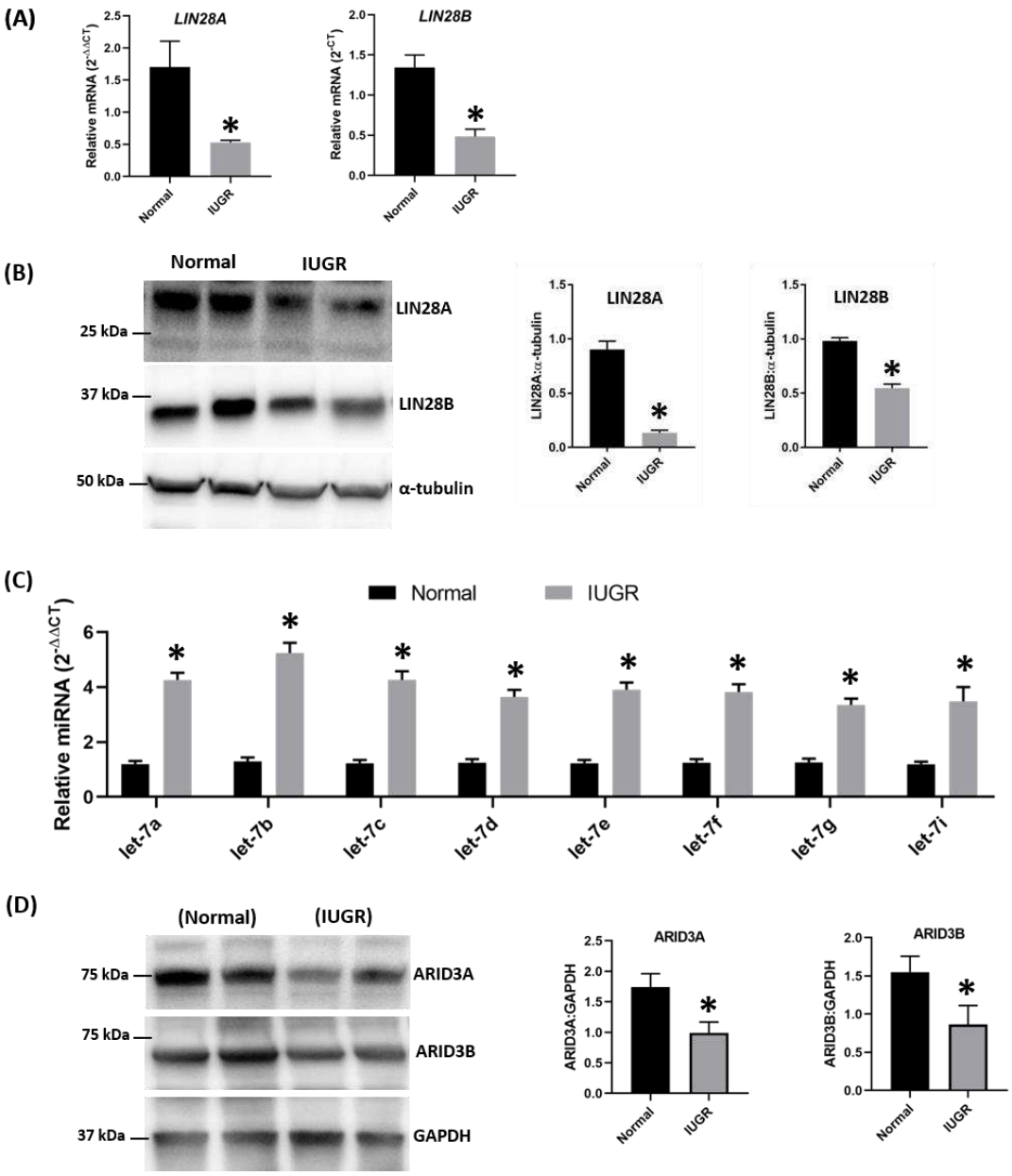

Figure 6. LIN28A, LIN28B and let-7 miRNAs in term human placentas from IUGR pregnancies and normal pregnancies. (A) LIN28A and LIN28B in term human placentas from IUGR pregnancies (n=8) compared to normal pregnancies (n=8). (B) Representative immunoblots for LIN28A, LIN28B and α-tubulin, and densitometric analysis of immunoblotting results for LIN28A and LIN28B in term human placentas from IUGR pregnancies (n=8) compared to normal pregnancies (n=8). (C) Let-7 miRNAs in term human placentas from IUGR pregnancies (n=8) compared to normal pregnancies (n=8). (D) Representative immunoblots for ARID3A, ARID3B and GAPDH, and densitometric analysis of immunoblotting results for ARID3A and ARID3B in term human placentas from IUGR pregnancies (n=6) compared to normal pregnancies (n=6). *P<0.05 vs. normal placentas.

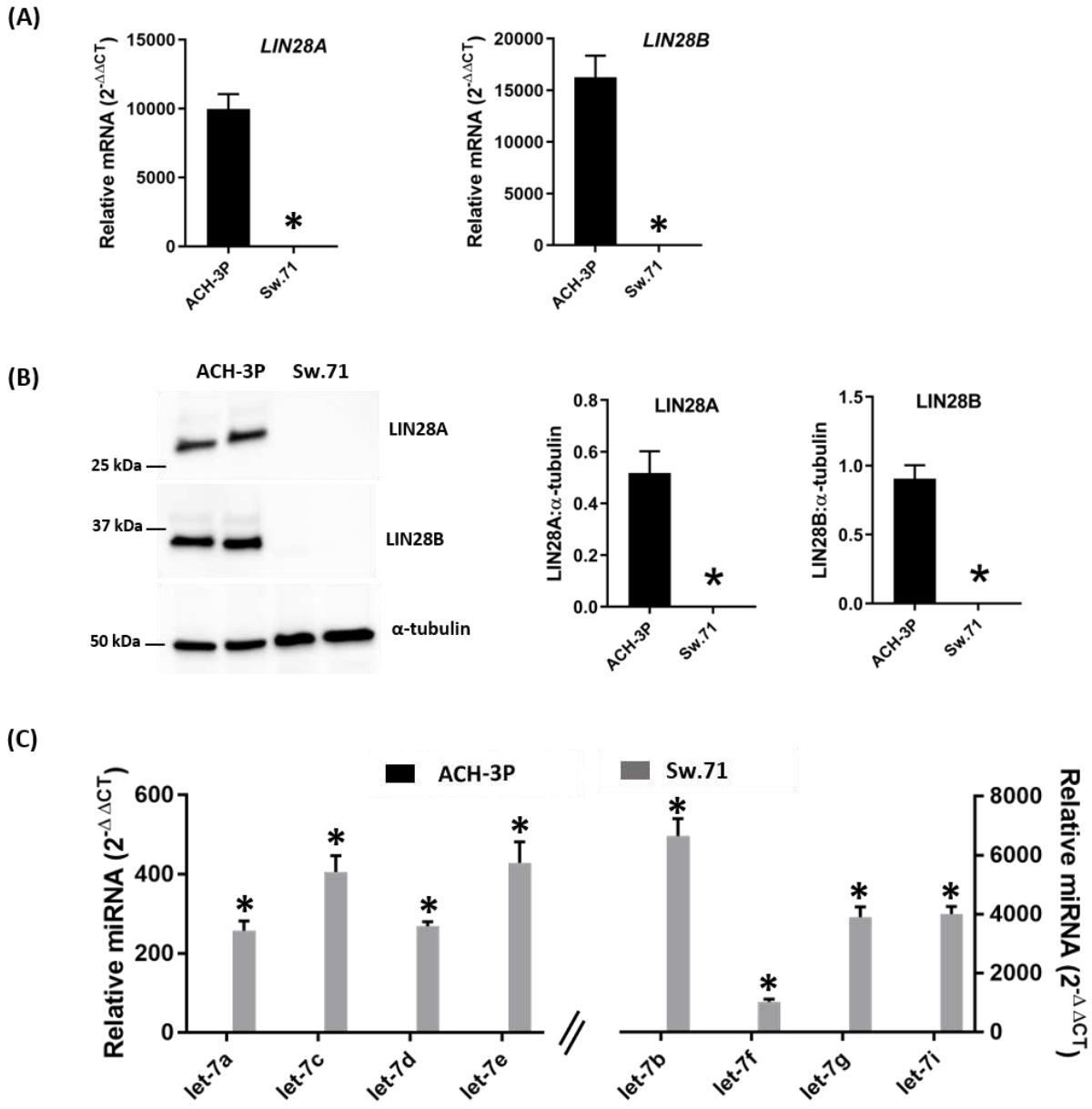

Figure 7. LIN28A, LIN28B and let-7 miRNAs in ACH-3P cells and Sw.71 cells. (A) LIN28A and LIN28B mRNA levels in ACH-3P cells compared to Sw.71 cells (n=3). (B) Representative immunoblots for LIN28A, LIN28B and α-tubulin, and densitometric analysis of immunoblotting results for LIN28A and LIN28B in ACH-3P cells compared to Sw.71 cells (n=3). (C) Let-7 miRNAs in ACH-3P cells compared to Sw.71 cells (n=3). *P<0.05 vs. ACH-3P cells.

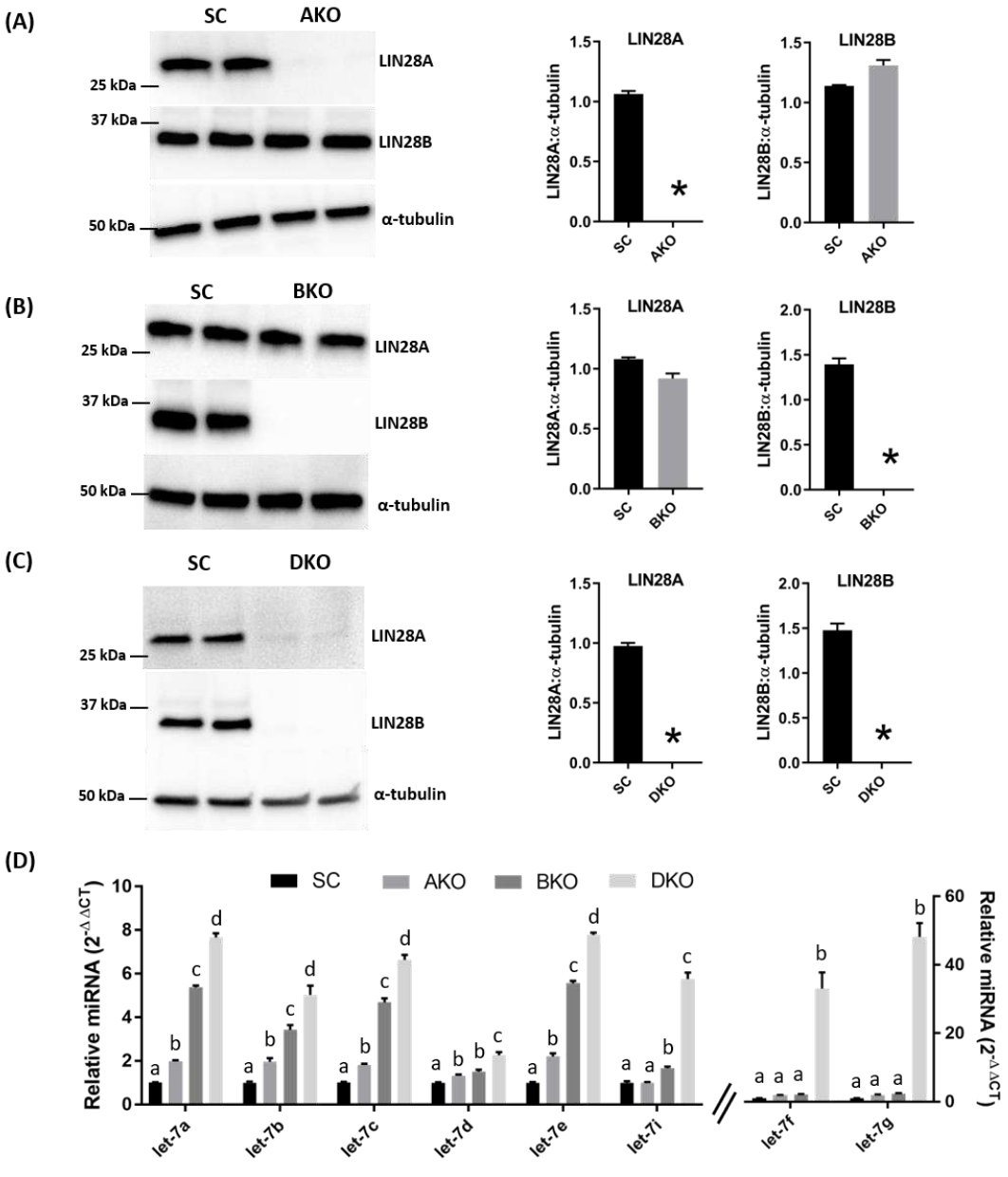

Figure 8. Knockout of LIN28A (AKO), LIN28B (BKO) and LIN28A-B (DKO) in ACH-3P cells and its effect on let-7 miRNAs. (A, B, C) Representative immunoblots for LIN28A, LIN28B and α-tubulin, and densitometric analysis of LIN28A and LIN28B in AKO, BKO and DKO ACH-3P cells compared to SC (n=3). (D) Comparison of let-7 miRNAs in SC vs AKO vs BKO vs DKO ACH-3P cells (n=3). *P<0.05 vs. SC.

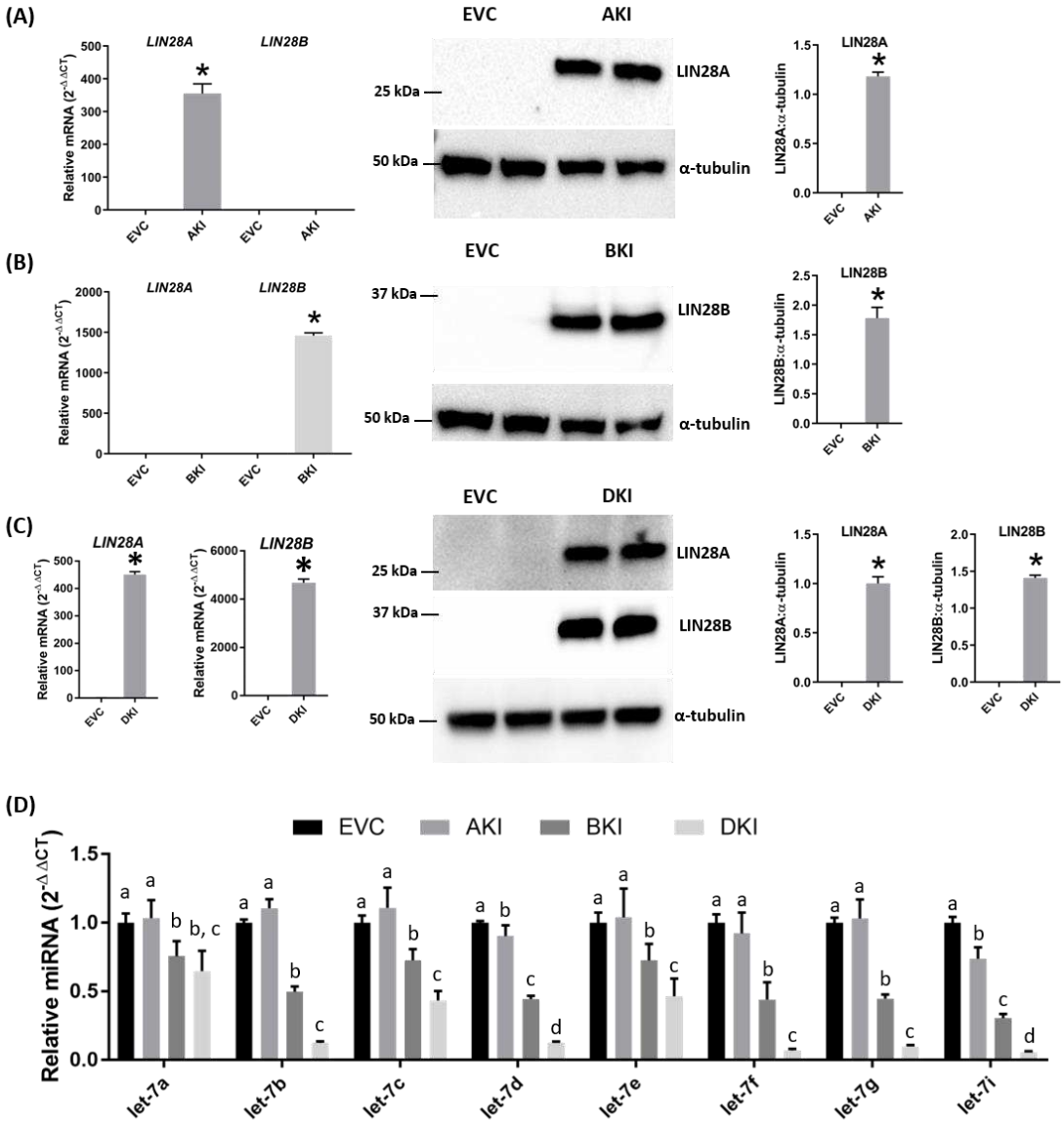

Figure 9. Knock-in of LIN28A (AKI), LIN28B (BKI) and LIN28A-B (DKI) in Sw.71 cells and its effect on let-7 miRNAs. (A, B, C) Detection of LIN28A and LIN28B mRNA and protein in AKI, BKI and DKI Sw.71 cells compared to EVC (n=3). (D) Comparison of let-7 miRNAs in EVC vs AKI vs BKI vs DKI Sw.71 cells (n=3). *P<0.05 vs. EVC.

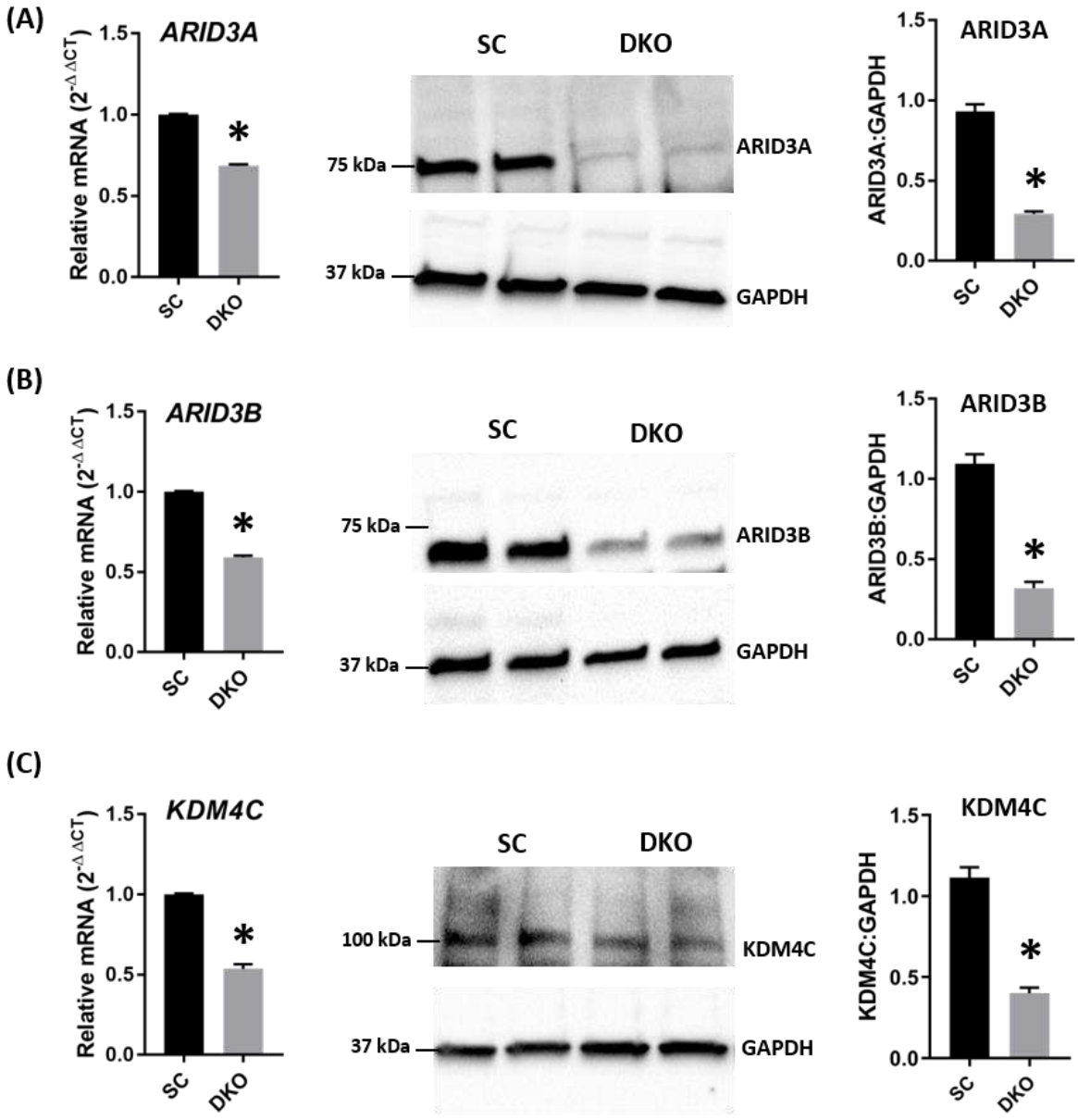

Figure 10. ARID3A, ARID3B and KDM4C in DKO ACH-3P cells. (A, B, C) Detection of ARID3A, ARID3B, and KDM4C mRNA and protein in LIN28 DKO ACH-3P cells compared to SC (n=3). *P<0.05 vs. SC.

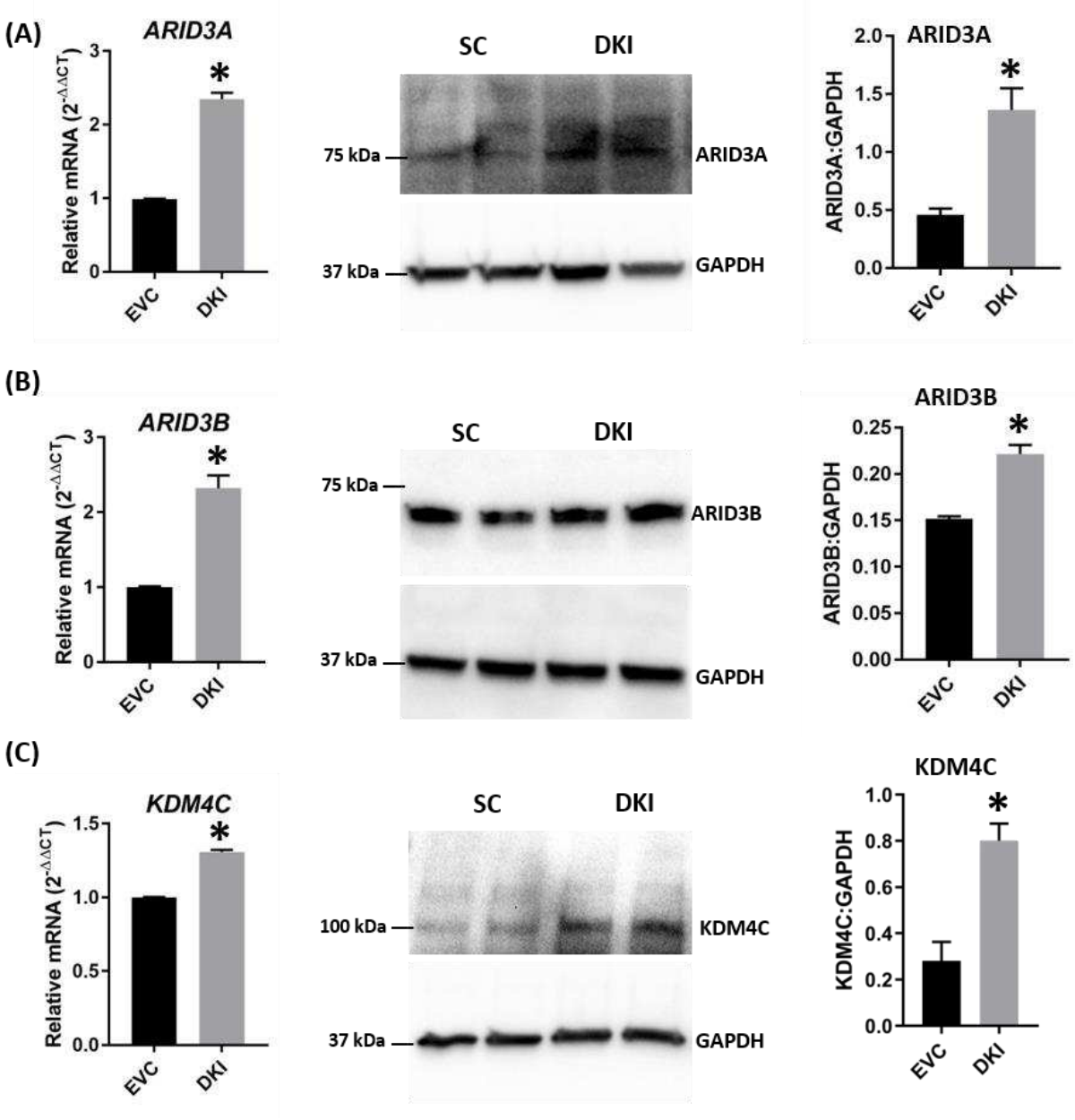

Figure 11. ARID3A, ARID3B and KDM4C in DKI Sw.71 cells. (A, B, C) Detection of ARID3A, ARID3B, and KDM4C mRNA and protein in DKI Sw.71 cells compared to EVC (n=3). *P<0.05 vs. EVC.

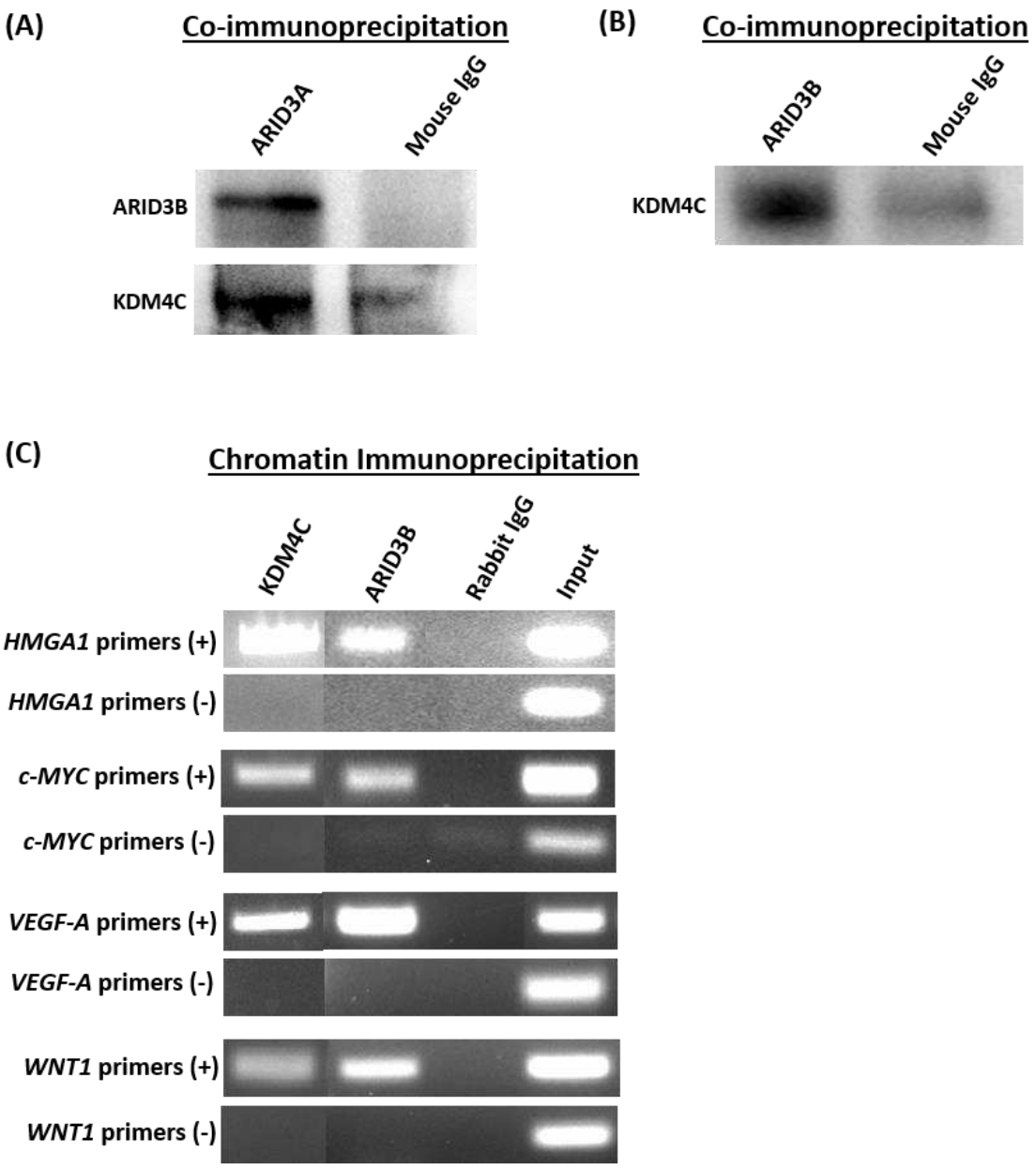

Figure 12. ARID3B-complex in ACH-3P cells. (A) Co-immunoprecipitation assay using ARID3A and normal mouse IgG for immunoprecipitation, and ARID3B and KDM4C for immunoblotting. (B) Co-immunoprecipitation using ARID3B and normal mouse IgG for immunoprecipitation, and KDM4C for immunoblotting. (C) Chromatin immunoprecipitation by KDM4C, ARID3B and normal rabbit IgG using sheared chromatin from ACH-3P cells, and end point PCR for HMGA1, c-MYC, VEGF-A and WNT1.

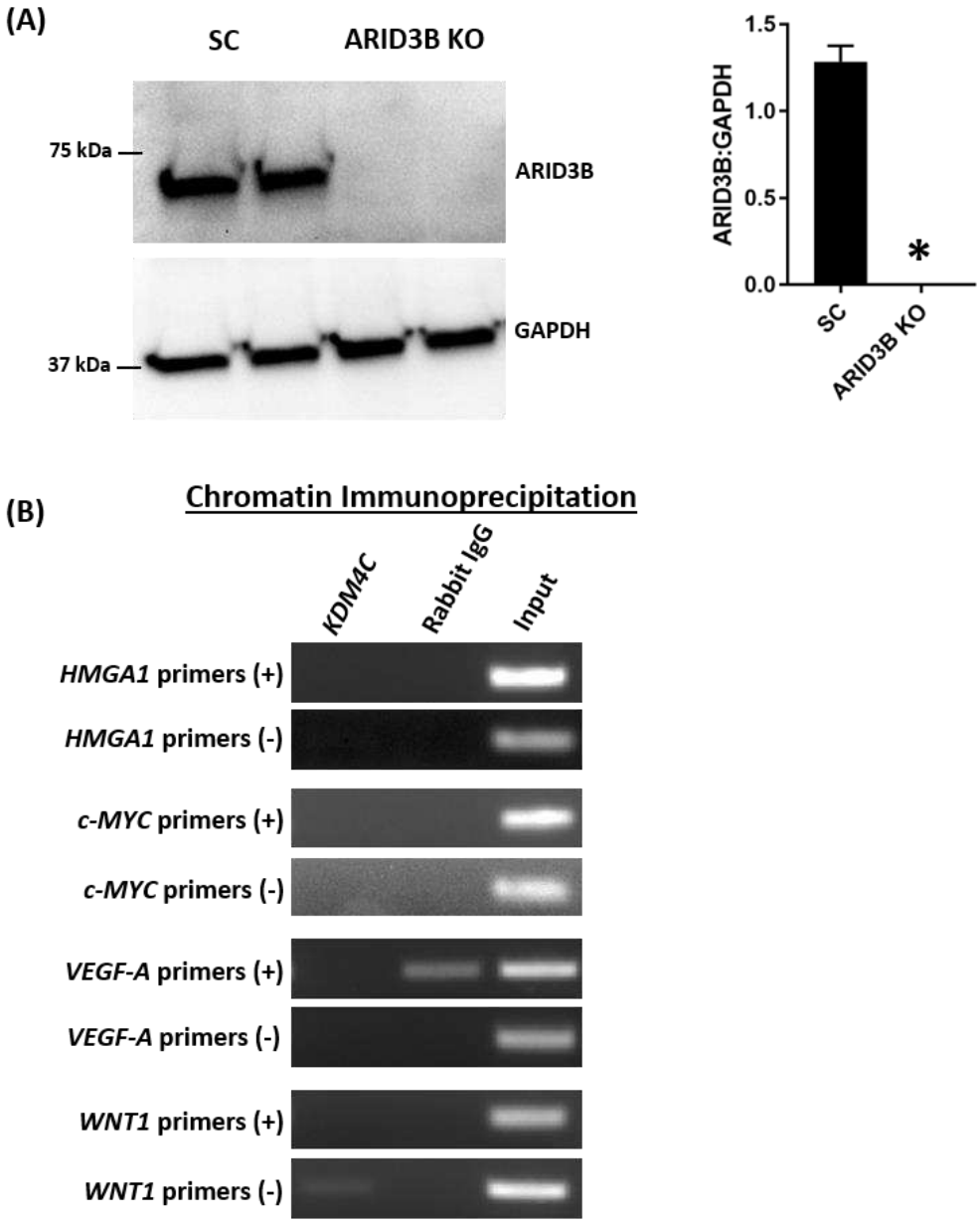

Figure 13. Chromatin binding of KDM4C in ARID3B KO ACH-3P cells. (A) Representative immunoblots for ARID3B and GAPDH, and densitometric analysis of immunoblotting results for ARID3B in ARID3B KO ACH-3P cells compared to SC (n=3). (B) Chromatin immunoprecipitation by KDM4C and normal rabbit IgG using sheared chromatin from ARID3B KO ACH-3P cells, and end point PCR for HMGA1, c-MYC, VEGF-A and WNT1. *P<0.05 vs. SC.

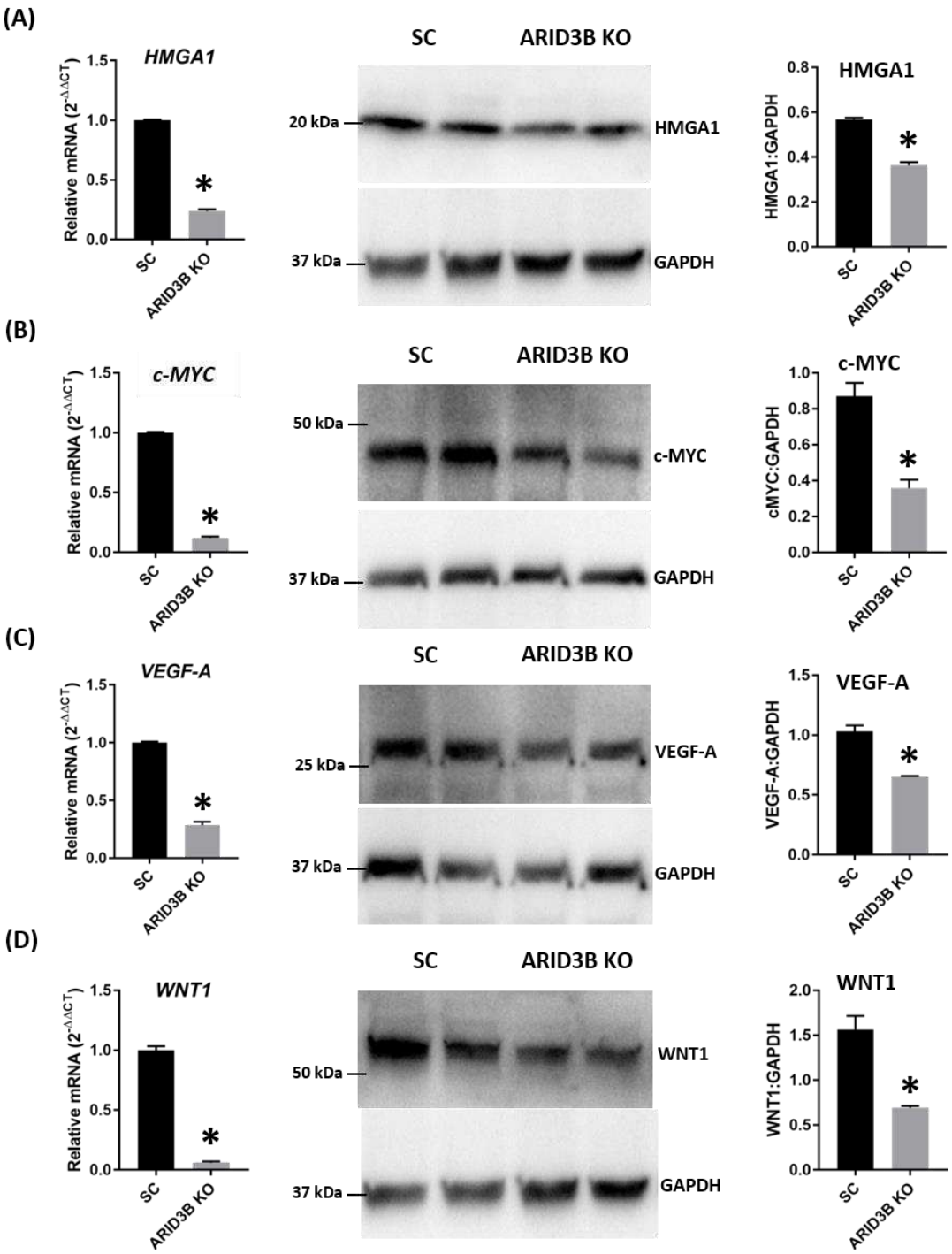

Figure 14. HMGA1, c-MYC, VEGF-A and WNT1 in ARID3B KO ACH-3P cells. (A, B, C, D) Detection of HMGA1, c-MYC, VEGF-A and WNT1 mRNA and protein in ARID3B KO ACH-3P cells compared to SC (n=3). *P<0.05 vs. SC.

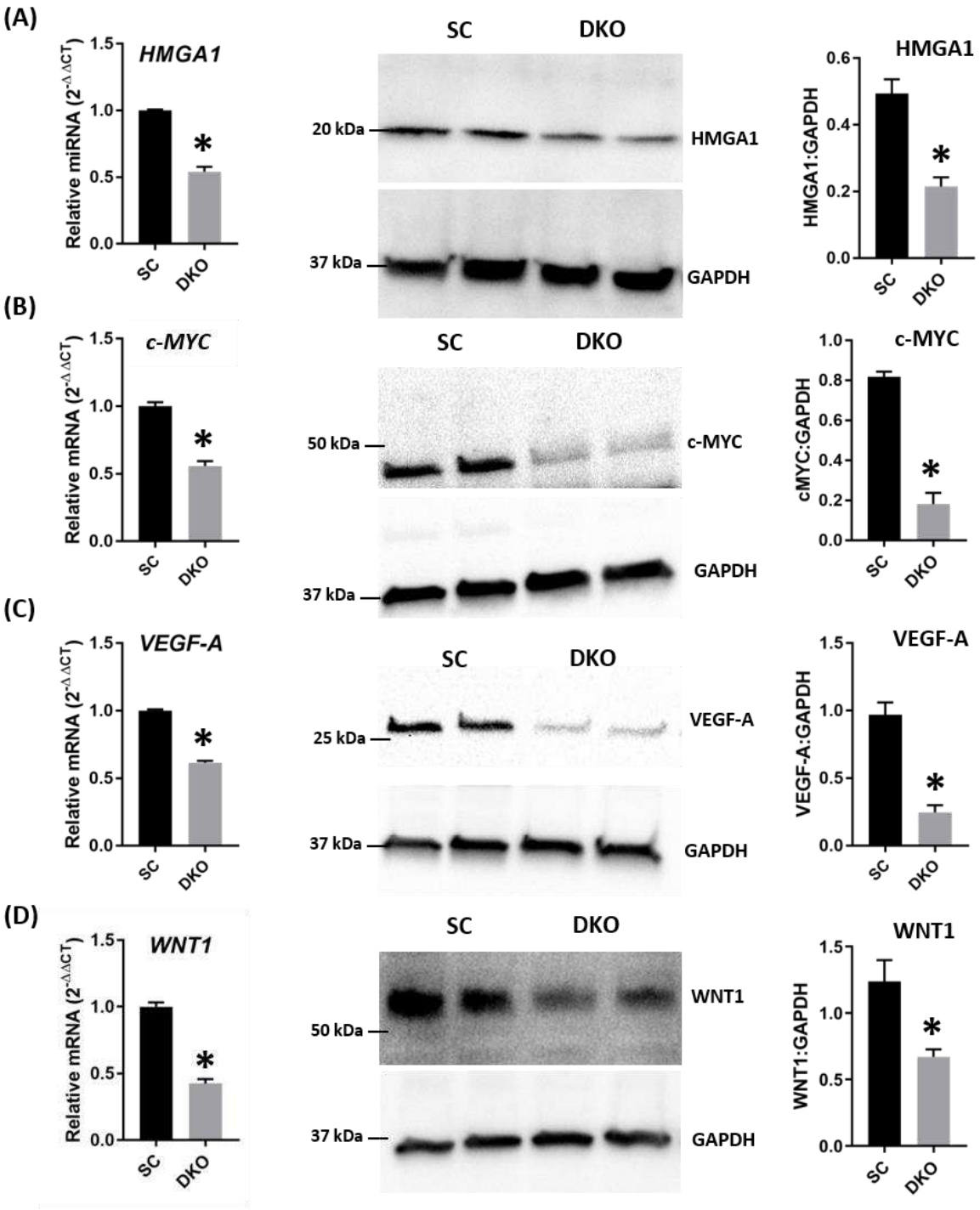

Figure 15. HMGA1, c-MYC, VEGF-A and WNT1 in DKO ACH-3P cells. (A, B, C, D) Detection of HMGA1, c-MYC, VEGF-A and WNT1 mRNA and protein in DKO ACH-3P cells compared to SC (n=3). *P<0.05 vs. SC.

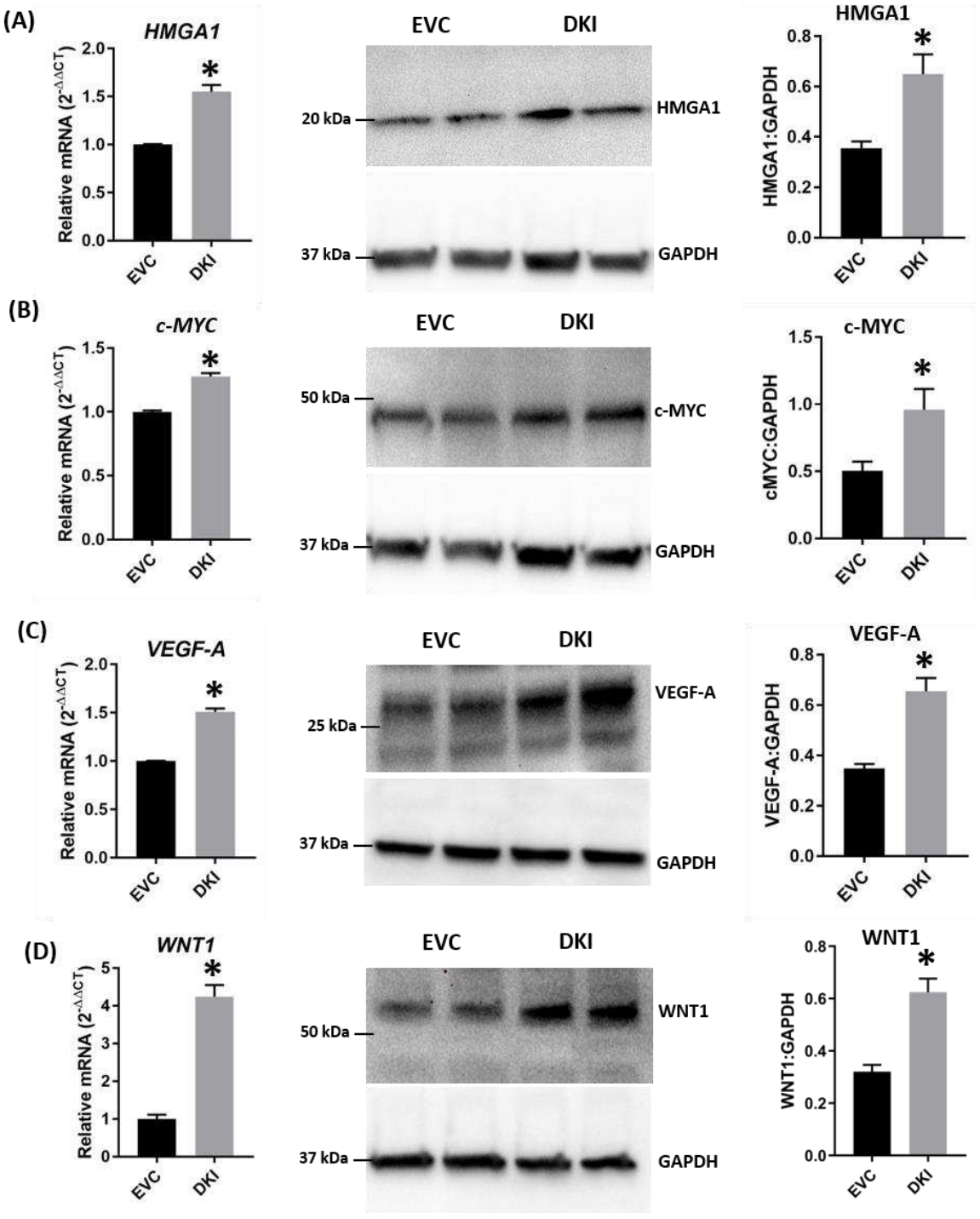

Figure 16. HMGA1, c-MYC, VEGF-A and WNT1 in DKI Sw.71 cells. (A, B, C, D) Detection of HMGA1, c-MYC, VEGF-A and WNT1 mRNA and protein in DKI Sw.71 cells compared to EVC (n=3). *P<0.05 vs. EVC.

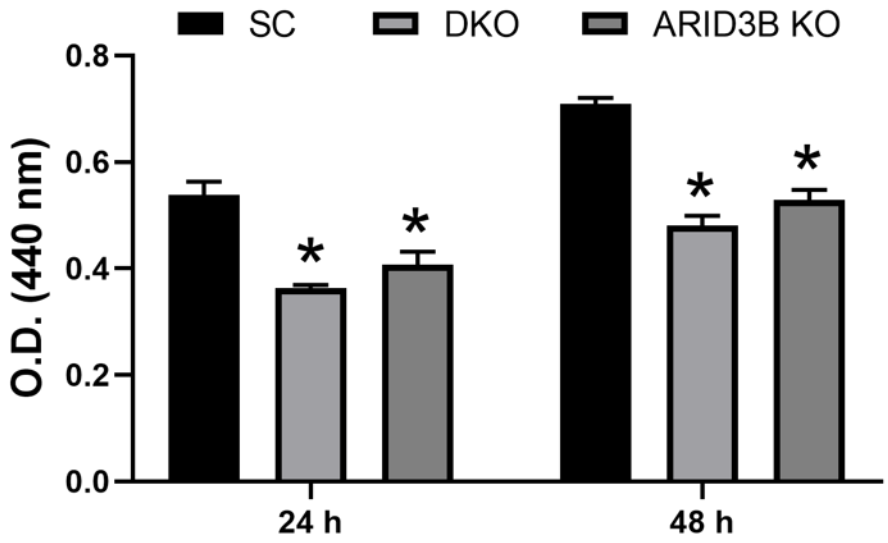

Figure 17. Cell proliferation of SC, LIN28 DKO and ARID3B KO ACH-3P cells measured after 24h and 48h using the Quick Cell Proliferation Assay Kit (n=3). *P<0.05 vs. SC.

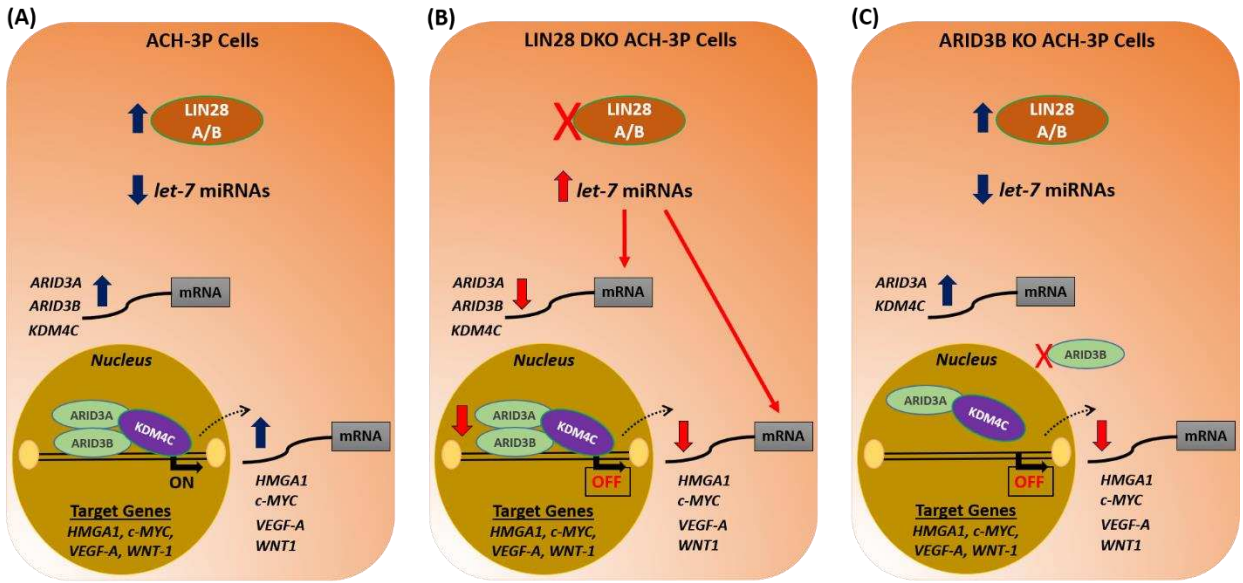

Figure 18. Graphical abstract. (A) In ACH-3P cells, let-7 miRNAs are low due to high LIN28A and LIN28B. Due to low levels of let-7 miRNAs, ARID3A, ARID3B and KDM4C are higher. ARID3B-complex binds the promoter regions of HMGA1, c-MYC, VEGF-A and WNT1, and turns on these genes by chromatin modification. (B) In LIN28 DKO ACH-3P cells, let-7 miRNAs are higher. Elevated let-7 miRNAs target HMGA1, c-MYC, VEGF-A and WNT1, leading to reduced expression of these genes. In addition, the elevated let-7 miRNAs also target ARID3A, ARID3B and KDM4C. This results in less binding of the ARID3B-complex to promoter regions of HMGA1, c-MYC, VEGF-A and WNT1, leading to reduced expression of these genes (C) In ARID3B KO ACH-3P cells, the ARID3B-complex is disrupted. KDM4C cannot bind to DNA in absence of ARID3B, which turns off this pathway of chromatin modification, and hence HMGA1, c-MYC, VEGF-A and WNT1 are reduced.

Table 2. *CRISPR-Cas9 oligos*

LIN28A	Forward oligo	5’ CACCGCTGTCCATGACCGCCCGCGC 3’
	Reverse oligo	5’ AAACGCGCGGGCGGTCATGGACAGC 3’
LIN28B	Forward oligo	5’ CACCGGCTGCCGGAGCCGGCAGAGG 3’
	Reverse oligo	5’ AAACCCTCTGCCGGCTCCGGCAGCC 3’
ARID3B	Forward oligo	5’ CACCGAGTGTTTGAACGGGGCAACA 3’
	Reverse oligo	5’ AAACTGTTGCCCCGTTCAAACACTC 3’
Scramble	Forward oligo	5’ CACCGGCTGATCTATCGCGGTCGTC 3’
	Reverse oligo	5’ AAACGACGACCGCGATAGATCAGCC 3’

Table 3. *Real-time RT-PCR primers*

LIN28A	Forward primer	5’ CTTTAAGAAGTCAGCCAAGGG 3’
	Reverse primer	5’ TGGCATGATGATCTAGACCTC 3’
LIN28B	Forward primer	5’ TAGGAAGTGAAAGAAGACCCA 3’
	Reverse primer	5’ ATGATGCTCTGACAGTAATGG 3’
ARID3A	Forward primer	5’ GATGCGGTTCACAGGTGTC 3’
	Reverse primer	5’ CGACTGGACTTACGAGGAGC 3’
ARID3B	Forward primer	5’ TCCATCTGCATCATCACTCC 3’
	Reverse primer	5’ GCCTCACCTTCTGTCTCCAC 3’
KDM4C	Forward primer	5’ TGGATCCCAGATAGCAATGA 3’
	Reverse primer	5’ TGTCTTCAAATCGCATGTCA 3’
IPO9	Forward primer	5’ TCTGCCAAGTGAACACCAAA 3’
	Reverse primer	5’ GGAAGCGTTAGTGGATACGC 3’
HMGA1	Forward primer	5’ AGGAAAAGGACGGCACTGAGAA 3’
	Reverse primer	5’ CCCCGAGGTCTCTTAGGTGTTGG 3’
c-MYC	Forward primer	5’ CTGGTGCTCCATGAGGAGA 3’
	Reverse primer	5’ CCTGCCTCTTTTCCACAGAA 3’
VEGF-A	Forward primer	5’ CCGGAGAGGGAGCGCGAGCCGCGCC 3’
	Reverse primer	5’ GATGTCCACCAGGGTCTCGATTG 3’
WNT1	Forward primer	5’ CACGACCTCGTCTACTTCGAG 3’
	Reverse primer	5’ ACAGACACTCGTGCAGTACGC 3’
GAPDH	Forward primer	5’ AAGGTCGGAGTCAACGGATTTG 3’
	Reverse primer	5’ CCATGGGTGGAATCATATTGGAA 3’

Table 4. *Antibodies used for western blotting, co-IP and ChIP*

Protein	Vendor	Catalog #	Host Species	Dilution used	Band size
LIN28A	Abcam	ab63740	Rabbit	1:1000	30 kDa
LIN28B	Bethyl Labs	A303-588A	Rabbit	1:2000	35 kDa
ARID3A	Bethyl Labs	A300-228A	Rabbit	1:4000	75 kDa
ARID3A	SCBT	sc-398367	Mouse	1:1000	co-IP
ARID3B	Bethyl Labs	A302-564A	Rabbit	1:4000	70 kDa
ARID3B	Bethyl Labs	A302-565A	Rabbit	1:4000	70 kDa
ARID3B	SCBT	sc-514741	Mouse	1:1000	co-IP
KDM4C	Bethyl Labs	A300-885A	Rabbit	1:2000	150 kDa
IPO9	Abcam	ab52605	Rabbit	1:1000	100 kDa
HMGA1	Abcam	ab226850	Rabbit	1:1000	20 kDa
c-MYC	Abcam	ab32	Mouse	1:1000	45 kDa
VEGF-A	SCBT	sc-7269	Mouse	1:500	30 kDa
WNT1	Abcam	ab63934	Rabbit	1:1000	50 kDa
GAPDH	Abcam	ab9485	Rabbit	1:3000	37 kDa
β-actin	SCBT	sc-47778	Mouse	1:2000	45 kDa
α-tubulin	Abcam	ab4074	Rabbit	1:3000	50 kDa
Goat anti-rabbit (HRP)	Abcam	ab97051	Goat	1:3000	Secondary (HRP)
Goat anti-mouse (HRP)	Abcam	ab97023	Goat	1:3000	Secondary (HRP)

Table 5: *PCR primers for ChIP assay*

HMGA1 (+)	Forward primer	5’	AACATTCCTGCCACATTCCT	3’
	Reverse primer	5’	ACACGGCTGTGACTCATGTT	3’
HMGA1 (-)	Forward primer	5’	TGAGATGAGACACCCTGGAG	3’
	Reverse primer	5’	CCTCCAGTTCTTCCAATGGT	3’
c-MYC (+)	Forward primer	5’	GGGACCAAGGATGAGAAGAA	3’
	Reverse primer	5’	ATGTAACCCGCAAACGTGTA	3’
c-MYC (-)	Forward primer	5’	TGTCCAAAAGGACCATAGCA	3’
	Reverse primer	5’	TTCCTTTGTTGAACCCCTTC	3’
VEGF-A (+)	Forward primer	5’	GTGAGCCTGGAGAAGTAGCC	3’
	Reverse primer	5’	CTGCGTGATGATTCAAACCT	3’
VEGF-A (-)	Forward primer	5’	GGAGTGGAACCTCATGCTTT	3’
	Reverse primer	5’	AGGAGGCAAGTAAGCCAAGA	3’
WNT1 (+)	Forward primer	5’	CCCATATTCACGTTGTTCCA	3’
	Reverse primer	5’	AGCGGTGGAGAGAAACCTAA	3’
WNT1 (-)	Forward primer	5’	GGCTATTTTGCCAGAGAGG	3’
	Reverse primer	5’	ACCACCAAGGAAGAGGTGAC	3’

REFERENCES

1. Beune, I. M., Bloomfield, F. H., Ganzevoort, W., Embleton, N. D., Rozance, P. J., van Wassenaer-Leemhuis, A. G., Wynia, K., and Gordijn, S. J. (2018) Consensus Based Definition of Growth Restriction in the Newborn. J. Pediatr. 196, 71-76.e1
2. Sharma, D., Shastri, S., Farahbakhsh, N., and Sharma, P. (2016) Intrauterine growth restriction - part 1. J. Matern.-Fetal Neonatal Med. Off. J. Eur. Assoc. Perinat. Med. Fed. Asia Ocean. Perinat. Soc. Int. Soc. Perinat. Obstet. 29, 3977–3987
3. Djakovic, A., Rieger, L., Wirbelauer, J., Kalla, J., and Dietl, J. (2007) [Severe foetal growth retardation in a patient with uterus bicornis, velamentous insertion and partial placental abruption in the 26th week of gestation--a case report]. Z. Geburtshilfe Neonatol. 211, 169–173
4. Wilkins-Haug, L., Quade, B., and Morton, C. C. (2006) Confined placental mosaicism as a risk factor among newborns with fetal growth restriction. Prenat. Diagn. 26, 428–432
5. Yu, K. M. (1992) [Relation between placental morphometry and fetal growth]. Zhonghua Fu Chan Ke Za Zhi 27, 217–219, 250
6. Heinonen, S., Taipale, P., and Saarikoski, S. (2001) Weights of placentae from small-for-gestational age infants revisited. Placenta 22, 399–404
7. Lyons, P., ed. (2006) Obstetrics in Family Medicine: A Practical Guide. Humana Press
8. Barker, D. J. P. (1999) Fetal origins of cardiovascular disease. Ann. Med. 31, 3–6
9. Norwitz, E. R. (2007) Defective implantation and placentation: laying the blueprint for pregnancy complications. Reprod. Biomed. Online 14 Spec No 1, 101–109

10. Scifres, C. M. and Nelson, D. M. (2009) Intrauterine growth restriction, human placental development and trophoblast cell death. J. Physiol. 587, 3453–3458

11. Devor, E. J., Reyes, H. D., Santillan, D. A., Santillan, M. K., Onukwugha, C., Goodheart, M. J., and Leslie, K. K. (2014) Placenta-Specific Protein 1: A Potential Key to Many Oncofetal-Placental OB/GYN Research Questions. Obstet. Gynecol. Int. 2014

12. Ma, W., Ma, J., Xu, J., Qiao, C., Branscum, A., Cardenas, A., Baron, A. T., Schwartz, P., Maihle, N. J., and Huang, Y. (2013) Lin28 regulates BMP4 and functions with Oct4 to affect ovarian tumor microenvironment. Cell Cycle Georget. Tex 12, 88–97

13. Feng, C., Neumeister, V., Ma, W., Xu, J., Lu, L., Bordeaux, J., Maihle, N. J., Rimm, D. L., and Huang, Y. (2012) Lin28 regulates HER2 and promotes malignancy through multiple mechanisms. Cell Cycle Georget. Tex 11, 2486–2494

14. Piskounova, E., Polytarchou, C., Thornton, J. E., LaPierre, R. J., Pothoulakis, C., Hagan, J. P., Iliopoulos, D., and Gregory, R. I. (2011) Lin28A and Lin28B inhibit let-7 microRNA biogenesis by distinct mechanisms. Cell 147, 1066–1079

15. Hagan, J. P., Piskounova, E., and Gregory, R. I. (2009) Lin28 recruits the TUTase Zcchc11 to inhibit let-7 maturation in mouse embryonic stem cells. Nat. Struct. Mol. Biol. 16, 1021–1025

16. Rybak, A., Fuchs, H., Smirnova, L., Brandt, C., Pohl, E. E., Nitsch, R., and Wulczyn, F. G. (2008) A feedback loop comprising lin-28 and let-7 controls pre-let-7 maturation during neural stem-cell commitment. Nat. Cell Biol. 10, 987–993

17. Newman, M. A., Thomson, J. M., and Hammond, S. M. (2008) Lin-28 interaction with the Let-7 precursor loop mediates regulated microRNA processing. RNA N. Y. N 14, 1539–1549

18. Heo, I., Joo, C., Kim, Y.-K., Ha, M., Yoon, M.-J., Cho, J., Yeom, K.-H., Han, J., and Kim, V. N. (2009) TUT4 in concert with Lin28 suppresses microRNA biogenesis through pre-microRNA uridylation. Cell 138, 696–708

19. Heo, I., Joo, C., Cho, J., Ha, M., Han, J., and Kim, V. N. (2008) Lin28 mediates the terminal uridylation of let-7 precursor MicroRNA. Mol. Cell 32, 276–284

20. West, R. C., McWhorter, E. S., Ali, A., Goetzman, L. N., Russ, J. E., Anthony, R. V., Bouma, G. J., and Winger, Q. A. (2018) HMGA2 is regulated by LIN28 and BRCA1 in human placental cells†. Biol. Reprod.

21. Canfield, J., Arlier, S., Mong, E. F., Lockhart, J., VanWye, J., Guzeloglu-Kayisli, O., Schatz, F., Magness, R. R., Lockwood, C. J., Tsibris, J. C. M., Kayisli, U. A., and Totary-Jain, H. (2018) Decreased LIN28B in preeclampsia impairs human trophoblast differentiation and migration. FASEB J. Off. Publ. Fed. Am. Soc. Exp. Biol. fj201801163R

22. Seabrook, J. L., Cantlon, J. D., Cooney, A. J., McWhorter, E. E., Fromme, B. A., Bouma, G. J., Anthony, R. V., and Winger, Q. A. (2013) Role of LIN28A in Mouse and Human Trophoblast Cell Differentiation. Biol. Reprod. 89, 95

23. Liao, T.-T., Hsu, W.-H., Ho, C.-H., Hwang, W.-L., Lan, H.-Y., Lo, T., Chang, C.-C., Tai, S.-K., and Yang, M.-H. (2016) let-7 Modulates Chromatin Configuration and Target Gene Repression through Regulation of the ARID3B Complex. Cell Rep. 14, 520–533

24. Wilsker, D., Probst, L., Wain, H. M., Maltais, L., Tucker, P. W., and Moran, E. (2005) Nomenclature of the ARID family of DNA-binding proteins. Genomics 86, 242–251

25. Kortschak, R. D., Tucker, P. W., and Saint, R. (2000) ARID proteins come in from the desert. Trends Biochem. Sci. 25, 294–299

26. Raney, B. J., Cline, M. S., Rosenbloom, K. R., Dreszer, T. R., Learned, K., Barber, G. P., Meyer, L. R., Sloan, C. A., Malladi, V. S., Roskin, K. M., Suh, B. B., Hinrichs, A. S., Clawson, H., Zweig, A. S., Kirkup, V., Fujita, P. A., Rhead, B., Smith, K. E., Pohl, A., Kuhn, R. M., Karolchik, D., Haussler, D., and Kent, W. J. (2011) ENCODE whole-genome data in the UCSC genome browser (2011 update). Nucleic Acids Res. 39, D871-875

27. Wood, J. J., Boyne, J. R., Paulus, C., Jackson, B. R., Nevels, M. M., Whitehouse, A., and Hughes, D. J. (2016) ARID3B: a Novel Regulator of the Kaposi's Sarcoma-Associated Herpesvirus Lytic Cycle. J. Virol. 90, 9543–9555

28. Bobbs, A., Gellerman, K., Hallas, W. M., Joseph, S., Yang, C., Kurkewich, J., and Cowden Dahl, K. D. (2015) ARID3B Directly Regulates Ovarian Cancer Promoting Genes. PloS One 10, e0131961

29. Roy, L., Samyesudhas, S. J., Carrasco, M., Li, J., Joseph, S., Dahl, R., and Cowden Dahl, K. D. (2014) ARID3B increases ovarian tumor burden and is associated with a cancer stem cell gene signature. Oncotarget 5, 8355–8366

30. Ratliff, M. L., Mishra, M., Frank, M. B., Guthridge, J. M., and Webb, C. F. (2016) The Transcription Factor ARID3a Is Important for In Vitro Differentiation of Human Hematopoietic Progenitors. J. Immunol. Baltim. Md 1950 196, 614–623

31. Habir, K., Aeinehband, S., Wermeling, F., and Malin, S. (2017) A Role for the Transcription Factor Arid3a in Mouse B2 Lymphocyte Expansion and Peritoneal B1a Generation. Front. Immunol. 8, 1387

32. Rhee, C., Edwards, M., Dang, C., Harris, J., Brown, M., Kim, J., and Tucker, H. O. (2017) ARID3A is required for mammalian placenta development. Dev. Biol. 422, 83–91

33. Takebe, A., Era, T., Okada, M., Martin Jakt, L., Kuroda, Y., and Nishikawa, S.-I. (2006) Microarray analysis of PDGFR alpha+ populations in ES cell differentiation culture identifies genes involved in differentiation of mesoderm and mesenchyme including ARID3b that is essential for development of embryonic mesenchymal cells. Dev. Biol. 293, 25–37

34. Kobayashi, K., Era, T., Takebe, A., Jakt, L. M., and Nishikawa, S.-I. (2006) ARID3B induces malignant transformation of mouse embryonic fibroblasts and is strongly associated with malignant neuroblastoma. Cancer Res. 66, 8331–8336

35. Casanova, J. C., Uribe, V., Badia-Careaga, C., Giovinazzo, G., Torres, M., and Sanz-Ezquerro, J. J. (2011) Apical ectodermal ridge morphogenesis in limb development is controlled by Arid3b-mediated regulation of cell movements. Dev. Camb. Engl. 138, 1195–1205

36. Webb, C. F., Bryant, J., Popowski, M., Allred, L., Kim, D., Harriss, J., Schmidt, C., Miner, C. A., Rose, K., Cheng, H.-L., Griffin, C., and Tucker, P. W. (2011) The ARID family transcription factor bright is required for both hematopoietic stem cell and B lineage development. Mol. Cell. Biol. 31, 1041–1053

37. Kim, D., Probst, L., Das, C., and Tucker, P. W. (2007) REKLES is an ARID3-restricted multifunctional domain. J. Biol. Chem. 282, 15768–15777

38. Hua, Z., Lv, Q., Ye, W., Wong, C.-K. A., Cai, G., Gu, D., Ji, Y., Zhao, C., Wang, J., Yang, B. B., and Zhang, Y. (2006) MiRNA-Directed Regulation of VEGF and Other Angiogenic Factors under Hypoxia. PLoS ONE 1

39. Jin, B., Wang, W., Meng, X., Du, G., Li, J., Zhang, S., Zhou, B., and Fu, Z. (2016) Let-7 inhibits self-renewal of hepatocellular cancer stem-like cells through regulating the epithelial-mesenchymal transition and the Wnt signaling pathway. BMC Cancer 16

40. Rahman, M. M., Qian, Z. R., Wang, E. L., Sultana, R., Kudo, E., Nakasono, M., Hayashi, T., Kakiuchi, S., and Sano, T. (2009) Frequent overexpression of HMGA1 and 2 in gastroenteropancreatic neuroendocrine tumours and its relationship to let-7 downregulation. Br. J. Cancer 100, 501–510

41. Wagner, S., Ngezahayo, A., Murua Escobar, H., and Nolte, I. (2014) Role of miRNA Let-7 and Its Major Targets in Prostate Cancer. BioMed Res. Int.

42. Yang, X., Cai, H., Liang, Y., Chen, L., Wang, X., Si, R., Qu, K., Jiang, Z., Ma, B., Miao, C., Li, J., Wang, B., and Gao, P. (2015) Inhibition of c-Myc by let-7b mimic reverses mutidrug resistance in gastric cancer cells. Oncol. Rep. 33, 1723–1730

43. Uchikura, Y., Matsubara, K., Matsubara, Y., and Mori, M. (2015) P34. Role of high-mobility group A1 protein in trophoblast invasion. Pregnancy Hypertens. Int. J. Womens Cardiovasc. Health 5, 243

44. Uchikura, Y., Matsubara, K., Muto, Y., Matsubara, Y., Fujioka, T., Matsumoto, T., and Sugiyama, T. (2017) Extranuclear Translocation of High-Mobility Group A1 Reduces the Invasion of Extravillous Trophoblasts Involved in the Pathogenesis of Preeclampsia: New Aspect of High-Mobility Group A1. Reprod. Sci. Thousand Oaks Calif 24, 1630–1638

45. Kumar, P., Luo, Y., Tudela, C., Alexander, J. M., and Mendelson, C. R. (2013) The c-Myc-regulated microRNA-17~92 (miR-17~92) and miR-106a~363 clusters target hCYP19A1 and hGCM1 to inhibit human trophoblast differentiation. Mol. Cell. Biol. 33, 1782–1796

46. Lala, N., Girish, G. V., Cloutier-Bosworth, A., and Lala, P. K. (2012) Mechanisms in decorin regulation of vascular endothelial growth factor-induced human trophoblast migration and acquisition of endothelial phenotype. Biol. Reprod. 87, 59

47. Li, Y., Zhu, H., Klausen, C., Peng, B., and Leung, P. C. K. (2015) Vascular Endothelial Growth Factor-A (VEGF-A) Mediates Activin A-Induced Human Trophoblast Endothelial-Like Tube Formation. Endocrinology 156, 4257–4268

48. Pang, V., Bates, D. O., and Leach, L. (2017) Regulation of human feto-placental endothelial barrier integrity by vascular endothelial growth factors: competitive interplay between VEGF-A165a, VEGF-A165b, PIGF and VE-cadherin. Clin. Sci. Lond. Engl. 1979 131, 2763–2775

49. Wu, K., Liu, F., Wu, W., Chen, Y., Wu, H., and Zhang, W. (2018) Long non-coding RNA HOX transcript antisense RNA (HOTAIR) suppresses the angiogenesis of human placentation by inhibiting vascular endothelial growth factor A expression. Reprod. Fertil. Dev.

50. Liu, F., Wu, K., Wu, W., Chen, Y., Wu, H., Wang, H., and Zhang, W. (2018) miR-203 contributes to pre-eclampsia via inhibition of VEGFA expression. Mol. Med. Rep. 17, 5627–5634

51. Sonderegger, S., Husslein, H., Leisser, C., and Knöfler, M. (2007) Complex expression pattern of Wnt ligands and frizzled receptors in human placenta and its trophoblast subtypes. Placenta 28 Suppl A, S97-102

52. Wang, X., Zhang, Z., Zeng, X., Wang, J., Zhang, L., Song, W., and Shi, Y. (2018) Wnt/β-catenin signaling pathway in severe preeclampsia. J. Mol. Histol. 49, 317–327

53. Jozwik, M., Pietrzycki, B., Jozwik, M., and Anthony, R. V. (2009) Expression of enzymes regulating placental ammonia homeostasis in human fetal growth restricted pregnancies. Placenta 30, 607–612

54. Hiden, U., Wadsack, C., Prutsch, N., Gauster, M., Weiss, U., Frank, H.-G., Schmitz, U., Fast-Hirsch, C., Hengstschläger, M., Pötgens, A., Rüben, A., Knöfler, M., Haslinger, P., Huppertz, B., Bilban, M., Kaufmann, P., and Desoye, G. (2007) The first trimester human trophoblast cell line ACH-3P: a novel tool to study autocrine/paracrine regulatory loops of human trophoblast subpopulations--TNF-alpha stimulates MMP15 expression. BMC Dev. Biol. 7, 137

55. Straszewski-Chavez, S. L., Abrahams, V. M., Alvero, A. B., Aldo, P. B., Ma, Y., Guller, S., Romero, R., and Mor, G. (2009) The isolation and characterization of a novel telomerase immortalized first trimester trophoblast cell line, Swan 71. Placenta 30, 939–948

56. Bae, S., Park, J., and Kim, J.-S. (2014) Cas-OFFinder: a fast and versatile algorithm that searches for potential off-target sites of Cas9 RNA-guided endonucleases. Bioinformatics 30, 1473–1475

57. Park, J., Bae, S., and Kim, J.-S. (2015) Cas-Designer: a web-based tool for choice of CRISPR-Cas9 target sites. Bioinformatics 31, 4014–4016

CHAPTER III: TROPHECTODERM-SPECIFIC KNOCKDOWN OF LIN28 DECREASES EXPRESSION OF GENES NECESSARY FOR CELL PROLIFERATION AND REDUCES ELONGATION OF SHEEP CONCEPTUS[45]

Synopsis

LIN28 inhibits *let-7* miRNA maturation which prevents cell differentiation and promotes proliferation. We hypothesize that the LIN28-*let-7* axis regulates proliferation-associated genes in sheep trophectoderm *in vivo*. Day 9 hatched sheep blastocysts were incubated with lentiviral particles to deliver shRNA targeting LIN28 specifically to trophectoderm cells. At day 16, conceptus elongation was significantly reduced in LIN28A and LIN28B knockdowns. *Let-7* miRNAs were significantly increased and IGF2BP1-3, HMGA1, ARID3B and c-MYC were decreased in trophectoderm from knockdown conceptuses. Ovine trophoblast (OTR) cells derived from day 16 trophectoderm are a useful tool for *in vitro* experiments. Surprisingly, LIN28 was significantly reduced and *let-7* miRNAs increased after only a few passages of OTR cells suggesting these passaged cells represent a more differentiated phenotype. To create an OTR cell line more similar to day 16 trophectoderm we overexpressed LIN28A and LIN28B, which significantly decreased *let-7* miRNAs and increased IGF2BP1-3, HMGA1, ARID3B and c-MYC compared to control. This is the first study showing the role of the LIN28-*let-7* axis in trophoblast proliferation and conceptus elongation *in vivo.* These results suggest that reduced LIN28 during

[4] This chapter has been published in International Journal of Molecular Sciences (IJMS).

[5]Authors List: Asghar Ali, Mark D Stenglein, Thomas E Spencer, Gerrit J Bouma, Russell V Anthony, Quinton A Winger

early placental development can lead to reduced trophoblast proliferation and sheep conceptus elongation at a critical period for successful establishment of pregnancy.

1. Introduction

Early placental development is one of the main factors determining perinatal fetal growth and postnatal fetal and maternal health. In humans, blastocyst implantation is an invasive process that occurs 7-9 days after fertilization [1]. Rapidly proliferating cytotrophoblast cells (CTBs) are the progenitor trophoblast cells which proliferate as well as differentiate into different trophoblast lineages throughout gestation [2]. If the balance between proliferation and differentiation of CTBs is dysregulated, it can result in severe disorders including pre-term birth, intrauterine growth restriction (IUGR) and pre-eclampsia [3,4]. These pregnancy related disorders affect about a third of human pregnancies [5].

In sheep, the blastocyst hatches out of the zona pellucida at day 8-9 and is surrounded by a single layer of mononuclear cells called trophectoderm (TE) [6]. Instead of invading the uterus, the hatched blastocyst elongates from day 11-16 due to rapid proliferation of trophoblast cells and adopts a filamentous shape comprised of mainly extraembryonic trophoblast cells [7–9]. Conceptus elongation is critical for implantation, placentation and successful establishment of pregnancy in sheep [10–12]. Reduced conceptus elongation and compromised placental function in domestic ruminants is one of the main causes of embryonic mortality resulting in reduced fertility [13–15]. Rapid trophoblast proliferation is an important phenomenon during early stages of pregnancy in both humans and domestic ruminants. The molecular mechanisms involved in regulating trophoblast proliferation and invasion are not well understood. Therefore, exploring the genes involved in sheep trophectoderm elongation can help to better understand the reasons for

reduced fertility in domestic ruminants and to improve the diagnosis and treatment of various pregnancy-related disorders in humans.

Trophoblast proliferation and differentiation is an intensively regulated process, and the role of several genes in placental development has been studied using various *in vivo* and *in vitro* models [16–20]. The pluripotency factor LIN28 is a highly conserved RNA binding protein which is expressed in placenta and has two paralogs, LIN28A and LIN28B [21,22]. It is usually described as a protooncogene due to its ability to regulate and stabilize oncogenes at the post-transcriptional level in tumor cells [23,24]. It also inhibits the biogenesis of lethal-7 (*let-7)* miRNAs in mammalian cells by binding pri-*let-7* and pre-*let-7* [25–30]. LIN28 is low and *let-7* miRNAs are high in differentiated cells and adult tissues, hence *let-7* miRNAs are considered markers of cell differentiation [31–33]. *Let-7* miRNAs reduce the expression of different proliferation factors either by directly targeting their mRNA or through chromatin dependent pathways by targeting the ARID3B-complex which is comprised of AT-Rich Interaction Domain 3A (ARID3A), AT-Rich Interaction Domain 3B (ARID3B) and lysine demethylase 4C (KDM4C) [18,34]. We have recently shown that term human placentas from IUGR pregnancies had reduced LIN28A and LIN28B and high *let-7* miRNAs compared to term human placentas from control pregnancies [18]. We further demonstrated that LIN28B is localized to cytotrophoblast cells in human placenta, and knockout of LIN28 in immortalized first trimester human trophoblast (ACH-3P) cells leads to an increase in *let-7* miRNAs, reduced expression of proliferation-associated genes, and reduced cell proliferation [18–20].

Insulin like growth factor 2 mRNA binding proteins (*IGF2BP1, IGF2BP2, IGF2BP3*), high mobility group AT-hook 1 (*HMGA1*), *ARID3B* and *c-MYC* are all *let-7* miRNA targets with known roles in cell proliferation [18,35–41]. IGF2BPs are highly conserved RNA binding

oncofetal proteins with three paralogs, IGF2BP1, IGF2BP2 and IGF2BP3[42]. By binding different mRNAs, IGF2BPs decide the fate of those mRNAs by controlling their localization, stability, and translation [40]. Many studies have reported the role of IGF2BPs in cell proliferation, cell invasion, tumorigenesis, and embryogenesis [40–51]. IGF2BPs have also been found in sheep trophoblast cells suggesting their role in rapid proliferation of these cells [52]. HMGA1 promotes invasion of trophoblast cells and reduced levels of HMGA1 has been linked to pathogenesis of preeclampsia [53,54]. ARID3B complexes with ARID3A and KDM4C to form the ARID3B-complex which plays a vital role in cell proliferation by transcriptional regulation of stemness genes including *HMGA1*, *c-MYC*, vascular endothelial growth factor A (*VEGF-A*), and Wnt family member 1 (*WNT1*) [18,34,55–59]. ARID3B knockout in immortalized first trimester human trophoblast cells results in reduced proliferation of these cells [18]. The *c-MYC* protooncogene has been identified as a proliferation factor in human cytotrophoblast cells and its level is reduced when cytotrophoblasts differentiate into syncytiotrophoblast [60].

To date, the role of LIN28-*let-7* miRNA axis in trophoblast cells has not been studied *in vivo*. The aim of this study is to demonstrate the role of LIN28-*let-7* axis in the regulation of proliferation-associated genes in trophoblast cells *in vivo*. We used sheep as an *in vivo* model to generate trophectoderm specific knockdown of LIN28A or LIN28B by infecting day 9 hatched blastocysts with shRNA-expressing lentiviral particles. This way, only the trophoblast cells will be infected by the lentiviral particles [61–63] and any phenotype will be due to knockdown of LIN28A or LIN28B in trophoblast cells. We hypothesize that the LIN28-*let-7* miRNAs axis plays an important role in sheep trophoblast cell proliferation and conceptus elongation by regulating the expression of genes associated with cell proliferation including *IGF2BP1, IGF2BP2, IGF2BP3*, *HMGA1*, *ARID3B* and *c-MYC*.

2. Materials and Methods

2.1.Lentivirus vector construction for shRNA expression

Lentiviral infection was used to stably integrate and express shRNA targeting LIN28A or LIN28B mRNA in the host cell. Lentiviral vectors were constructed using the protocol previously described by Baker et al. [61]. Briefly, LIN28A targeting shRNA, LIN28B targeting shRNA, or scrambled control shRNA sequence (Table 6) were first cloned into the pLKO.1 vector (plasmid 10878; Addgene, Cambridge, MA, USA), which contains the human U6 promoter upstream of cloning site for shRNA cassettes. The human U6 promoter and downstream LIN28A/LIN28B/SC shRNA sequence within pLKO.1 was PCR amplified using a forward primer with a 5′ XbaI restriction site(5′-TCTAGATTCACCGAGGGCCTATTTCCC-3′) and a reverse primer containing a 3′ XhoI restriction site (5′-GAATACTGCCATTTGTCTCGAGGTCG-3′). The resulting PCR amplicon was gel purified and cloned into the StrataClone PCR cloning vector using StrataClone PCR Cloning KIT (Agilent, Santa Clara, CA). The human U6 promoter and LIN28A/LIN28B/SC shRNA DNA fragment was digested from StrataClone PCR cloning vector using XbaI/XhoI restriction enzymes. Subsequently, the DNA fragment was ligated into the pLL3.7 vector also digested with XbaI/XhoI. Insertion of the human U6 promoter and LIN28A/LIN28B/SC shRNA sequence into pLL3.7 was verified by sanger sequencing.

2.2.Lentivirus vector construction for overexpression of LIN28A and LIN28B

To overexpress LIN28A and LIN28B, pCDH lentiviral expression vector (System Biosciences, Palo Alto, CA, USA) was used. The mRNA was extracted from day 16 TE using RNeasy Mini Kit (Qiagen Inc. Germantown, MD, USA) following the manufacturer's protocol, and then reverse transcribed to cDNA using iScript cDNA synthesis kit (Bio-Rad Laboratories, Hercules, CA, USA). cDNA was amplified using PCR primers for LIN28A or LIN28B (Table 7).

The PCR primers included restriction sites for NheI and SwaI restriction enzymes. The resulting PCR amplicons were gel purified and cloned into the StrataClone PCR cloning vector using StrataClone PCR Cloning KIT (Agilent, Santa Clara, CA). StrataClone vector with successful cloning of PCR product were double digested using NheI/SwaI. The double digested product was cloned in double digested pCDH vector and confirmed by sanger sequencing.

2.3.Lentiviral vector for immortalizing passaged ovine trophoblast cells

To immortalize the OTR cells, pLV-hTERT-IRES-hygro was used (Addgene, Watertown, MA, USA, Plasmid # 85140) [64]. pLV-hTERT-IRES-hygro vector-based lentiviral particles express human telomerase reverse transcriptase (hTERT) in the infected cells.

2.4.Production of lentiviral particles

To generate lentiviral particles, three vectors were used including transfer vector (LL3.7 or pCDH or pLV-hTERT-IRES-hygro), packaging plasmid (psPAX2 from Addgene, Watertown, MA, USA, Plasmid # 12260) and envelope plasmid (pMD2.G from Addgene, Watertown, MA, USA, Plasmid # 12259). 293FT cells (Invitrogen, Carlsbad, CA, USA) were cultured in DMEM high-glucose media supplemented with 10% heat-inactivated fetal bovine serum (FBS) and 1x penicillin-streptomycin-amphotericin B (PSA) solution, at 37°C and 5% CO_2. 8.82 µg transfer vector DNA, 6.66 µg psPAX2 packaging plasmid DNA and 2.70 µg pMD2.G envelope plasmid DNA was mixed with 180 µl of polyfect transfection reagent (Qiagen Inc., Germantown, MD, USA) and final volume was brought up to 855 µl using DMEM high-glucose media without any supplements. The plasmids-polyfect mixture was incubated at room temperature for 10 min and then gently mixed in the media on 70-80 % confluent 293FT cells. Cells were incubated for 4–6 h at 37°C and 5% CO2. After incubation time, the transfection media was replaced by fresh DMEM high glucose media supplemented with 10% FBS and 1x PSA solution. After 72 h, the medium

containing lentiviral particles was collected and ultra-centrifuged over a 20% sucrose cushion at 25,000 RPM for 2 h at 4°C. LL3.7 vector-based lentiviral particles were resuspended in CDM-2 media whereas pCDH or pLV-hTERT-IRES-hygro vector-based lentiviral particles were resuspended in 1x PBS, aliquoted and stored at −80°C.

To infect the cells by pCDH or pLV-hTERT-IRES-hygro based-lentiviral particle, the TCID50 of lentiviral particles was calculated. The frozen viral aliquot was resuspended in 0.5-1 ml of appropriate media with 8 μg/ml polybrene. The target cells were incubated with lentiviral particles (MOI = 10) for 24 h, at 37˚C and 5% CO_2. After 72 h of culture, cells were selected with appropriate selection antibiotic. The LL3.7 vector-based lentiviral particles were tittered by infecting HEK cells and counting GFP-positive cells [61].

2.5.Blastocyst collection and transfer

All animal procedures were approved by Institutional Animal Care and Use Committee at Colorado State University, Fort Collins, Colorado, USA. Blastocysts collection and transfer was done following the procedure previously described by Baker at al [61]. A group of 12 ewes at day 6-12 of estrus were synchronized by two intramuscular injections of PGF-2α (10 mg/dose) given at interval of 4 h (Lutalyse; Pfizer, New York, NY). After 48 h of estrus synchronization, 4 ewes were separated to be used as recipients while 8 donor ewes were bred by intact rams. At day 9, donor ewes were euthanized using pentobarbital sodium (90 mg/kg iv, Pentasol; Vibrac, Fort Worth, TX, USA), and blastocysts were flushed from the uterus using DMEM-F-12 (1:1) medium supplemented with 0.25% BSA. The hatched blastocysts were infected with 100,000 shRNA expressing lentiviral particles in a 100μl drop of CDM-2 media with 5μg/ml polybrene (Sigma-Aldrich, St. Louis, MO, USA). Blastocysts with lentiviral particles were kept in incubator for 4-5 h at 5% CO2, 5% O2 and 38.5°C. Overnight fasted recipient ewes were sedated using ketamine

(12.5 mg/kg iv, Ketacine; VetOne, Boise, ID, USA) and diazepam (0.125 mg/kg iv; Hospira, Lake Forest, IL, USA). Surgical procedure was performed under general anesthesia on 2 l/min O2 and 2–4% isoflurane (Fluriso; VetOne, Boise, IS, USA). A total of 23 blastocysts were transferred including 6 SC, 7 AKD and 10 BKD. One blastocyst was transferred in each recipient.

2.6.Tissue collection

For analysis of LIN28A or LIN28B knockdown and its effect on conceptus elongation, terminal surgeries were conducted on recipient ewes 16 dGA, and tissues were collected. Conceptuses were flushed from the uterus using DMEM-F-12 (1:1) medium. After separating the embryo, trophectoderm length was measured, and both embryo and TE were snap frozen. TE samples were used to extract mRNA, miRNA or proteins for further analysis.

2.7.Cell lines

Day 16 TE from 3 non-infected pregnancies was minced in DMEM-F-12 (1:1) medium supplemented with 10% bovine serum albumin, 1x penicillin-streptomycin-amphotericin B solution, 10 µg/ml insulin, 0.1 mM non-essential amino acids, 2mM glutamine, and 1 mM sodium pyruvate. The minced tissue was spun down at 1000 rpm for 5 minutes and the supernatant was incubated in a 100 mm collagen treated tissue culture dish, at 37°C and 5% CO_2. After 24 h, the cells attached to the plate were washed and incubated with fresh complete medium. After 48-72 h, the cells were passaged and later collected at passage number 4-6 at 70-80% confluency to extract mRNA, miRNA and proteins for further analysis. Western blot analysis for cytokeratin-7 (CK-7) was done to confirm if the phenotype of OTR cells. To generate immortalized ovine trophoblast cells (iOTR cells), the OTR cells were infected with pLV-hTERT-IRES-hygro based-lentiviral particles resuspended in complete DMEM-F12 (1:1) medium supplemented with 8 µg/ml polybrene transfection reagent. The media with viral particles was replaced with fresh media after

24 h. The cells were selected in complete DMEM-F12 (1:1) medium supplemented with 300-500 µg/ml hygromycin B (Sigma-Aldrich, St. Louis, MO, USA).

2.8.Overexpression of LIN28A and LIN28B

To overexpress *LIN28* genes in iOTR cells, pCDH-LIN28A or pCDH-LIN28B-based lentiviral particles were used to infect iOTR cells at 70-80% confluency in one well of a 12-well plate (Corning Inc., Corning, NY, USA). After 48-72 hours, the infected cells were selected using 2-4 µg/ml puromycin. Successful gene knock-in was confirmed using real-time RT-PCR and western blot analysis. iOTR cells with knock-in of LIN28A (AKI) or LIN28B (BKI). iOTR cells infected with empty-expression vector based lentiviral particles were used to generate expression vector control (EVC) iOTR cells.

2.9.RNA extraction and real-time RT-PCR

For real-time RT-PCR analysis, mRNA was isolated from day 16 sheep TE, OTR cells and iOTR cells using RNeasy Mini Kit (Qiagen Inc. Germantown, MD, USA), following the manufacturer's protocol. The mRNA was reverse transcribed to cDNA using iScript cDNA synthesis kit (Bio-Rad Laboratories, Hercules, CA, USA). Real-time RT-PCR reactions were run in triplicate in 384-well plates, using 10µl reaction volume in each well. The reaction volume included 5µl of 2x Light-Cycler 480 SYBR Green I Master (Roche Applied Science, Penzberg, Germany), 50ng reverse-transcribed mRNA and 1µM of target specific forward and reverse primers. Primer sequences used for real-time RTPCR are listed in table 8. PCR reactions were incubated in the Light-Cycler 480 PCR machine (Roche Applied Science, Penzberg, Germany) at the following cycling conditions: 95˚C for 10 min, 45 cycles of 95˚C for 30 seconds, 55˚C for 1 minute, and 72˚C for 1 min. Relative mRNA levels were normalized using *RPS15.* For miRNA profiling, total RNA was extracted using a miRNeasy Mini Kit (Qiagen Inc. Germantown, MD,

USA), following the manufacturer's protocol. 300 ng total RNA was reverse transcribed to cDNA using miScript RT II kit (Qiagen Inc. Germantown, MD, USA). Real-time RT-PCR reactions were run in triplicate in 384-well plates, using 10µl reaction volume in each well. The reaction volume included 5µl of 2x QuantiTech SYBR Green Master Mix (Qiagen Inc. Germantown, MD, USA), 3ng cDNA, 1x miScript universal primer (Qiagen Inc. Germantown, MD, USA) and 1x miScript assay for *let-7* miRNAs (*let-7a, let-7b, let-7c, let-7d, let-7e, let-7f, let-7g, let-7i*). These reactions were incubated in the Light-Cycler 480 PCR machine (Roche Applied Science, Penzberg, Germany) at following cycling conditions: 95˚C for 15 minutes, 45 cycles of 94˚C for 15 seconds, 55˚C for 30 seconds, and 70˚C for 30 seconds. Relative miRNA levels were normalized using *SNORD-48*.

2.10. Protein Extraction and Western Blot

Western blot analysis was performed using whole cell lysate to quantify proteins in cells and tissue samples. For protein extraction, cell pellets were resuspended in 200-400 µl RIPA buffer (20 mM Tris, 137 mM NaCl, 10% glycerol, 1% nonidet P-40, 3.5 mM SDS, 1.2 mM sodium deoxycholate, 1.6 mM EDTA, pH 8) containing 1x protease/phosphate inhibitor cocktail (Sigma-Aldrich, St. Louis, MO, USA). Whole cell lysate was incubated on ice for 5 min and then centrifuged at 14,000 g for 5 min to remove cell debris. To extract protein from day 16 TE, the tissue was homogenized in RIPA buffer. Homogenized samples were sonicated using a Bioruptor Sonication System (Diagenode, Denville, NJ, USA) for 5 cycles of 30 seconds "ON" and 30 seconds "OFF". Sonicated samples were centrifuged at 14,000 g for 5 minutes to remove debris. Protein concentration was measured using the BCA protein assay kit (ThermoFisher, Waltham, MA, USA). Protein was separated in 4-15% Bis-Tris gels (Bio-Rad Laboratories, Hercules, CA, USA) at 90 volts for 15 min and 125 volts for 60 min, and then transferred to 0.45 µm pore size

nitrocellulose membrane (Bio-Rad Laboratories, Hercules, CA, USA) at 100 volts for 2 hours at 4°C. The membranes were then blocked in 5% non-fat dry milk solution in TBST (50 mM Tris, 150 mM NaCl, 0.05% Tween 20, pH 7.6) for 1 hour at room temperature. After blocking, the membranes were washed 3 times with 1x TBST for 5 min each, and then incubated at 4°C overnight with specific primary antibody. After overnight incubation, the membranes were washed 3 times with 1x TBST for 5 min each. After washing, the membranes were incubated with appropriate secondary antibody conjugated to horseradish peroxidase for 1 hour at room temperature. After removing the secondary antibody, the membranes were washed following the same procedure and developed using Super Signal WestDura Extended Duration Substrate (ThermoFisher, Waltham, MA, USA) and imaged using ChemiDoc XRS+ chemiluminescence system (Bio-Rad Laboratories, Hercules, CA, USA). The images were quantified using Image-Lab software (Bio-Rad Laboratories, Hercules, CA, USA). To normalize protein quantity, β-actin, α-tubulin, or GAPDH were used as loading control. Each experiment was repeated on three replicates. The antibodies used and their dilutions are listed in table 9.

2.11. Cell Proliferation Assay

Cell proliferation was measured using Quick Cell Proliferation Assay Kit (Abcam, Cambridge, MA, USA) following manufacturer's protocol. This assay is based on cleavage of tetrazolium salt (WST-1) to formazan by mitochondrial dehydrogenases. EVC, AKI and BKI iOTR cells were plated to a density of 1000 cells/100 µl in 96-well tissue culture plates, with four replicates of each cell type. After 4, 24, 48 or 96 hours of plating the cells, 10 µl WST-1 reagent was added in each well followed by incubation for 2 hours in standard culture conditions. Absorbance was measured using Cytation 3 Multi-Mode Reader (BioTek Instruments, Inc., VT, USA) at 440 nm with reference wavelength of 650 nm.

2.12. Matrigel Invasion Assay

Cell invasion was measured using Corning BioCoat Tumor Invasion System (Corning, New York, NY, USA) following manufacturer's protocol. EVC, AKI and BKI iOTR cells were stained with CellTracker™ Green 5-chloromethylfluorescein diacetate (CMFDA) (Invitrogen, Carlsbad, CA, USA). Four replicates of each cell line were plated at a density of 10,000 cells/500 µl DMEM/F-12 (1:1) media without phenol red and fetal bovine serum, in a 24-multiwell insert plate with 8 µm pore size polyethylene terephthalate membrane coated with uniform layer of matrigel matrix. DMEM/F-12 (1:1) media without any cells was added in four wells to be used as blank. In the bottom wells, 750 µl of DMEM/F-12 (1:1) media with 10% fetal bovine serum was added. Plates were read at 2, 4, 24 and 48 hours after plating the cells using Cytation 3 Multi-Mode Reader (BioTek Instruments, Inc., VT, USA) with top and bottom reading ability, at 492 nm excitation and 517 nm emission wavelengths. The invasion index was calculated using the formula: (RFU of cells at the bottom/RFU of cells at top + RFU of cells at bottom) x 100.

2.13. Statistics

All data were analyzed using GraphPad Prism 7 Software. To determine significance of mRNAs, miRNAs and proteins, t-test was used when comparing two groups and analysis of variance followed by Tukey's HSD post-hoc test was done when comparing three groups. P values less than 0.05 were considered statistically significant. The error bars in the figures indicate standard error of the mean (SEM).

3. Results

3.1.LIN28 knockdown in trophectoderm results in reduced proliferation of trophoblast cells and lower expression of proliferation-associated genes

Day 9 hatched blastocysts were infected with lentiviral particles expressing shRNA to knockdown LIN28A (AKD) or LIN28B (BKD), or scramble control shRNA (SC). The blastocysts treated with lentiviral particles were surgically transferred to synchronized ewes at day 9 of estrus. The conceptuses were collected at day 16 of gestation and trophectoderm (TE) was separated from embryo. LIN28A and LIN28B mRNAs and proteins were quantified by real-time RT-PCR and western blot. LIN28A mRNA and protein was significantly reduced in AKD TE while LIN28B mRNA and protein was significantly reduced in BKD TE compared to SC (Fig. 19A-B). As expected due to reduced LIN28, *let-7* miRNAs (*let-7a, let-7b, let-7c, let-7d, let-7e, let-7f, let-7g, let-7i*) were significantly higher in AKD and BKD TE compared to SC, and there was no significant change in *let-7* miRNAs between AKD and BKD TE (Fig. 19C). These results suggest that reduced LIN28A or LIN28B led to significant increase in *let-7* miRNAs.

To determine the effect of LIN28 knockdown on conceptus elongation, we measured the length of TE. Knockdown of LIN28A or LIN28B resulted in a significant reduction in day 16 TE length compared to SC (Fig. 20A-B). There was no significant difference in elongation of AKD *vs* BKD TE. This data suggests knockdown of either LIN28A or LIN28B *in vivo* resulted in reduced proliferation of trophoblast cells.

Due to the potential for reduced proliferation of trophoblast cells in the AKD and BKD conceptuses, we measured the mRNA and protein levels of *let-7*-regulated proliferation-associated genes. The mRNA and protein levels of IGF2BP1, IGF2BP2, IGF2BP3, HMGA1, ARID3B and c-MYC were significantly reduced in AKD and BKD day 16 TE compared to SC (Fig. 21, 22).

These results suggest that high *let-7* miRNAs in AKD and BKD TE led to a significant reduction in expression of IGF2BP1, IGF2BP2, IGF2BP3, HMGA1, ARID3B and c-MYC, and the reduced proliferation of trophoblast cells in AKD and BKD TE is due to significantly reduced expression of these proliferation-associated genes.

3.2.Ovine trophoblast cells generated from day 16 trophectoderm have a significant reduction in LIN28

To further investigate the regulation of ovine trophoblast cell proliferation by LIN28 *in vitro,* we used day 16 TE to generate ovine trophoblast cells. The day 16 TE was minced and plated in collagen coated plates and were passaged to obtain a cell line. The cells used for further experiments were collected at passage 4-6, so we called these cells non-immortalized ovine trophoblast (OTR) cells. Interestingly, real-time RT-PCR data showed that OTR cells had a significant reduction in *LIN28A* and *LIN28B* mRNAs compared to day 16 TE (Fig. 23A). Densitometric analysis of western blots showed that LIN28A and LIN28B proteins were also significantly reduced in OTR cells compared to day 16 TE (Fig. 23B). Furthermore, real-time RT-PCR data showed significant increase in *let-7* miRNAs (*let-7a, let-7b, let-7c, let-7d, let-7e, let-7f, let-7g, let-7i*) in OTR cells compared to day 16 TE (Fig. 23C). The significantly reduced LIN28 and high *let-7* miRNAs in OTR cells after only 4-6 passages suggest that these cells have differentiated to a different phenotype compared to trophoblast cells in day 16 TE.

The effect of low LIN28 and high *let-7* miRNAs on proliferation-associated genes in OTR cells was determined by measuring IGF2BP1, IGF2BP2, IGF2BP3, HMGA1, ARID3B and c-MYC mRNAs and proteins. Real-time RT-PCR showed that mRNA levels of *IGF2BP1, IGF2BP2, IGF2BP3, HMGA1, ARID3B* and *c-MYC* were significantly reduced in OTR cells compared to day 16 TE (Fig. 24). Densitometric analysis of western blots revealed a significant

reduction in protein levels of IGF2BP1, IGF2BP2, IGF2BP3, HMGA1, ARID3B and c-MYC in OTR cells compared to day 16 TE (Fig. 25). These results suggest that reduced LIN28 and high *let-7* miRNAs led to reduced expression of proliferation-associated genes in OTR cells.

The OTR cells originated from day 16 TE undergo senescence after only a few passages. Therefore, the OTR cells were immortalized by overexpressing hTERT to keep them growing for further *in vitro* experiments. The newly generated immortalized cells were referred to as immortalized ovine trophoblast (iOTR) cells.

3.3.Overexpression of LIN28 in iOTR cells results in increased proliferation and expression of proliferation-associated genes

To determine if LIN28 overexpression will rescue the expression of proliferation-associated genes, the iOTR cells were infected with lentiviral particles expressing LIN28A (AKI) or LIN28B (BKI), or lentiviral particles with empty expression vector as expression vector control (EVC). Real-time RT-PCR data showed that AKI iOTR cells had a significant increase in *LIN28A* mRNA while BKI iOTR cells had a significant increase in *LIN28B* mRNA compared to EVC (Fig. 26A). The densitometric analysis of western blots showed a significant increase in LIN28A protein in AKI and significant increase in LIN28B protein in BKI iOTR cells compared to EVC (Fig. 26B). Moreover, the real-time RT-PCR data showed that *let-7* miRNAs (*let-7a, let-7b, let-7c, let-7d, let-7e, let-7f, let-7g, let-7i*) were significantly reduced in both AKI and BKI iOTR cells compared to EVC (Fig. 26C). These results suggest that increased expression of either LIN28A or LIN28B leads to reduction in *let-7* miRNAs.

To determine the effect of LIN28 overexpression and reduction in *let-7* miRNAs on expression of proliferation-associated genes, real-time RT-PCR and western blot analysis were done. Real-time RT-PCR showed that mRNA levels of *IGF2BP1, IGF2BP2, IGF2BP3, HMGA1,*

ARID3B and *c-MYC* were significantly increased in both AKI and BKI iOTR cells compared to EVC (Fig. 27). Densitometric analysis of western blots showed significant increase in IGF2BP1, IGF2BP2, IGF2BP3, HMGA1, ARID3B and c-MYC proteins in both AKI and BKI iOTR cells compared to EVC (Fig. 28). These results suggest that the expression of proliferation-associated genes in immortalized ovine trophoblast cells is regulated by the LIN28-*let-7* axis.

3.4.Overexpression of LIN28 led to significant increase in trophoblast cell proliferation

The role of LIN28-*let-7* miRNA axis on the functionality of iOTR cells was determined by measuring proliferation of AKI and BKI iOTR cells compared to EVC after 4 h, 24 h, 48 h and 72 h. The results showed that proliferation of both AKI and BKI iOTR cells was significantly increased at 24 h, 48 h and 72 h compared to EVC (Fig. 29A). Furthermore, proliferation of BKI iOTR cells was not different at 24 h but was significantly higher at 48 h and 72 h compared to AKI iOTR cells (Fig. 29A). The matrigel invasion assay showed that there was no significant change in the invasion index of AKI and BKI iOTR cells compared to EVC (Fig. 29B). These results suggest that increased proliferation of AKI and BKI iOTR cells is due to increased expression of proliferation-associated genes in these cells compared to EVC.

4. Discussion

The pluripotency factors LIN28A and LIN28B inhibit the maturation of *let-7* miRNAs [39,62]. Recently, we showed that both Lin28A and LIN28B were significantly decreased and levels of *let-7* miRNAs (*let-7a, let-7b, let-7c, let-7d, let-7e, let-7f, let-7g, let-7i*) were significantly increased in term human placentas from IUGR pregnancies compared to control pregnancies [18]. We further demonstrated that double knockout of LIN28A and LIN28B in immortalized first trimester human trophoblast (ACH-3P) cells resulted in significantly increased *let-7* miRNAs [18]. In this study, we show that RNA interference (RNAi) of LIN28A or LIN28B in sheep TE *in vivo*

resulted in significant increase in *let-7* miRNAs (*let-7a, let-7b, let-7c, let-7d, let-7e, let-7f, let-7g, let-7i*). Moreover, the conceptus elongation was significantly reduced after RNAi of LIN28A or LIN28B in TE.

Although animal models with global gene knockout or knockdown have been extensively and successfully used in many studies, it is difficult to exclude the effect of global gene manipulation while focusing on mechanisms involved in one tissue type or organ. Incubating the day 9 hatched sheep blastocyst with shRNA expressing lentiviral particles causes viral infection of only trophoblast cells while all other cells including the inner cell mass are spared of lentiviral infection [61]. Hence, significant reduction in LIN28A or LIN28B in day 16 TE conceptus is restricted to the trophoblast cells only. Conceptus elongation in sheep is due to rapid proliferation of trophoblast cells [7–9], therefore a significant reduction in conceptus length at day 16 after trophectoderm-specific LIN28A or LIN28B knockdown indicates reduced proliferation of trophoblast cells.

LIN28 is a part of a complex genetic pathway known to regulate multiple downstream targets [66]. Inhibition of biogenesis of mature *let-7* miRNAs is one of the main pathways through which LIN28 regulates the expression of its downstream targets [67]. *Let-7* miRNAs reduce expression of many genes by degrading their mRNAs or inhibiting translation [39]. Our results show that RNAi of LIN28A or LIN28B and resultant increase in *let-7* miRNAs in day 16 TE significantly reduced IGF2BP1, IGF2BP2, IGF2BP3, HMGA1, ARID3B and c-MYC. Previous studies have shown the role of IGF2BP1, IGF2BP2, IGF2BP3, HMGA1, ARID3B and c-MYC in cell proliferation [17,38–40,40,43,45,46,48,51], suggesting that reduced proliferation of trophoblast cells after LIN28A or LIN28B knockdown in TE is due to reduced expression of proliferation-associated genes (Fig. 30).

To further investigate the role of the LIN28-*let-7* miRNA axis in sheep trophoblast cells *in vitro*, OTR cells were generated from day 16 TE. Surprisingly, both LIN28A and LIN28B were depleted and the *let-7* miRNAs were significantly higher in OTR cells compared to day 16 TE. The senescence of OTR cells after only a few passages along with high *let-7* miRNAs suggests that these cells are a differentiated phenotype of trophoblast cells compared to day 16 TE. Furthermore, the expression of proliferation-associated genes including IGF2BP1, IGF2BP2, IGF2BP3, HMGA1, ARID3B and c-MYC was also significantly reduced in OTR cells compared to day 16 TE. To overcome the OTR cell senescence, we generated immortalized ovine trophoblast (iOTR) cells by expressing hTERT in these cells. Immortalized human first trimester trophoblast cells (Sw.71 cells) were also generated by expressing hTERT in first trimester human trophoblast cells at passage 3 [68]. Sw.71 cells also have depleted LIN28A and LIN28B and high *let-7* miRNAs compared to other trophoblast-derived cell lines such as ACH-3P cells [18]. The iOTR cells generated in this study are similar to Sw.71 cells in terms of LIN28 and *let-7* miRNAs expression, which may be because both cell lines were generated by immortalizing the passaged trophoblast cells. The contrasting levels of LIN28, *let-7* miRNAs and *let-7* miRNA target genes between day 16 TE and iOTR cells should be taken in consideration if using these cells for further studies.

To generate iOTR cells that are more similar to day 16 TE, we overexpressed LIN28A or LIN28B in iOTR cells. Overexpression of LIN28A or LIN28B in iOTR cells led to a significant decrease in *let-7* miRNAs and significant increase in expression of IGF2BP1, IGF2BP2, IGF2BP3, HMGA1, ARID3B and c-MYC compared to control. Additionally, the proliferation of both AKI and BKI iOTR cells was significantly increased compared to control. These results suggest that the LIN28-*let-7* miRNA axis plays a role in proliferation of iOTR cells by regulating the

expression of genes associated with cell proliferation. We suggest that the iOTR cells overexpressing LIN28A and LIN28B would be a better choice to study molecular mechanisms in ovine trophoblast cells compared to iOTR cells with depleted LIN28A and LIN28B.

To our knowledge, this is the first *in vivo* study defining the role of LIN28-*let*-7 miRNA axis in early placental development by trophoblast specific RNAi of LIN28A or LIN28B. Due to wide range of *let-7* miRNAs target genes, as well as the ability of LIN28 to directly bind the mRNA of different genes, LIN28 knockdown might be affecting many different genetic pathways in trophoblast cells which are yet to be explored. Reduced conceptus elongation in LIN28A or LIN28B knockdown TE can lead to impaired placentation, fetal growth restriction, loss of pregnancy and reduced fertility in domestic ruminants.

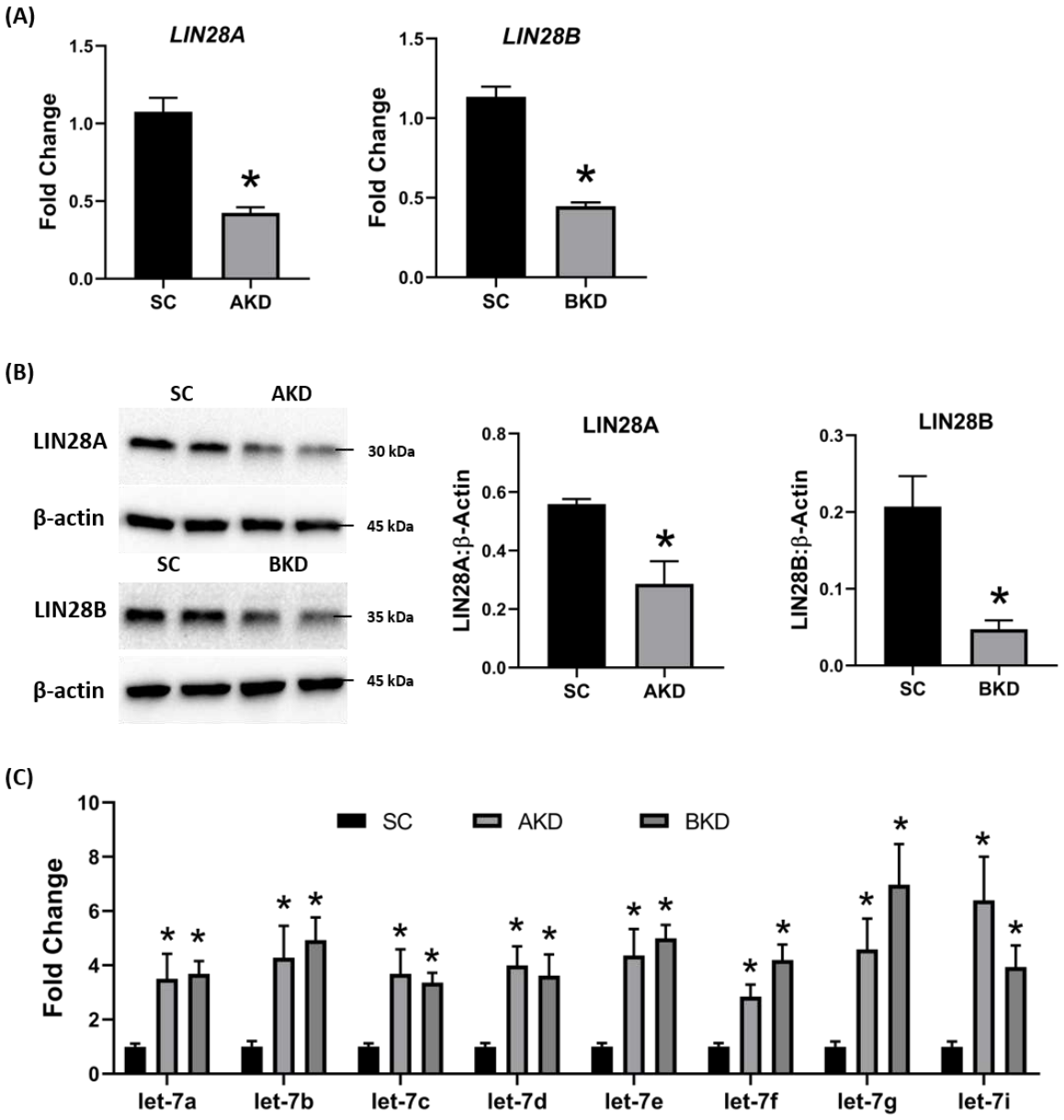

Figure 19. LIN28A or LIN28B knockdown and *let-7* miRNAs in day 16 sheep TE. (A) *LIN28A* and *LIN28B* mRNA in AKD (n=5) and BKD (n=6) day 16 TE compared to SC (n=6). (B) Representative immunoblots for LIN28A, LIN28B and β-actin in AKD, BKD and SC day 16 TE, and densitometric analysis. (C) *Let-7* miRNAs in AKD and BKD day 16 TE and SC. *P<0.05 *vs.* SC.

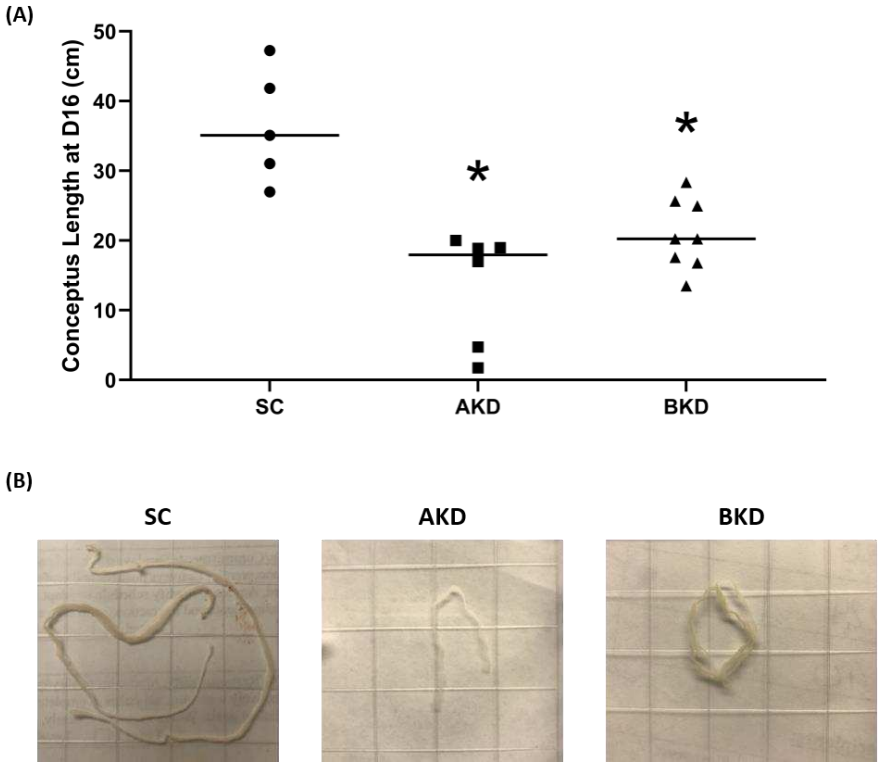

Figure 20. (A) Conceptus length at day 16 after LIN28A knockdown (n=6) and LIN28B knockdown (n=8) compared to SC (n=5). (B) Representative images of day 16 sheep conceptuses for LIN28A KD, LIN28B KD, and SC day 16 TE. *P<0.05 *vs.* SC.

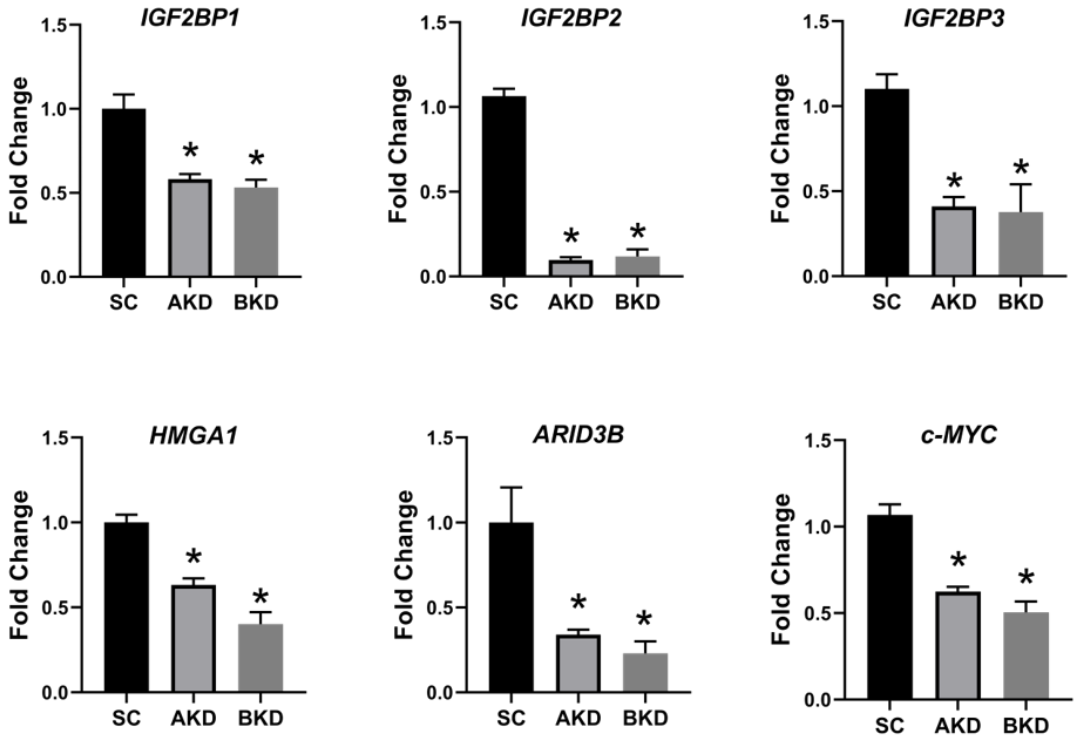

Figure 21. *IGF2BP1, IGF2BP2, IGF2BP3, HMGA1, ARID3B* and *c-MYC* mRNA in AKD and BKD day 16 TE compared to SC (n=5/treatment). *P<0.05 *vs.* SC.

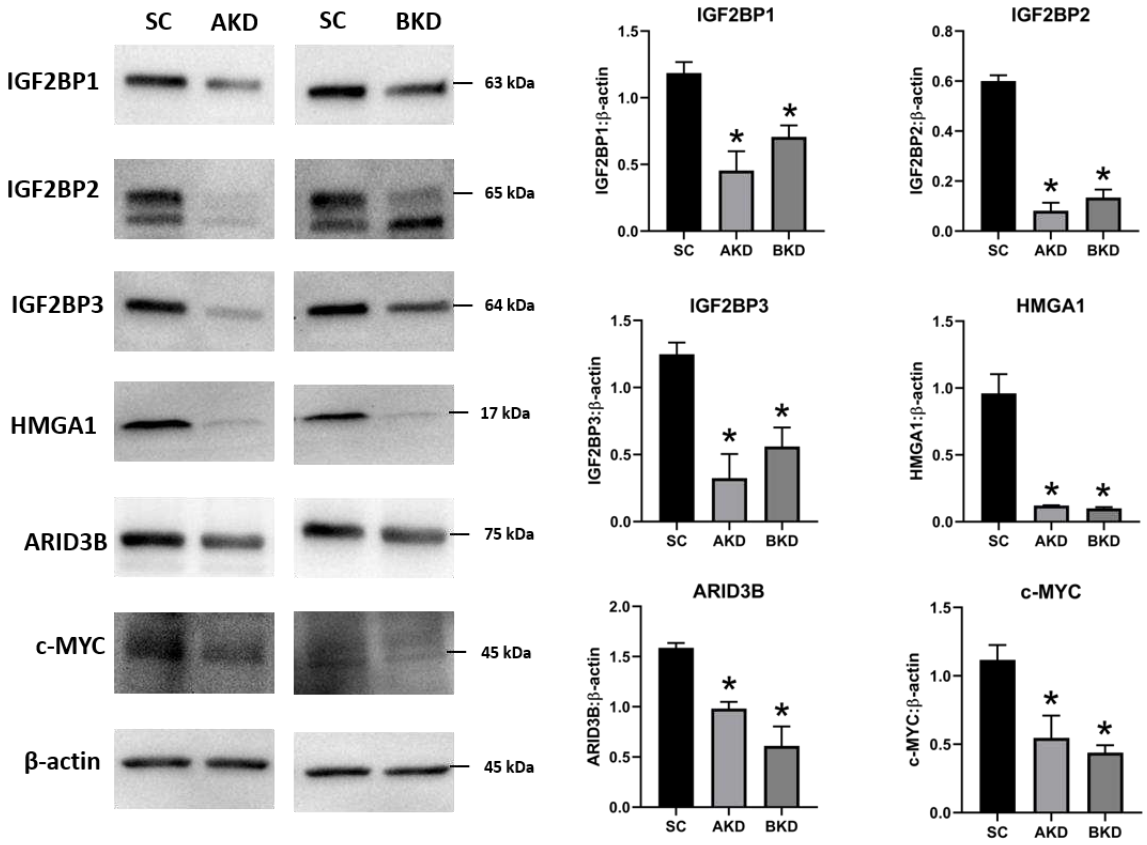

Figure 22. Representative immunoblots for IGF2BP1, IGF2BP2, IGF2BP3, HMGA1, ARID3B, c-MYC and β-actin, and densitometric analysis of immunoblotting results in AKD and BKD day 16 sheep TE compared to SC (n=3/treatment). *P<0.05 *vs.* SC.

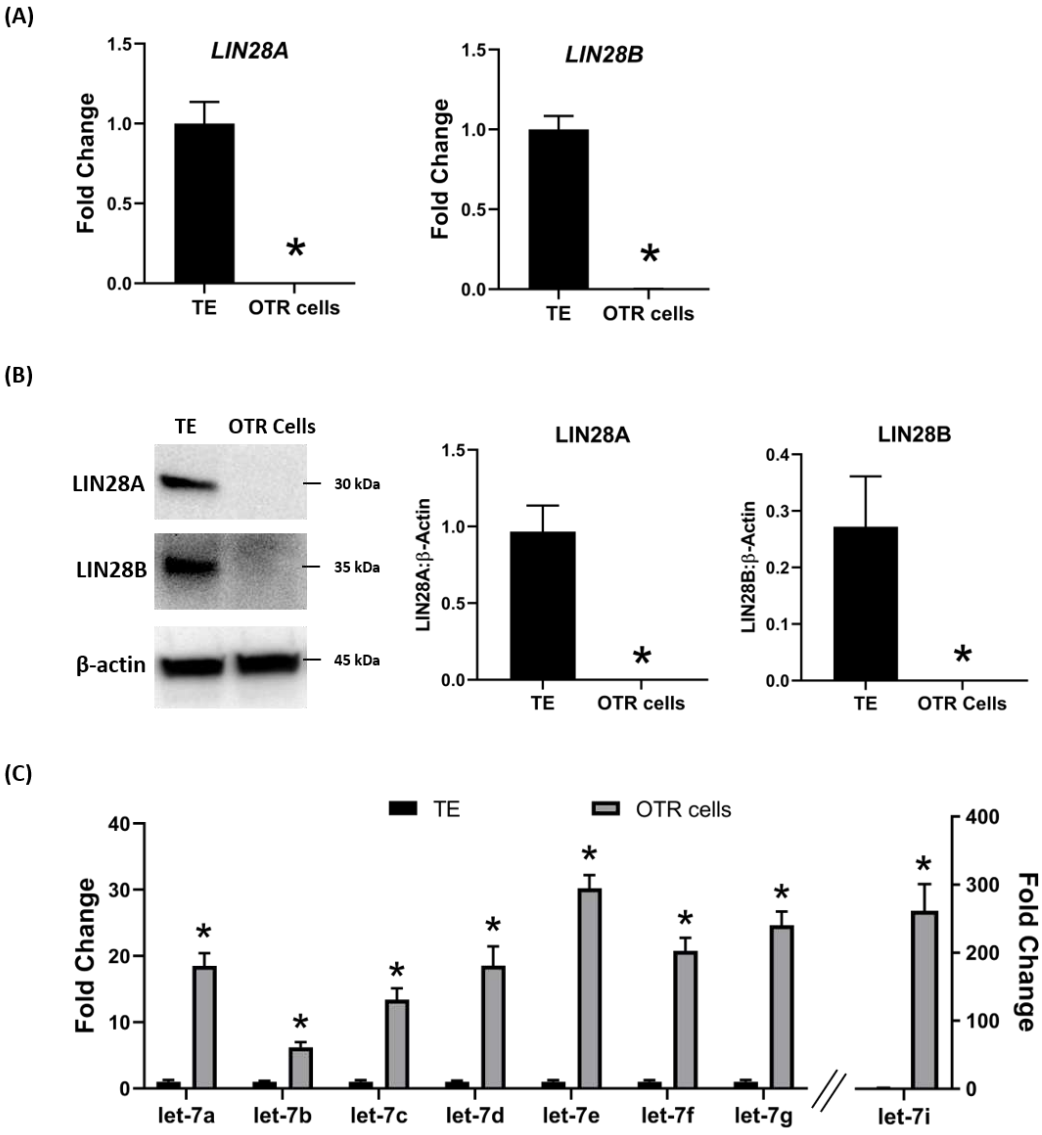

Figure 23. LIN28A, LIN28B and *let-7* miRNAs in OTR cells. (A) *LIN28A* and *LIN28B* mRNA in OTR cells compared to day 16 sheep TE. (B) Representative immunoblots for LIN28A, LIN28B and β-actin, and densitometric analysis of immunoblotting results in OTR cells compared to day 16 TE. (C) *Let-7* miRNAs in OTR cells (n=3/treatment) compared to day 16 TE (n=3). *P<0.05 *vs.* TE.

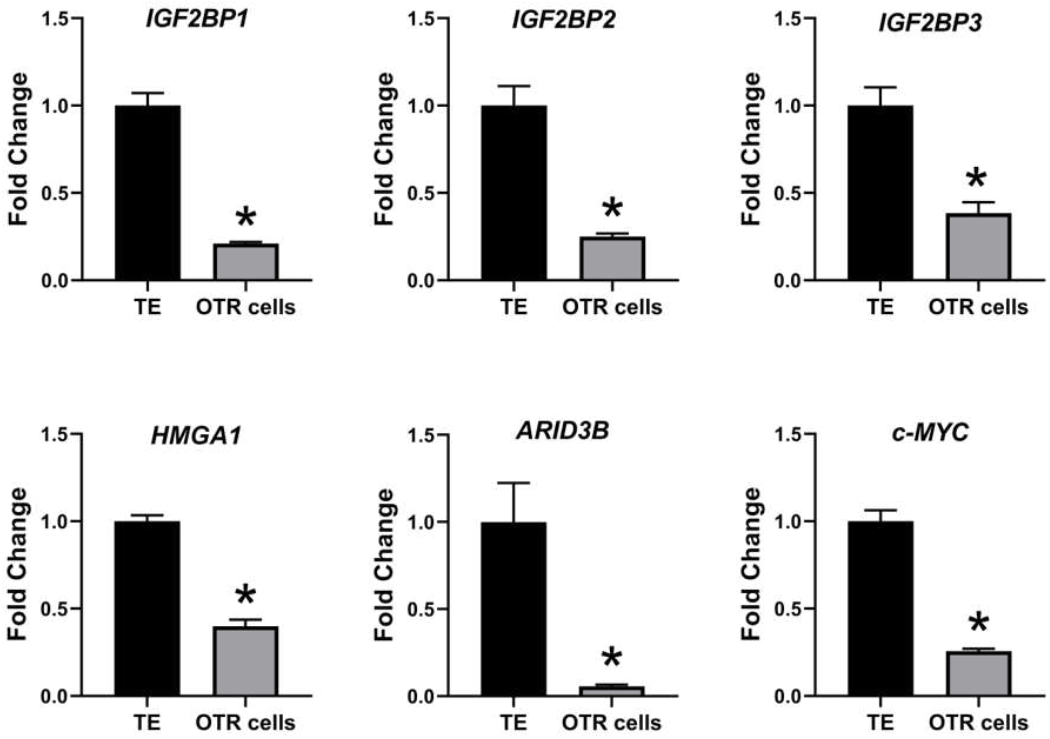

Figure 24. *IGF2BP1, IGF2BP2, IGF2BP3, HMGA1, ARID3B* and *c-MYC* mRNA in OTR cells compared to day 16 TE (n=3/treatment). *P<0.05 *vs.* TE.

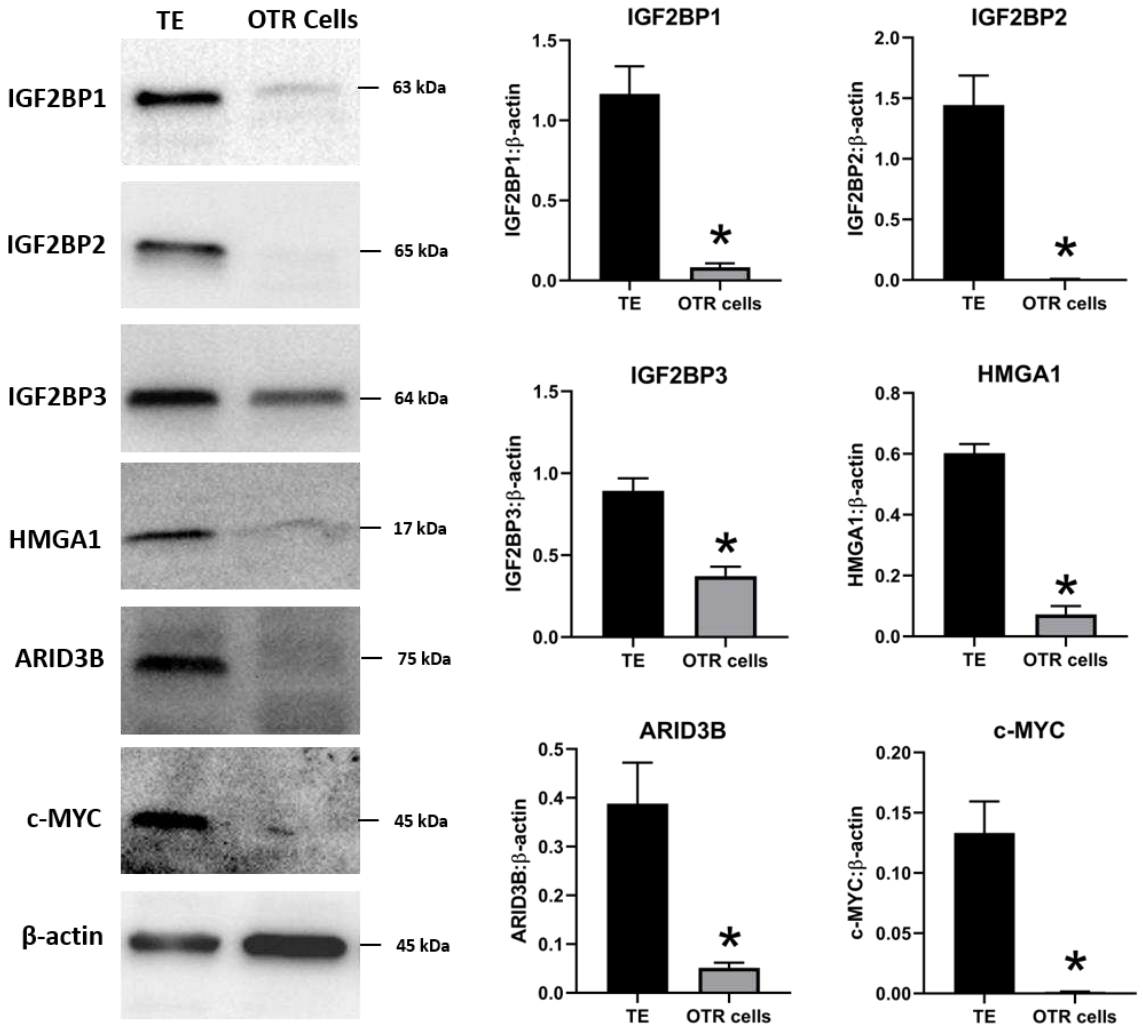

Figure 25. Representative immunoblots for IGF2BP1, IGF2BP2, IGF2BP3, HMGA1, ARID3B, c-MYC and β-actin, and densitometric analysis of immunoblotting results in OTR cells compared to day 16 TE (n=3/treatment). *P<0.05 *vs.* TE.

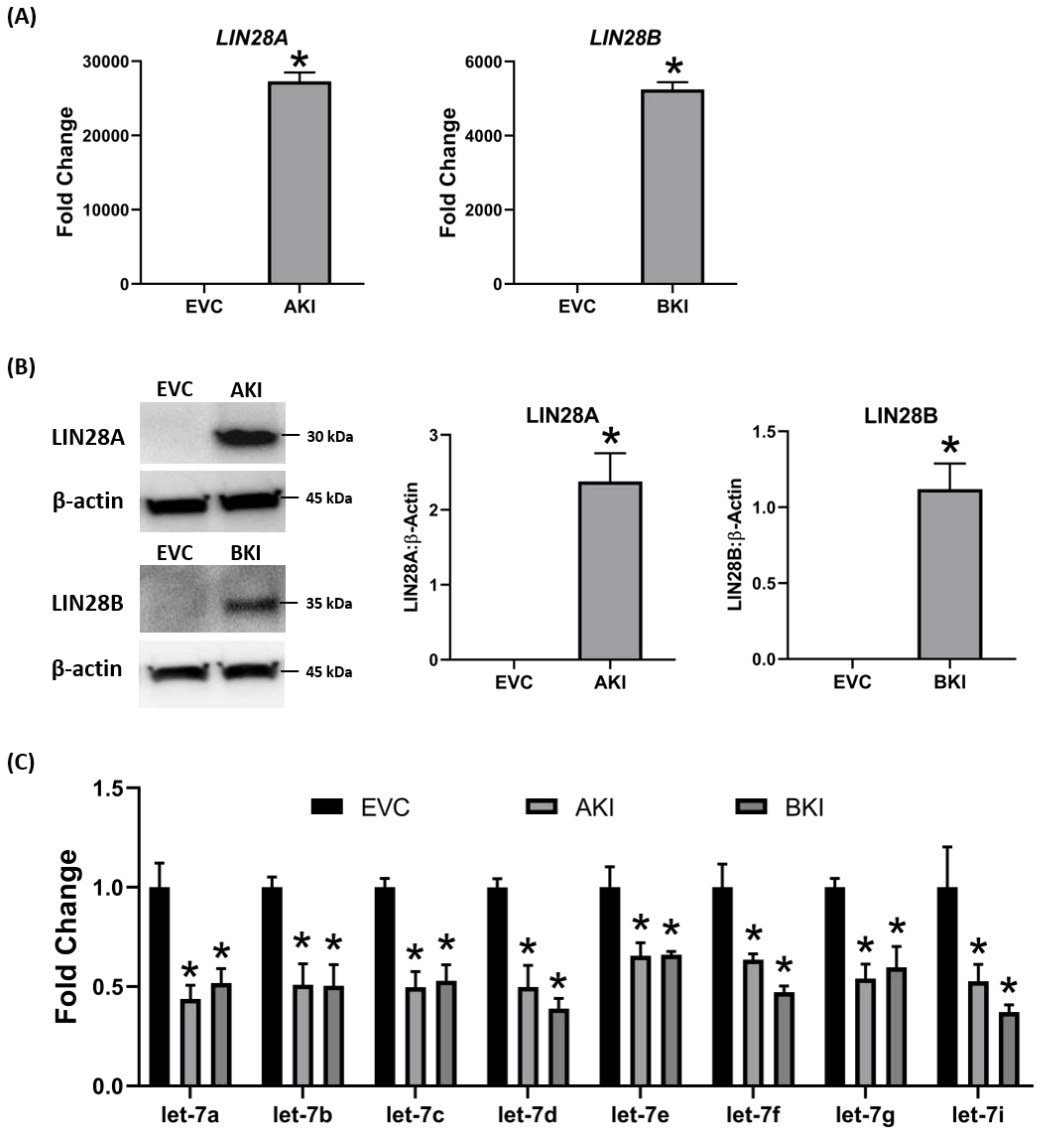

Figure 26. LIN28A, LIN28B and *let-7* miRNAs in AKI and BKI iOTR cells. (A) *LIN28A* and *LIN28B* mRNA in AKI and BKI iOTR cells compared to EVC. (B) Representative immunoblots for LIN28A, LIN28B and β-actin, and densitometric analysis of immunoblotting results in AKI and BKI iOTR cells compared to EVC. (C) *Let-7* miRNAs in AKI and BKI iOTR cells compared to EVC (n=3/treatment). *P<0.05 *vs.* EVC.

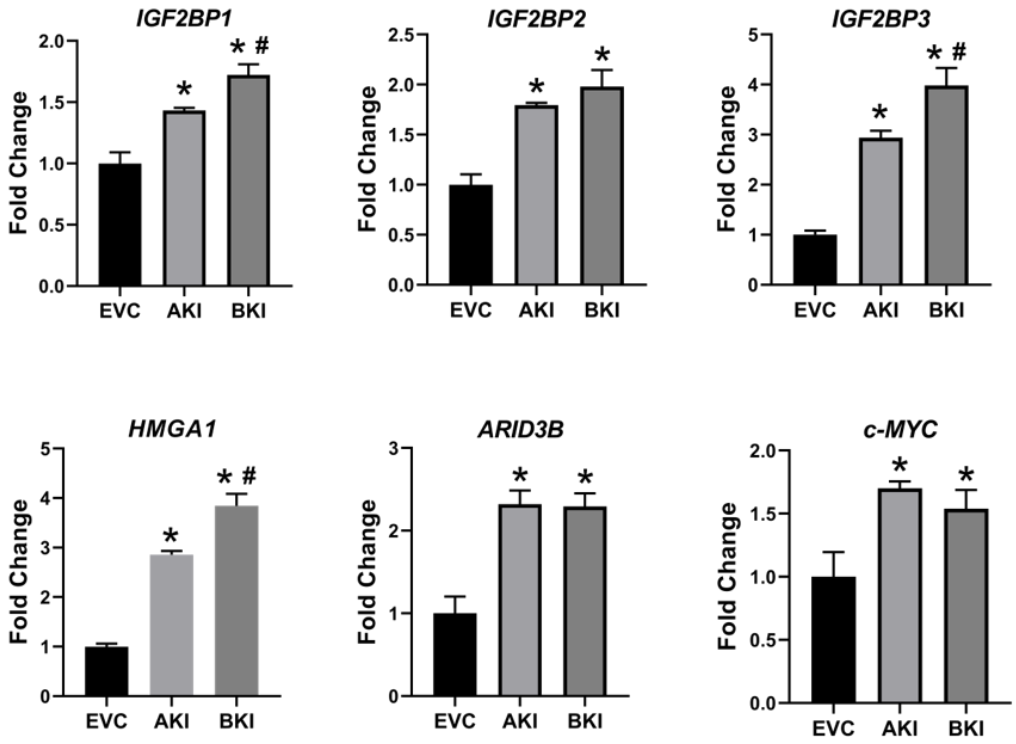

Figure 27. *IGF2BP1, IGF2BP2, IGF2BP3, HMGA1, ARID3B* and *c-MYC* mRNA in AKI and BKI iOTR cells compared to EVC (n=3/treatment). *P<0.05 *vs.* EVC; # P<0.05 vs AKI.

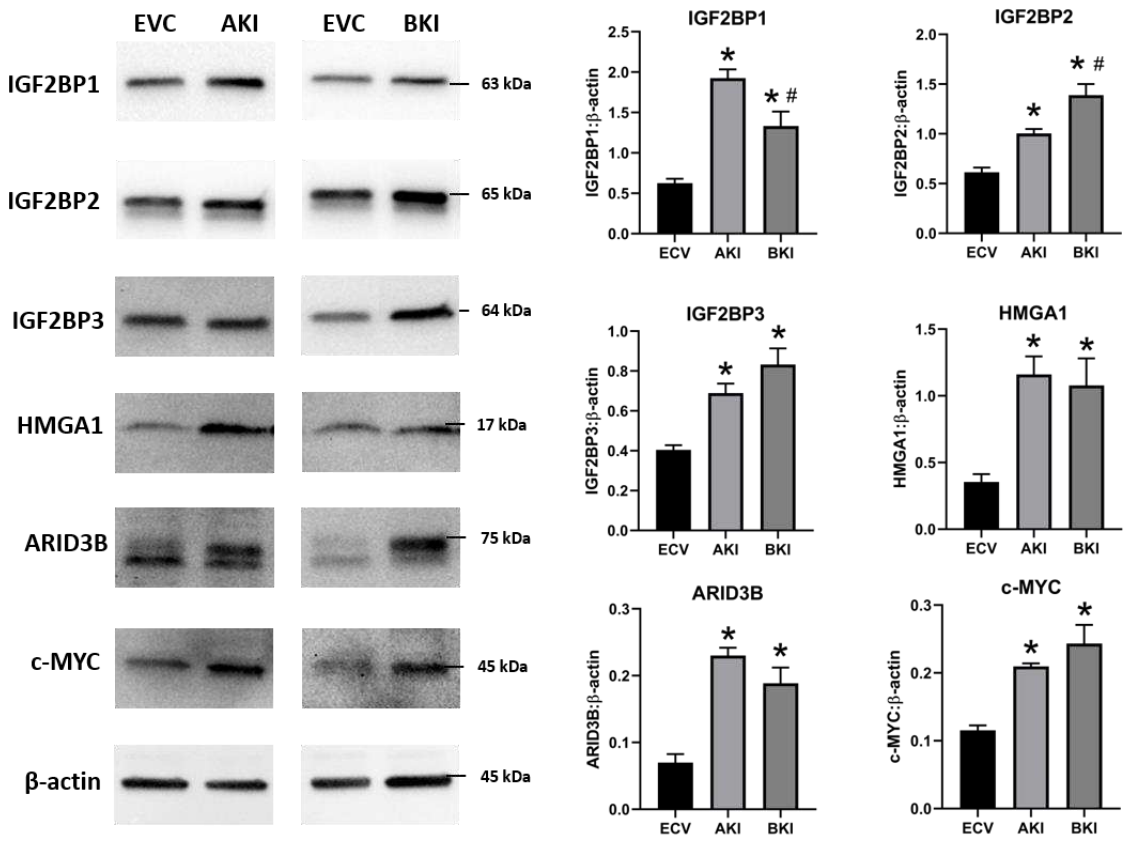

Figure 28. Representative immunoblots for IGF2BP1, IGF2BP2, IGF2BP3, HMGA1, ARID3B, c-MYC and β-actin, and densitometric analysis of immunoblotting results in AKI and BKI iOTR cells compared to EVC (n=3/treatment). *P<0.05 *vs.* EVC; # P<0.05 vs AKI.

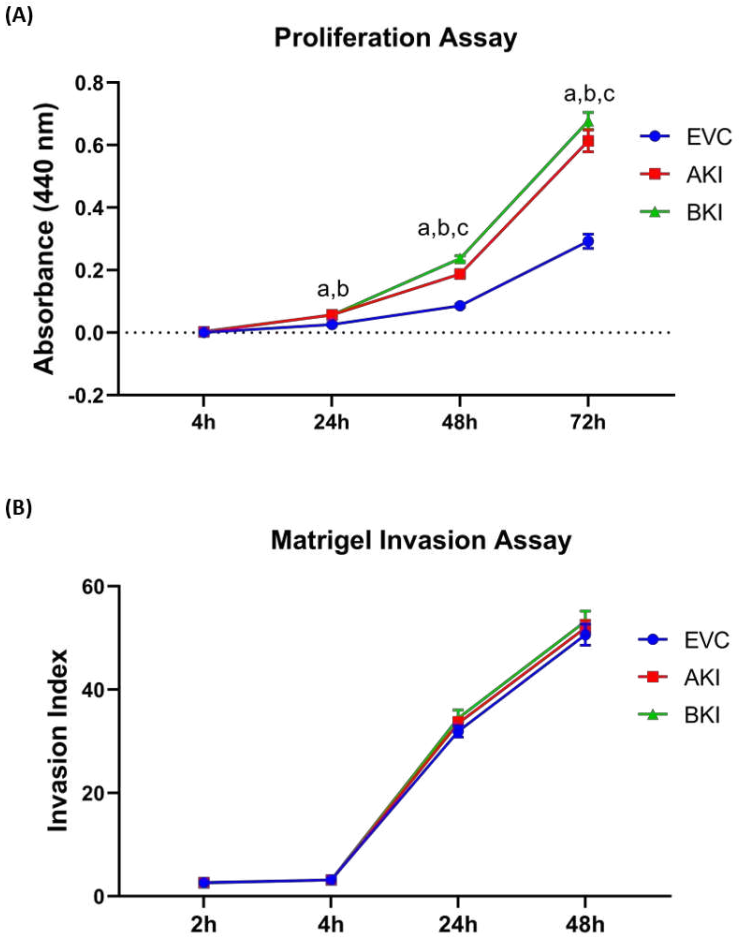

Figure 29. Proliferation and invasion of AKI, BKI and EVC iOTR cells. (A) Proliferation of AKI, BKI and EVC iOTR cells (n=4/treatment) was measured after 4h, 24h, 48h and 72h using Quick Cell Proliferation Assay Kit. (B) Invasion of AKI, BKI and EVC iOTR cells (n=4) measured after 2h, 4h, 24h and 48h using the Matrigel Invasion Assay Kit. a, $P<0.05$ for AKI vs EVC; b, $P<0.05$ for BKI vs EVC; c, $P<0.05$ for BKI vs AKI.

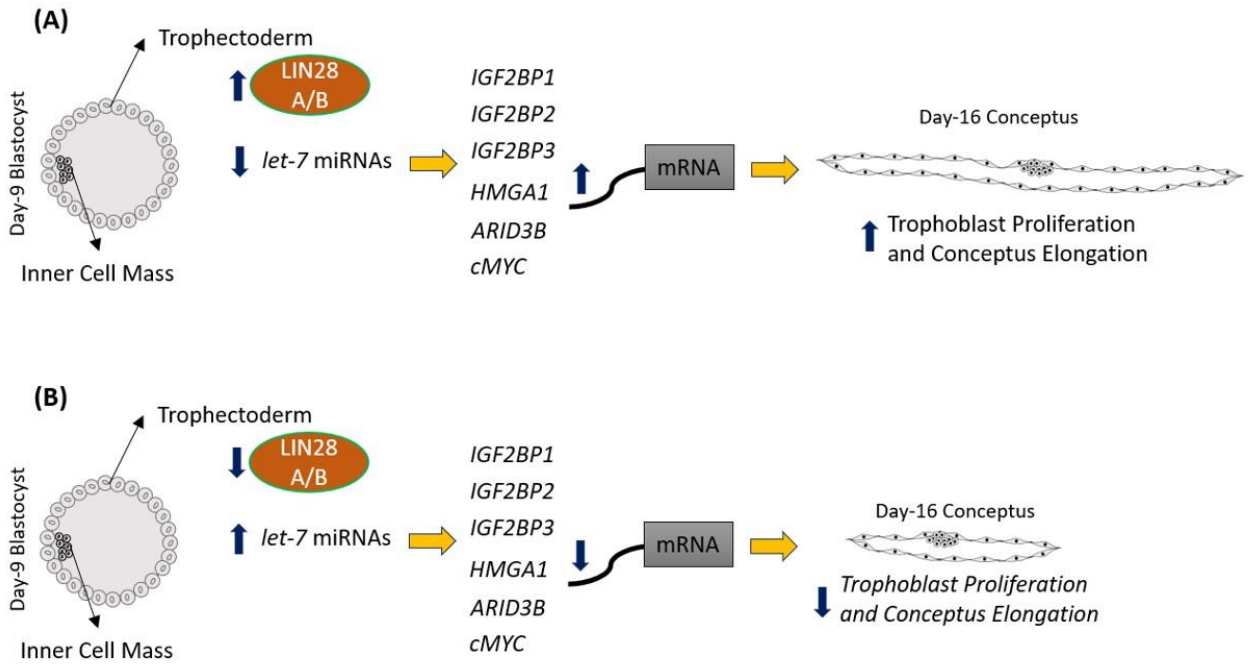

Figure 30. Graphical abstract. A) In control day 9 TE, *let-7* miRNAs are low because of high LIN28A and LIN28B. Because of low levels of let-7 miRNAs, IGF2BP1, IGF2BP2, IGF2BP3, HMGA1, ARID3B, and c-MYC are higher leading to increased proliferation of trophoblast cells and hence conceptus elongation. B) In LIN28A or LIN28B KD day 9 TE, *let-7* miRNAs are higher. Elevated let-7 miRNAs target *IGF2BP1, IGF2BP2, IGF2BP3, HMGA1, ARID3B* and *c-MYC*, leading to reduced expression of these genes leading to reduced proliferation of trophoblast cells and hence reduced conceptus elongation.

Table 6: shRNA oligos

LIN28A	Forward Oligo	5’ CCGGGCATCTGTAAGTGGTTCAACGTTCAAGAGACG TTGAACCACTTACAGATGCTTTTTG 3’
	Reverse Oligo	5’ AATTCAAAAAGCATCTGTAAGTGGTTCAACGTCTCT TGAACGTTGAACCACTTACAGATGC 3’
LIN28B	Forward Oligo	5’ CCGGGGATTCATCTCCATGATAAGCTTCAAGAGAGC TTATCATGGAGATGAATCCTTTTTG 3’
	Reverse Oligo	5’ AATTCAAAAAGGATTCATCTCCATGATAAGCTCTCT TGAAGCTTATCATGGAGATGAATCC 3’
SC	Forward Oligo	5’ CCGGAGTTAAAGGTTCGGCACGAATTCAAGAGATTC GTGCCGAACCTTTAACTCTTTTTG 3’
	Reverse Oligo	5’ AATTCAAAAAGAGTTAAAGGTTCGGCACGAATCTC TTGAATTCGTGCCGAACCTTTAACT 3’

Table 7: Primers for LIN28A and LIN28B Expression

LIN28A Expression	Forward Oligo	5’ GCTAGCCAGACTACCATGGGCTCTGTG 3’
	Reverse Oligo	5’ ATTTAAATACCCACTGTGGCTTCAATTC 3’
LIN28B Expression	Forward Oligo	5’ GCTAGCGCCGGAAAGAATTAGTTTCGC 3’
	Reverse Oligo	5’ ATTTAAATACATAACACATGACACCCT 3’

Table 8: Realtime RTPCR Primers

LIN28A	Forward Oligo	5’ GACAGGTGCTACAACTGTGGAG 3’
	Reverse Oligo	5’ ATGGCAGAGCTATGGATCTCTT 3’
LIN28B	Forward Oligo	5’ GCCTTGAATCAATACGGGTAAC 3’
	Reverse Oligo	5’ CTTCTTTGGCTGAGGAGGTAGA 3’
IGF2BP1 (IMP1)	Forward Oligo	5’ GCAACCTGAAGAAGGTGGAG 3’
	Reverse Oligo	5’ GCAGCCACGTCATTCTCATA 3’
IGF2BP2 (IMP2)	Forward Oligo	5’ TCCCGGGTAGACATCCATAG 3’
	Reverse Oligo	5’ GTGGGCCAAGATCTTCAGAG 3’
IGF2BP3 (IMP3)	Forward Oligo	5’ TGCCGCTGAGAAGTCAATTA 3’
	Reverse Oligo	5’ TCCGTCCTTCCTTACCAATG 3’
HMGA1	Forward Oligo	5’ AAGGGGAGCAAAAACAAGG 3’
	Reverse Oligo	5’ CCTCCTCTTCCTCCTTCTCC 3’
ARID3B	Forward Oligo	5’ AAGGTGATGGAGTCCCAGTG 3’
	Reverse Oligo	5’ CCTCTTCTGACAGCCTGGAC 3’
c-MYC	Forward Oligo	5’ CTTCTCCCCCTCCTCTGACT 3’
	Reverse Oligo	5’ GCCTCTTTTCCACAGAGACAA 3’
S15	Forward Oligo	5’ ATCATTCTGCCCGAGATGGTG 3’
	Reverse Oligo	5’ TGCTTGACGGGCTTGTAGGTG 3’

Table 9: Antibodies

Protein	**Vendor**	**Catalog #**	**Host Species**	**Dilution used**	**Band size**
LIN28A	Abcam	ab63740	Rabbit	1:1000	30 kDa
LIN28B	Bethyl Labs	A303-588A	Rabbit	1:2000	35 kDa
IGF2BP1	Abcam	ab82968	Rabbit	1:500	63 kDa
IGF2BP2	Abcam	ab124930	Rabbit	1:3000	60-66 kDa
IGF2BP3	Abcam	Ab225697	Rabbit	1:3000	64 kDa
c-MYC	Abcam	ab32	Mouse	1:1000	45 kDa
HMGA1	Abcam	ab226850	Rabbit	1:1000	17 kDa
ARID3B	Bethyl Labs	A302-565A	Rabbit	1:4000	70 kDa
GAPDH	Abcam	ab9485	Rabbit	1:3000	37 kDa
β-actin	SCBT	sc-47778	Mouse	1:2000	45 kDa
α-tubulin	Abcam	ab4074	Rabbit	1:3000	50 kDa
Goat anti-rabbit (HRP)	Abcam	ab97051	Goat	1:3000	Secondary (HRP)
Goat anti-mouse (HRP)	Abcam	ab97023	Goat	1:3000	Secondary (HRP)

REFERENCES

1. Knöfler, M.; Haider, S.; Saleh, L.; Pollheimer, J.; Gamage, T.K.J.B.; James, J. Human placenta and trophoblast development: key molecular mechanisms and model systems. Cell. Mol. Life Sci. 2019, 76, 3479–3496.
2. Aplin, J.D. The cell biological basis of human implantation. *Baillieres Best Pract. Res. Clin. Obstet. Gynaecol.* 2000, *14*, 757–764.
3. Red-Horse, K.; Zhou, Y.; Genbacev, O.; Prakobphol, A.; Foulk, R.; McMaster, M.; Fisher, S.J. Trophoblast differentiation during embryo implantation and formation of the maternal-fetal interface. *J. Clin. Invest.* 2004, *114*, 744–754.
4. Brosens, I.; Pijnenborg, R.; Vercruysse, L.; Romero, R. THE "GREAT OBSTETRICAL SYNDROMES" ARE ASSOCIATED WITH DISORDERS OF DEEP PLACENTATION. *Am. J. Obstet. Gynecol.* 2011, *204*, 193–201.
5. Jauniaux, E.; Poston, L.; Burton, G.J. Placental-related diseases of pregnancy: involvement of oxidative stress and implications in human evolution. *Hum. Reprod. Update* 2006, *12*, 747–755.
6. Spencer, T.E.; Johnson, G.A.; Bazer, F.W.; Burghardt, R.C. Implantation mechanisms: insights from the sheep. *Reprod. Camb. Engl.* 2004, *128*, 657–668.
7. Rowson, L.E.; Moor, R.M. Development of the sheep conceptus during the first fourteen days. *J. Anat.* 1966, *100*, 777–785.
8. Wintenberger-Torrés, S.; Fléchon, J.E. Ultrastructural evolution of the trophoblast cells of the pre-implantation sheep blastocyst from day 8 to day 18. *J. Anat.* 1974, *118*, 143–153.

9. Wang, J.; Guillomot, M.; Hue, I. Cellular organization of the trophoblastic epithelium in elongating conceptuses of ruminants. *C. R. Biol.* 2009, *332*, 986–997.

10. Spencer, T.E.; Hansen, T.R. Implantation and Establishment of Pregnancy in Ruminants. *Adv. Anat. Embryol. Cell Biol.* 2015, *216*, 105–135.

11. Shorten, P.R.; Ledgard, A.M.; Donnison, M.; Pfeffer, P.L.; McDonald, R.M.; Berg, D.K. A mathematical model of the interaction between bovine blastocyst developmental stage and progesterone-stimulated uterine factors on differential embryonic development observed on Day 15 of gestation. *J. Dairy Sci.* 2018, *101*, 736–751.

12. Farin, C.E.; Imakawa, K.; Hansen, T.R.; McDonnell, J.J.; Murphy, C.N.; Farin, P.W.; Roberts, R.M. Expression of trophoblastic interferon genes in sheep and cattle. *Biol. Reprod.* 1990, *43*, 210–218.

13. Thatcher, W.W.; Guzeloglu, A.; Mattos, R.; Binelli, M.; Hansen, T.R.; Pru, J.K. Uterine-conceptus interactions and reproductive failure in cattle. *Theriogenology* 2001, *56*, 1435–1450.

14. Roberts, R.M.; Chen, Y.; Ezashi, T.; Walker, A.M. Interferons and the maternal-conceptus dialog in mammals. *Semin. Cell Dev. Biol.* 2008, *19*, 170–177.

15. Aires, M.B.; Degaki, K.Y.; Dantzer, V.; Yamada, A.T. Bovine placentome development during early pregnancy.; 2014.

16. Lopez-Tello, J.; Arias-Alvarez, M.; Gonzalez-Bulnes, A.; Sferuzzi-Perri, A.N. Models of Intrauterine growth restriction and fetal programming in rabbits. *Mol. Reprod. Dev. 0*.

17. Devor, E.J.; Reyes, H.D.; Santillan, D.A.; Santillan, M.K.; Onukwugha, C.; Goodheart, M.J.; Leslie, K.K. Placenta-Specific Protein 1: A Potential Key to Many Oncofetal-Placental OB/GYN Research Questions. *Obstet. Gynecol. Int.* 2014, *2014*.

18. Ali, A.; Anthony, R.V.; Bouma, G.J.; Winger, Q.A. LIN28-let-7 axis regulates genes in immortalized human trophoblast cells by targeting the ARID3B-complex. *FASEB J. Off. Publ. Fed. Am. Soc. Exp. Biol.* 2019, *33*, 12348–12363.

19. West, R.C.; McWhorter, E.S.; Ali, A.; Goetzman, L.N.; Russ, J.E.; Anthony, R.V.; Bouma, G.J.; Winger, Q.A. HMGA2 is regulated by LIN28 and BRCA1 in human placental cells†. *Biol. Reprod.* 2018.

20. Seabrook, J.L.; Cantlon, J.D.; Cooney, A.J.; McWhorter, E.E.; Fromme, B.A.; Bouma, G.J.; Anthony, R.V.; Winger, Q.A. Role of LIN28A in Mouse and Human Trophoblast Cell Differentiation. *Biol. Reprod.* 2013, *89*, 95.

21. Moss, E.G.; Tang, L. Conservation of the heterochronic regulator Lin-28, its developmental expression and microRNA complementary sites. *Dev. Biol.* 2003, *258*, 432–442.

22. Chan, H.W.; Lappas, M.; Yee, S.W.Y.; Vaswani, K.; Mitchell, M.D.; Rice, G.E. The expression of the let-7 miRNAs and Lin28 signalling pathway in human term gestational tissues. *Placenta* 2013, *34*, 443–448.

23. Feng, C.; Neumeister, V.; Ma, W.; Xu, J.; Lu, L.; Bordeaux, J.; Maihle, N.J.; Rimm, D.L.; Huang, Y. Lin28 regulates HER2 and promotes malignancy through multiple mechanisms. *Cell Cycle Georget. Tex* 2012, *11*, 2486–2494.

24. Ma, W.; Ma, J.; Xu, J.; Qiao, C.; Branscum, A.; Cardenas, A.; Baron, A.T.; Schwartz, P.; Maihle, N.J.; Huang, Y. Lin28 regulates BMP4 and functions with Oct4 to affect ovarian tumor microenvironment. *Cell Cycle Georget. Tex* 2013, *12*, 88–97.

25. Hagan, J.P.; Piskounova, E.; Gregory, R.I. Lin28 recruits the TUTase Zcchc11 to inhibit let-7 maturation in mouse embryonic stem cells. *Nat. Struct. Mol. Biol.* 2009, *16*, 1021–1025.

26. Heo, I.; Joo, C.; Cho, J.; Ha, M.; Han, J.; Kim, V.N. Lin28 mediates the terminal uridylation of let-7 precursor MicroRNA. *Mol. Cell* 2008, *32*, 276–284.

27. Heo, I.; Joo, C.; Kim, Y.-K.; Ha, M.; Yoon, M.-J.; Cho, J.; Yeom, K.-H.; Han, J.; Kim, V.N. TUT4 in concert with Lin28 suppresses microRNA biogenesis through pre-microRNA uridylation. *Cell* 2009, *138*, 696–708.

28. Piskounova, E.; Polytarchou, C.; Thornton, J.E.; LaPierre, R.J.; Pothoulakis, C.; Hagan, J.P.; Iliopoulos, D.; Gregory, R.I. Lin28A and Lin28B inhibit let-7 microRNA biogenesis by distinct mechanisms. *Cell* 2011, *147*, 1066–1079.

29. Rybak, A.; Fuchs, H.; Smirnova, L.; Brandt, C.; Pohl, E.E.; Nitsch, R.; Wulczyn, F.G. A feedback loop comprising lin-28 and let-7 controls pre-let-7 maturation during neural stem-cell commitment. *Nat. Cell Biol.* 2008, *10*, 987–993.

30. Newman, M.A.; Thomson, J.M.; Hammond, S.M. Lin-28 interaction with the Let-7 precursor loop mediates regulated microRNA processing. *RNA N. Y. N* 2008, *14*, 1539–1549.

31. Ibarra, I.; Erlich, Y.; Muthuswamy, S.K.; Sachidanandam, R.; Hannon, G.J. A role for microRNAs in maintenance of mouse mammary epithelial progenitor cells. *Genes Dev.* 2007, *21*, 3238–3243.

32. Lee, H.; Han, S.; Kwon, C.S.; Lee, D. Biogenesis and regulation of the let-7 miRNAs and their functional implications. *Protein Cell* 2016, *7*, 100–113.

33. Viswanathan, S.R.; Daley, G.Q. Lin28: A MicroRNA Regulator with a Macro Role. *Cell* 2010, *140*, 445–449.

34. Liao, T.-T.; Hsu, W.-H.; Ho, C.-H.; Hwang, W.-L.; Lan, H.-Y.; Lo, T.; Chang, C.-C.; Tai, S.-K.; Yang, M.-H. let-7 Modulates Chromatin Configuration and Target Gene Repression through Regulation of the ARID3B Complex. *Cell Rep.* 2016, *14*, 520–533.

35. Rahman, M.M.; Qian, Z.R.; Wang, E.L.; Sultana, R.; Kudo, E.; Nakasono, M.; Hayashi, T.; Kakiuchi, S.; Sano, T. Frequent overexpression of HMGA1 and 2 in gastroenteropancreatic neuroendocrine tumours and its relationship to *let-7* downregulation. *Br. J. Cancer* 2009, *100*, 501–510.

36. Yang, X.; Cai, H.; Liang, Y.; Chen, L.; Wang, X.; Si, R.; Qu, K.; Jiang, Z.; Ma, B.; Miao, C.; et al. Inhibition of c-Myc by let-7b mimic reverses mutidrug resistance in gastric cancer cells. *Oncol. Rep.* 2015, *33*, 1723–1730.

37. Uchikura, Y.; Matsubara, K.; Matsubara, Y.; Mori, M. P34. Role of high-mobility group A1 protein in trophoblast invasion. *Pregnancy Hypertens. Int. J. Womens Cardiovasc. Health* 2015, *5*, 243.

38. Sampson, V.B.; Rong, N.H.; Han, J.; Yang, Q.; Aris, V.; Soteropoulos, P.; Petrelli, N.J.; Dunn, S.P.; Krueger, L.J. MicroRNA Let-7a Down-regulates MYC and Reverts MYC-Induced Growth in Burkitt Lymphoma Cells. *Cancer Res.* 2007, *67*, 9762–9770.

39. Boyerinas, B.; Park, S.-M.; Shomron, N.; Hedegaard, M.M.; Vinther, J.; Andersen, J.S.; Feig, C.; Xu, J.; Burge, C.B.; Peter, M.E. Identification of Let-7–Regulated Oncofetal Genes. *Cancer Res.* 2008, *68*, 2587–2591.

40. Bell, J.L.; Wächter, K.; Mühleck, B.; Pazaitis, N.; Köhn, M.; Lederer, M.; Hüttelmaier, S. Insulin-like growth factor 2 mRNA-binding proteins (IGF2BPs): post-transcriptional drivers of cancer progression? *Cell. Mol. Life Sci.* 2013, *70*, 2657–2675.

41. JnBaptiste, C.K.; Gurtan, A.M.; Thai, K.K.; Lu, V.; Bhutkar, A.; Su, M.-J.; Rotem, A.; Jacks, T.; Sharp, P.A. Dicer loss and recovery induce an oncogenic switch driven by transcriptional activation of the oncofetal Imp1–3 family. *Genes Dev.* 2017, *31*, 674–687.

42. Degrauwe, N.; Suvà, M.-L.; Janiszewska, M.; Riggi, N.; Stamenkovic, I. IMPs: an RNA-binding protein family that provides a link between stem cell maintenance in normal development and cancer. *Genes Dev.* 2016, *30*, 2459–2474.

43. Zhao, W.; Lu, D.; Liu, L.; Cai, J.; Zhou, Y.; Yang, Y.; Zhang, Y.; Zhang, J. Insulin-like growth factor 2 mRNA binding protein 3 (IGF2BP3) promotes lung tumorigenesis via attenuating p53 stability. *Oncotarget* 2017, *8*, 93672–93687.

44. Li, Y.; Francia, G.; Zhang, J.-Y. p62/IMP2 stimulates cell migration and reduces cell adhesion in breast cancer. *Oncotarget* 2015, *6*, 32656–32668.

45. Mahapatra, L.; Andruska, N.; Mao, C.; Le, J.; Shapiro, D.J. A Novel IMP1 Inhibitor, BTYNB, Targets c-Myc and Inhibits Melanoma and Ovarian Cancer Cell Proliferation. *Transl. Oncol.* 2017, *10*, 818–827.

46. Zhou, Y.; Meng, X.; Chen, S.; Li, W.; Li, D.; Singer, R.; Gu, W. IMP1 regulates UCA1-mediated cell invasion through facilitating UCA1 decay and decreasing the sponge effect of UCA1 for miR-122-5p. *Breast Cancer Res. BCR* 2018, *20*, 32.

47. Schmiedel, D.; Tai, J.; Yamin, R.; Berhani, O.; Bauman, Y.; Mandelboim, O. The RNA binding protein IMP3 facilitates tumor immune escape by downregulating the stress-induced ligands ULPB2 and MICB. *eLife* 2016, *5*.

48. Lederer, M.; Bley, N.; Schleifer, C.; Hüttelmaier, S. The role of the oncofetal IGF2 mRNA-binding protein 3 (IGF2BP3) in cancer. *Semin. Cancer Biol.* 2014, *29*, 3–12.

49. Wu, C.; Ma, H.; Qi, G.; Chen, F.; Chu, J. Insulin-like growth factor II mRNA-binding protein 3 promotes cell proliferation, migration and invasion in human glioblastoma. *OncoTargets Ther.* 2019, *12*, 3661–3670.

50. Wan, B.-S.; Cheng, M.; Zhang, L. Insulin-like growth factor 2 mRNA-binding protein 1 promotes cell proliferation via activation of AKT and is directly targeted by microRNA-494 in pancreatic cancer. *World J. Gastroenterol.* 2019, *25*, 6063–6076.

51. Cao, J.; Mu, Q.; Huang, H. The Roles of Insulin-Like Growth Factor 2 mRNA-Binding Protein 2 in Cancer and Cancer Stem Cells Available online: https://www.hindawi.com/journals/sci/2018/4217259/ (accessed on Nov 18, 2019).

52. Brooks, K.; Burns, G.W.; Moraes, J.G.N.; Spencer, T.E. Analysis of the Uterine Epithelial and Conceptus Transcriptome and Luminal Fluid Proteome During the Peri-Implantation Period of Pregnancy in Sheep. *Biol. Reprod.* 2016, *95*.

53. Uchikura, Y.; Matsubara, K.; Muto, Y.; Matsubara, Y.; Fujioka, T.; Matsumoto, T.; Sugiyama, T. Extranuclear Translocation of High-Mobility Group A1 Reduces the Invasion of Extravillous Trophoblasts Involved in the Pathogenesis of Preeclampsia: New Aspect of High-Mobility Group A1. *Reprod. Sci. Thousand Oaks Calif* 2017, *24*, 1630–1638.

54. Kumar, P.; Luo, Y.; Tudela, C.; Alexander, J.M.; Mendelson, C.R. The c-Myc-regulated microRNA-17~92 (miR-17~92) and miR-106a~363 clusters target hCYP19A1 and hGCM1 to inhibit human trophoblast differentiation. *Mol. Cell. Biol.* 2013, *33*, 1782–1796.

55. Bobbs, A.; Gellerman, K.; Hallas, W.M.; Joseph, S.; Yang, C.; Kurkewich, J.; Cowden Dahl, K.D. ARID3B Directly Regulates Ovarian Cancer Promoting Genes. *PloS One* 2015, *10*, e0131961.

56. Roy, L.; Samyesudhas, S.J.; Carrasco, M.; Li, J.; Joseph, S.; Dahl, R.; Cowden Dahl, K.D. ARID3B increases ovarian tumor burden and is associated with a cancer stem cell gene signature. *Oncotarget* 2014, *5*, 8355–8366.

57. Ratliff, M.L.; Mishra, M.; Frank, M.B.; Guthridge, J.M.; Webb, C.F. The Transcription Factor ARID3a Is Important for In Vitro Differentiation of Human Hematopoietic Progenitors. *J. Immunol. Baltim. Md 1950* 2016, *196*, 614–623.

58. Habir, K.; Aeinehband, S.; Wermeling, F.; Malin, S. A Role for the Transcription Factor Arid3a in Mouse B2 Lymphocyte Expansion and Peritoneal B1a Generation. *Front. Immunol.* 2017, *8*, 1387.

59. Rhee, C.; Edwards, M.; Dang, C.; Harris, J.; Brown, M.; Kim, J.; Tucker, H.O. ARID3A is required for mammalian placenta development. *Dev. Biol.* 2017, *422*, 83–91.

60. Lala, N.; Girish, G.V.; Cloutier-Bosworth, A.; Lala, P.K. Mechanisms in decorin regulation of vascular endothelial growth factor-induced human trophoblast migration and acquisition of endothelial phenotype. *Biol. Reprod.* 2012, *87*, 59.

61. Baker, C.M.; Goetzmann, L.N.; Cantlon, J.D.; Jeckel, K.M.; Winger, Q.A.; Anthony, R.V. Development of ovine chorionic somatomammotropin hormone-deficient pregnancies. *Am. J. Physiol. - Regul. Integr. Comp. Physiol.* 2016, *310*, R837–R846.

62. Jeckel, K.J.; Boyarko, A.C.; Bouma, G.J.; Winger, Q.A.; Anthony, R.V. Chorionic Somatomammotropin Impacts Early Fetal Growth and Placental Gene Expression. *J. Endocrinol.* 2018, *237*, 301–310.

63. Purcell, S.H.; Cantlon, J.D.; Wright, C.D.; Henkes, L.E.; Seidel, G.E.; Anthony, R.V. The Involvement of Proline-Rich 15 in Early Conceptus Development in Sheep. *Biol. Reprod.* 2009, *81*, 1112–1121.

64. Hayer, A.; Shao, L.; Chung, M.; Joubert, L.-M.; Yang, H.W.; Tsai, F.-C.; Bisaria, A.; Betzig, E.; Meyer, T. Engulfed cadherin fingers are polarized junctional structures between collectively migrating endothelial cells. *Nat. Cell Biol.* 2016, *18*, 1311–1323.

65. Su, J.-L.; Chen, P.-S.; Johansson, G.; Kuo, M.-L. Function and regulation of let-7 family microRNAs. *MicroRNA Shariqah United Arab Emir.* 2012, *1*, 34–39.

66. Tsialikas, J.; Romer-Seibert, J. LIN28: roles and regulation in development and beyond. *Development* 2015, *142*, 2397–2404.

67. Lee, H.; Han, S.; Kwon, C.S.; Lee, D. Biogenesis and regulation of the let-7 miRNAs and their functional implications. *Protein Cell* 2016, *7*, 100–113.

68. Straszewski-Chavez, S.L.; Abrahams, V.M.; Alvero, A.B.; Aldo, P.B.; Ma, Y.; Guller, S.; Romero, R.; Mor, G. The isolation and characterization of a novel telomerase immortalized first trimester trophoblast cell line, Swan 71. *Placenta* 2009, *30*, 939–948.

CHAPTER IV: KDM1A REGULATES GENES IMPORTANT FOR PLACENTAL DEVELOPMENT IN HUMAN TROPHOBLAST-DERIVED CELLS

Synopsis

Compromised placentation can lead to serious pregnancy related disorders including preeclampsia (PE), intrauterine growth restriction (IUGR), preterm birth and gestational diabetes mellitus (GDM). The important steps during early placental development include rapid proliferation of trophoblast cells and remodeling of spiral arteries. These processes are regulated by complex molecular mechanisms which are not well understood. We recently showed that LIN28-*let-7* miRNA axis regulates genes important for trophoblast cell proliferation and angiogenesis. Lysine-specific demethylase 1(LSD1/KDM1A) is the first discovered histone demethylase which regulates gene transcription by chromatin remodeling. In the current study we used *in vitro* and *in vivo* approaches to determine the function of KDM1A in placental development. We hypothesize that KDM1A regulate the expression of genes important for early placental development including LIN28, androgen receptors (AR), vascular endothelial growth factor A (*VEGF-A*), high mobility group AT-hook 1 (*HMGA1*) and MYC protooncogene (cMYC). Using CRISPR-Cas 9 based genome editing, ACH-3P cells with KDM1A knockout (KDM1AKO) were generated. KDM1AKO cells had significantly reduced LIN28A and LIN28B and significantly increased *let-7* miRNAs (*let-7a, b, c, d, e, g)* compared to scramble control (SC). Moreover, the mRNAs and proteins of AR, VEGF-A, HMGA1 and cMYC were significantly reduced in KDM1AKO cells compared to SC. An *in vivo* experiment was conducted to demonstrate the role for KDM1A in placental development, using the sheep as a model. Briefly, day 9 hatched blastocysts were flushed and infected with a Lenti-CRISPRv2 KDM1A target

construct (n=4) to knockout KDM1A specifically in the trophectoderm or with SC (n=5). Infected embryos were transferred to recipient ewes and embryos were collected at gestational day 16. The results show that KDM1A is necessary for embryo elongation. Collectively these results suggest that KDM1A plays a role in AR signaling in trophoblast cells and is necessary for early placental development.

1. Introduction

Human placental development starts with the implantation of blastocyst. Throughout the gestation, fetus is dependent on placenta for nutrition. Structural and functional placental abnormalities can cause sever pregnancy disorders including IUGR, PE, stillbirth, spontaneous abortion, and placental abruption [1]. These disorders result into around 60000 maternal mortalities every year [2]. Understanding the placental development and associated pathologies can help to reduce this loss. Development of human planta starts with the interaction of trophectoderm with uterine luminal epithelium [3]. The cytotrophoblasts undergo rapid proliferation and differentiate into multinucleated syncytiotrophoblast and extravillous trophoblast cells [4]. Syncytiotrophoblast helps the blastocyst to invade the decidualized uterus and the extravillous trophoblast cells invade deep in the maternal uterus and transform the spiral arteries [5]. These steps are critical in development of hemochorial human placenta and are not well understood.

The transcription factors bind the promoter or enhancer regions of genes and recruit co-repressors and co-activators which activate or repress gene transcription by histone modifications. Methylation or demethylation of is an example of histone modifications which occur at lysine and arginine of histones [6]. Until the discovery of lysine specific demethylase 1 (LSD1 or KDM1A) in 2004, histone methylation was thought to be an irreversible epigenetic mark [7]. KDM1A is a

flavin adenine-dinucleotide dependent enzyme which catalyzes the demethylation of mono- and di-methylated lysine 4 or 9 in histone 3 (H3K4me1/2 or H3K9me1/2) [7,8]. Demethylation at H3K4me1/2 leads to transcriptional repression, whereas demethylation at H3K9me1/2 causes transcriptional activation [7–9].

KDM1A regulates important biological functions in cells and tissues. KDM1A knockout in mice leads to developmental arrest and embryonic lethality before E7.5 [10,11]. Undifferentiated human cells have high expression of KDM1A which gradually decreases as the cells differentiate, indicating the role of KDM1A in cell proliferation [12]. It is also required to maintain the pluripotency of cells by suppressing the lineage-specific cell differentiation [12]. Various studies have defined KDM1A as an oncogene due to its role in cancer development [13–17]. Inhibition of KDM1A leads to reduced proliferation of tumor cells while overexpression of KDM1A promotes cells proliferation, invasion and migration [18]. The ENCODE transcription factor targets dataset shows that KDM1A bind in the promoter regions of many genes including LIN28, HMGA1, VEGF-A and cMYC [19].

Androgen receptors (AR) signaling has been shown to promote cell proliferation [20,21]. AR binds the androgen response elements (ARE) in promoter regions of target genes and recruits KDM1A which activates the transcription of target gene by H3K9me1/2 demethylation [22]. The expression of AR is regulated by different mechanisms. Oncogene cMYC activates AR transcription by binding in its promoter region [23]. The miRNA *let-7c* suppresses the expression of AR either by directly targeting *AR* mRNA or through downregulation of *cMYC* [23,24]. AR-KDM1A duplex binds in the promoter region of VEGF-A and activate its transcription [25]. Knockdown of KDM1A leads to decreased expression of VEGF-A through inhibition of AR function [26].

The role of KDM1A in regulation of genes important for placental development has not been described previously. In this study, we show that knockout of KDM1A in first trimester human trophoblast-derived cells (ACH-3P cells), leads to reduced expression of AR by modulating various molecular pathways. We further show that KDM1A is required for early placental development in sheep.

2. Materials and Methods

2.1.Cell line

The first trimester human trophoblast (ACH-3P) cells were used in this study. ACH-3P cells are hybrid cells obtained by fusion of primary first trimester human trophoblast cells (week 12 of gestation) with a human choriocarcinoma cell line (AC1-1) [27].

2.2.CRISPR-Cas9 based genome editing

Knockout ACH-3P cells were generated using CRISPR-Cas9 based genome editing technique. Target specific gRNAs for human and sheep KDM1A were designed [28,29], and cloned in lentiCRISPR v2 plasmid. The lentiviral particles were generated and used to infect ACH-3P cells following the same procedure described in our previous study [30]. The gRNA sequences used in this study are listed in table 10.

2.3.Embryo Transfer and Tissue Collection

All animal procedures were approved by Institutional Animal Care and Use Committee at Colorado State University, Fort Collins, Colorado, USA. The blastocysts were collected and transferred following the procedure described by Baker et al [31].

2.4.RNA extraction and real-time RT-PCR

For real-time RT-PCR analysis, mRNA and miRNA were isolated from ACH-3P cells using RNeasy and miRNeasy Mini Kits (Qiagen Inc. Germantown, MD, USA). The mRNA was reverse transcribed to cDNA using iScript cDNA synthesis kit (Bio-Rad Laboratories, Hercules, CA, USA). Real-time RT-PCR reactions were run in triplicate in 384-well plates, using 10µl reaction volume in each well containing 50ng cDNA. Primer sequences used for real-time RTPCR are listed in table 11. PCR reactions were incubated in the Light-Cycler 480 PCR machine (Roche Applied Science, Penzberg, Germany). Relative mRNA levels were normalized using *GAPDH*. For miRNA profiling, 300 ng total RNA was reverse transcribed to cDNA using miScript RT II kit (Qiagen Inc. Germantown, MD, USA). Real-time RT-PCR reactions were run in triplicate in 384-well plates, using 10µl reaction volume in each well. These reactions were incubated in the Light-Cycler 480 PCR machine (Roche Applied Science, Penzberg, Germany) at following cycling conditions: 95˚C for 15 minutes, 45 cycles of 94˚C for 15 seconds, 55˚C for 30 seconds, and 70˚C for 30 seconds. Relative miRNA levels were normalized using *SNORD-48*.

2.5.Protein Extraction and Western Blot

Western blot analysis was performed using whole cell lysate to quantify proteins in cells. Protein was extracted using RIPA buffer and quantified using BCA protein assay kit (ThermoFisher, Waltham, MA, USA). Protein was separated in 4-14% Bis-Tris gels (Bio-Rad Laboratories, Hercules, CA, USA) at 90 volts for 15 min and 125 volts for 60 min, and then transferred to 0.45 µm pore size nitrocellulose membrane (Bio-Rad Laboratories, Hercules, CA, USA) at 100 volts for 2 hours at 4°C. The membranes were then blocked in 5% non-fat dry milk solution in TBST (50 mM Tris, 150 mM NaCl, 0.05% Tween 20, pH 7.6) for 1 hour and incubated at 4°C overnight with specific primary antibody. After overnight incubation, the membranes were

washed 3 times with 1x TBST and incubated with appropriate secondary antibody conjugated to horseradish peroxidase for 1 hour at room temperature. The blots were imaged using ChemiDoc XRS+ chemiluminescence system (Bio-Rad Laboratories, Hercules, CA, USA). To normalize protein quantity, α-tubulin or GAPDH were used. Each experiment was repeated on three replicates. The antibodies used are listed in table 12.

2.6.Co-immunoprecipitation

Proteins extracted from ACH-3P cells were incubated with and KDM1A antibody conjugated protein-G magnetic beads (Bio-Rad Laboratories, Hercules, CA, USA) to immunoprecipitate KDM1A protein. After immunoprecipitation, proteins were eluted using 1x laemmli buffer and used for western blot following the same procedure described earlier. The membranes were probed using AR antibody. Normal rabbit IgG was used as a negative control in this experiment.

2.7.Chromatin Immunoprecipitation Assay

Chromatin immunoprecipitation (ChIP) assay was performed using Magna ChIP G (EMD Millipore Corp., Burlington, MA, USA). 70-80% confluent ACH-3P cells were used in this procedure. Cells were fixed with formaldehyde and chromatin was extracted and sheared to produce 100-1000 bp strands using Bioruptor Sonication System (Diagenode, Denville, NJ, USA). Immunoprecipitation was done using KDM1A antibodies and immunoprecipitated DNA was eluted and used to run end-point PCR for *AR*. The primers used in ChIP assay are listed in table 13. ChIP input DNA was used as positive controls for PCR, and sheared chromatin immunoprecipitated by normal Rabbit IgG was used as negative control.

2.8.Cell Proliferation Assay

Cell proliferation was measured using Quick Cell Proliferation Assay Kit (Abcam, Cambridge, MA, USA). SC, KDM1A KO or ACH-3P cells treated with LSD1 inhibitor (Millipore Sigma, CA, USA) at 13 nM final concentration were plated to a density of 1000 cells/100 µl in 96-well tissue culture plates, with four replicates of each cell type. After 24 hours of plating the cells, 10 µl WST-1 reagent was added in each well followed by incubation for 2 hours in standard culture conditions. Absorbance was measured using Cytation 3 Multi-Mode Reader (BioTek Instruments, Inc., VT, USA) at 440 nm with reference wavelength of 650 nm.

2.9.Statistics

All data were analyzed using GraphPad Prism 7 Software. To determine significance of mRNAs, miRNAs and proteins, all values were compared between SC and KDM1A KO ACH-3P cells using student t-test. P values less than 0.05 were considered statistically significant.

3. Results

3.1.Knockout of KDM1A resulted in reduced expression of AR in ACH-3P cells

ACH-3P cells were infected with lentiCRISPR-V2 based lentiviral particles expressing gRNA to target *KDM1A*. Western blot data showed significant reduction in KDM1A protein in KDM1A KO ACH-3P cells compared to SC (Fig. 31A). The real-time RT-PCR and western blot data showed significant reduction in mRNA and protein of AR in KDM1A KO ACH-3P cells compared to SC (Fig. 31B). Co-immunoprecipitation assay showed that AR and KDM1A proteins physically bind with each other in ACH-3P cells (Fig. 32A). Chromatin immunoprecipitation assay showed that KDM1A binds the promoter region and untranslated region of axon 1 of *AR* (Fig. 32B-C). From these results we interpret that KDM1A regulates the expression of AR by directly

binding in its promoter region. Additionally, AR-KDM1A duplex might play role in gene regulation in human trophoblast-derived cells.

3.2.KDM1A KO ACH-3P cells had significant reduction in LIN28 and significant increase in let-7 miRNAs

To access the effect of KDM1A KO on expression of LIN28, real-time and western blot analysis were done. The results demonstrated that mRNA and proteins of both LIN28A and LIN28B were significantly reduced in KDM1A KO ACH-3P cells compared to SC (Fig. 33A-B). As expected, the real-time RT-PCR data showed that levels of *let-7a, b, c, d, e* and *g* miRNAs were significantly increased in KDM1A KO cells compared to SC (Fig. 33C). These results suggest that reduction in AR expression in KDM1A KO cells is potentially due to increase in *let-7* miRNA.

3.3.KDM1A KO ACH-3P cells had significantly reduced expression of VEGF-A, HMGA1 and cMYC

The effect of KDM1A knockout on proliferation and angiogenesis associated genes was accessed using real-time RT-PCR and western blot analysis. The results showed that KDM1A KO ACH-3P cells had significant reduction in mRNA and protein levels of VEGF-A, HMGA1 and cMYC (Fig. 34A-C). These results suggest that reduced expression of these genes is either an effect of KDM1A knockout or increased *let-7* miRNAs.

3.4.KDM1A knockout or inhibition leads to reduced proliferation of ACH-3P cells

Proliferation of ACH-3P cells with knockout of KDM1A or inhibition of KDM1A was measured using Cell Proliferation Assay. The results showed significant reduction in proliferation of ACH-3P cells with KDM1A knockout or inhibition compared to control (Fig. 35).

3.5.KDM1A is required for conceptus elongation in sheep

After trophectoderm specific targeting with lentiviral particles, the sheep conceptus collected at day 16 were smaller in KDM1A KO treatment compared to control. This indicated that KDM1A is required for initial conceptus development in sheep (Fig. 36A). Moreover, real-time RT-PCR data showed significant reduction in KDM1A and AR mRNA in KDM1A KO TE compared to SC (Fig. 36B). These results suggest that KDM1A regulated AR expression in sheep TE *in vivo.*

4. Discussion

KDM1A complexes with AR and binds promoter regions of AR-stimulated genes, where KDM1A acts as a co-activator by causing demethylation of H3K9me1/2 [16,26,32]. In this study we showed that KDM1A and AR bind with each other in ACH-3P cells suggesting that KDM1A regulates AR-stimulated genes in these cells. We further demonstrated that AR itself is potentially regulated by KDM1A. KDM1A binds the promoter region and untranslated region of exon 1 of *AR* gene. Knockout of KDM1A lead to reduction of AR expression which suggests that, KDM1A activates AR transcription by binding in its promoter region by the well-known mechanism of H3K8me1/2 demethylation. Previous studies have shown that KDM1A increased proliferation and invasion of cancer cell and is considered as a promising target for cancer therapy [33–36]. In immortalized first trimester human trophoblast (ACH-3P) cells, KDM1A knockout lead to significant reduction in cell proliferation suggesting a role of KDM1A in early placental development. The activity of KDM1A can be inhibited by using KDM1A inhibitors. Reduced

proliferation of ACH-3P cells after inhibition of KDM1A activity suggests that such inhibitor can be useful in controlling tumor progression in human and animals.

KDM1A binds the promoter areas of more than 7000 genes in humans indicating its role in major biological processes. LIN28, a pluripotency factor that suppresses *let-7* miRNAs, is also a potential target of KDM1A [19]. Our results show that KDM1A KO ACH-3P cells had significant reduction in LIN28A and LIN28B and significant increase in *let-7* miRNAs. *Let-7* miRNAs target several genes and inhibit their translation. AR is targeted by *let-7c* in human trophoblast cells [24]. Significant reduction in AR expression in KDM1A KO ACH-3P cells can be either due to direct effect of KDM1A knockout or due to increased *let-7c* in these cells.

Similar to AR and LIN28B, HMGA1 and cMYC are also regulated by KDM1A as well as by *let-7* miRNAs [30]. KDM1A KO ACH-3P cells had reduced expression of HMGA1 and cMYC. Both HMGA1 and cMYC are proliferation-associated genes and play a role in placental development. HMGA1 promotes trophoblast cell invasion and its reduced expression is involved in pathogenesis of preeclampsia [37,38]. Reduced expression of *cMYC* drives the cytotrophoblast cells towards differentiation [39]. Although KDM1A promoter proliferation, reduced expression of HMGA1 and cMYC might also contribute towards reduced proliferation of KDM1A KO ACH-3P cells. The AR receptor transcription is activated by cMYC [23]. The data from this study suggests that knockout of KDM1A, high *let-7c* miRNA, and reduced cMYC can all contribute towards reduced expression of AR in KDM1A KO ACH-3P cells.

Other than rapid proliferation and invasion, one critical role of trophoblast cells is to transform the spiral arteries. VEGF-A is a key regulator in differentiation of trophoblast cells to endovascular trophoblast cells and plays major role in spiral artery remodeling [40]. *VEGF-A* is an AR-receptor stimulated gene and we have previously shown that AR-KDM1A complex bind

the androgen response element (ARE) in *VEGF-A* promoter region [41]. Our results suggest that knockout of KDM1A and resultant reduction in AR expression leads to reduced expression of VEGF-A.

Although we transferred only 4 blastocysts with TE-specific knockout of KDM1A, only two of them were able to elongate by day 16 and were smaller (average length = 5 cm) compared to control conceptuses (average length = 35 cm). This data might not be enough to draw a concrete conclusion, but it suggests that KDM1A might be playing critical role in early conceptus elongation. KDM1A KO ACH-3P cells have reduced proliferation, suggesting that reduced elongation from KDM1A KO conceptuses might be due to reduced proliferation of trophoblast cells. In humans, spiral artery remodeling is a critical process for successful placentation. Reduced VEGF-A due to KDM1A knockout suggests its role in spiral artery remodeling. AR-KDM1A acts as transcriptional activator for many genes by binding the ARE in their promoter regions. These pathways and their role in placental development is yet to be explored.

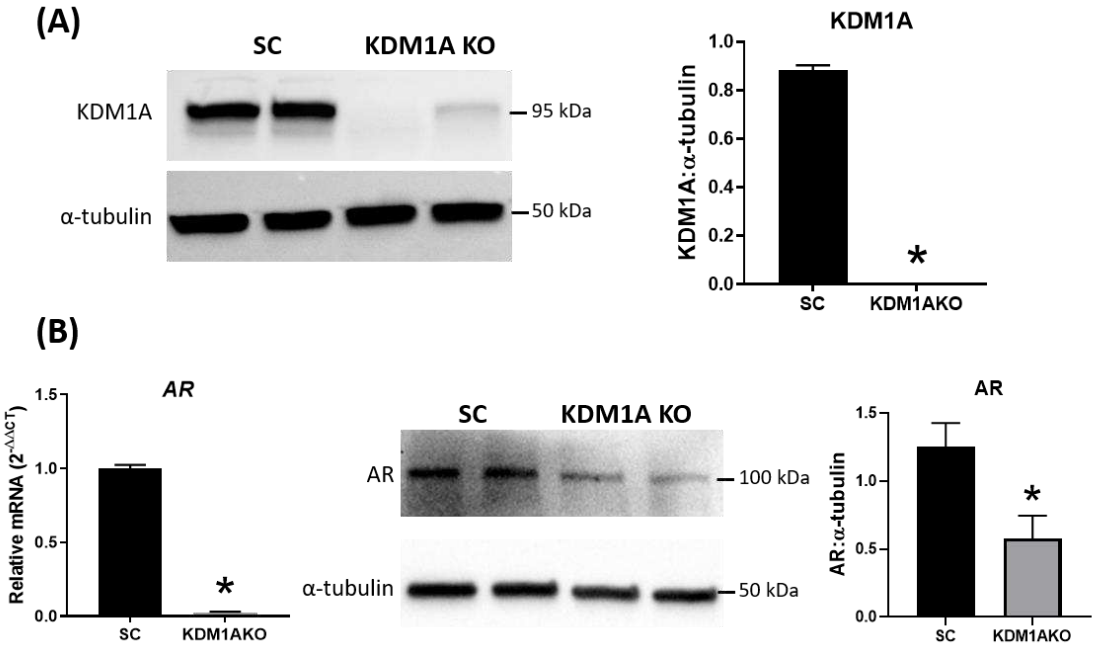

Figure 31. AR in KDM1A KO ACH-3P cells. (A) Representative immunoblots for KDM1A and α-tubulin and densitometric analysis in KDM1A KO ACH-3P cells compared to SC. (B) AR mRNA, representative immunoblots for AR and α-tubulin in KDM1A KO ACH-3P cells compared to SC. (n=3/treatment). *P<0.05 *vs.* control.

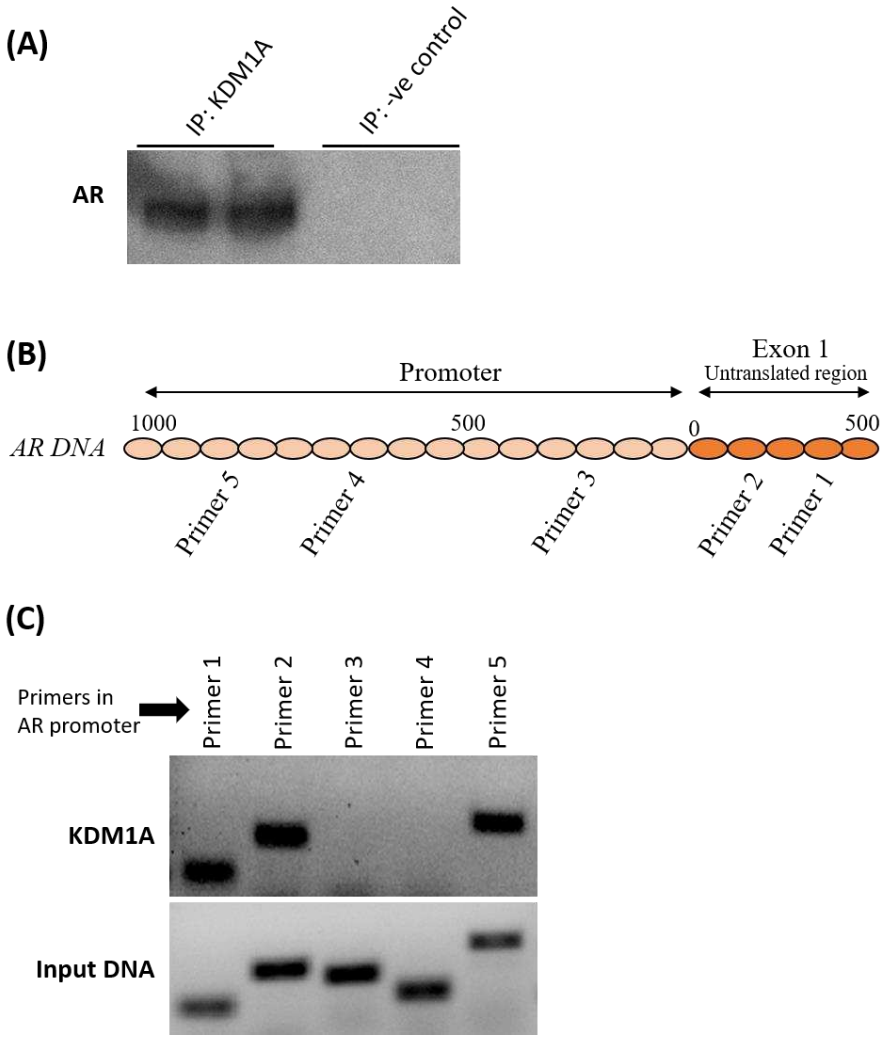

Figure 32. Interaction between KDM1A and AR in ACH-3P cells. (A) Co-immunoprecipitation assay using KDM1A and normal rabbit IgG for immunoprecipitation, and AR for immunoblotting. (B) Schematic diagram indicating the AR DNA regions amplified by PCR primers. (C) Chromatin immunoprecipitation assay using KDM1A for immunoprecipitation, and end point PCR for primers amplifying different areas in *AR* DNA.

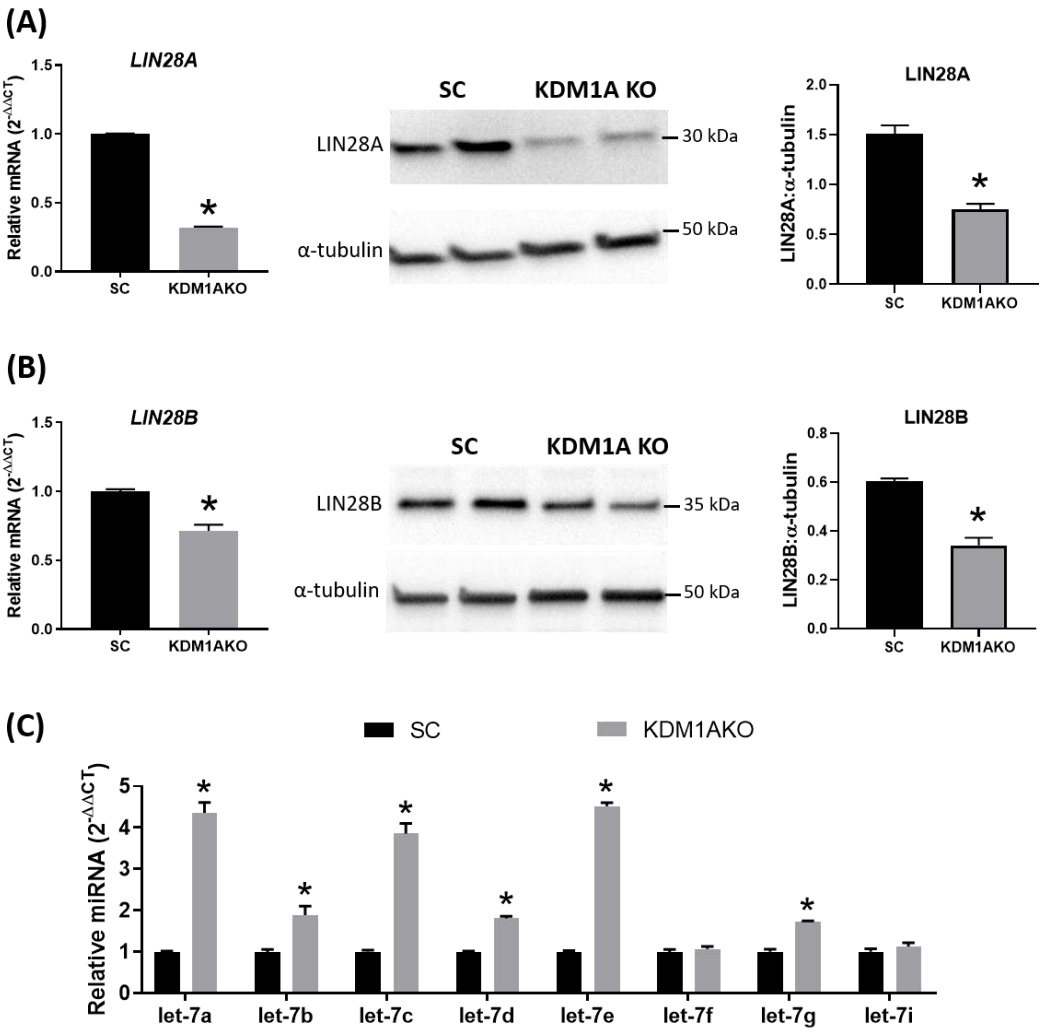

Figure 33. LIN28-*let-7* axis in KDM1A KO ACH-3P cells. (A) LIN28A and LIN28B mRNA, representative immunoblots for LIN28A, LIN28B and α-tubulin, and densitometric analysis in KDM1A KO ACH-3P cells compared to SC. (B) *Let-7* miRNAs in KDM1A KO ACH-3P cells compared to SC. (n=3/treatment). *P<0.05 *vs.* control.

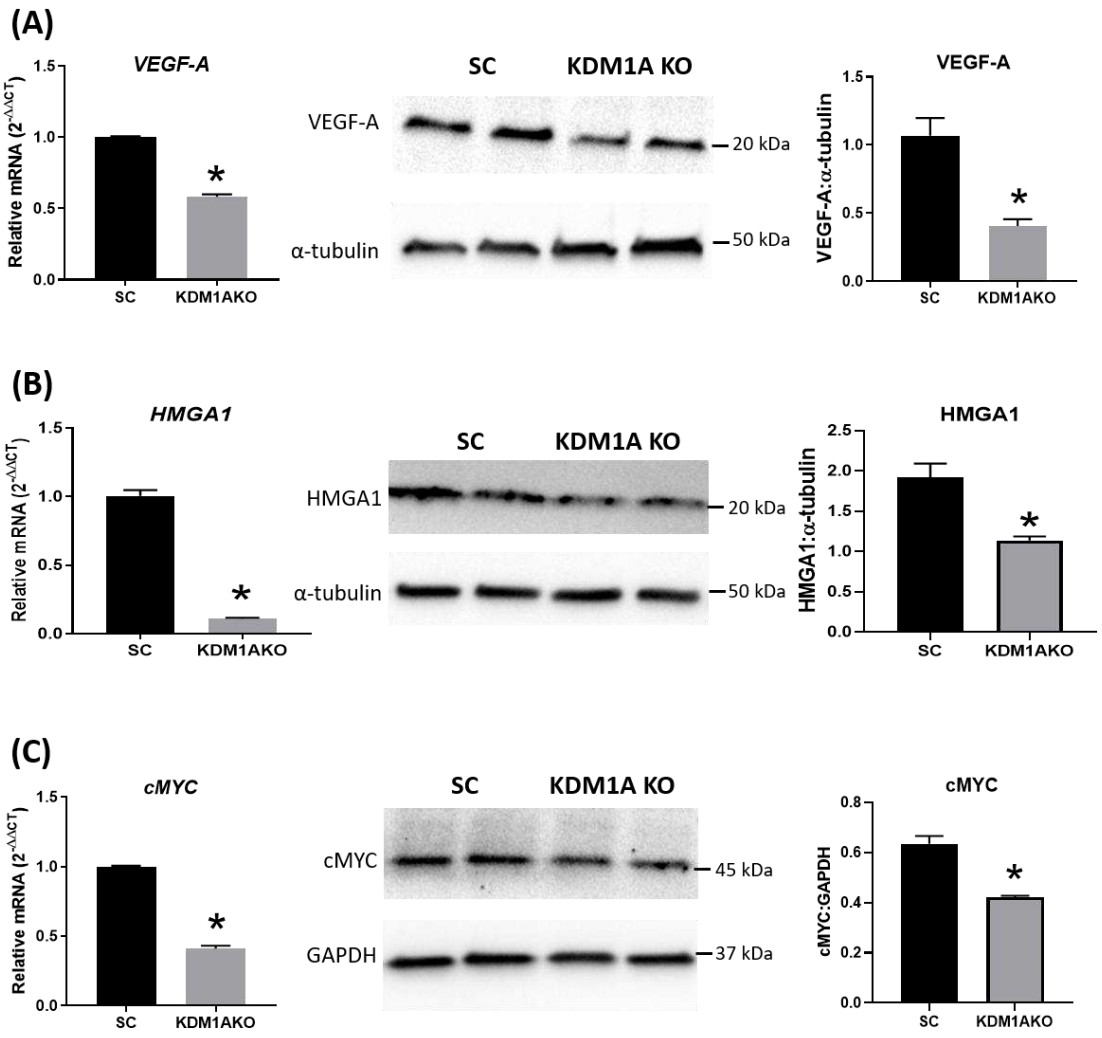

Figure 34. VEGF-A, HMGA1 and cMYC in KDM1A KO ACH-3P cells. (A-C) VEGF-A, HMGA1 and cMYC mRNA, representative immunoblots and densitometric analysis for VEGF-A, HMGA1, cMYC and α-tubulin in KDM1A KO cells compared to SC. (n=3/treatment). *P<0.05 *vs.* control.

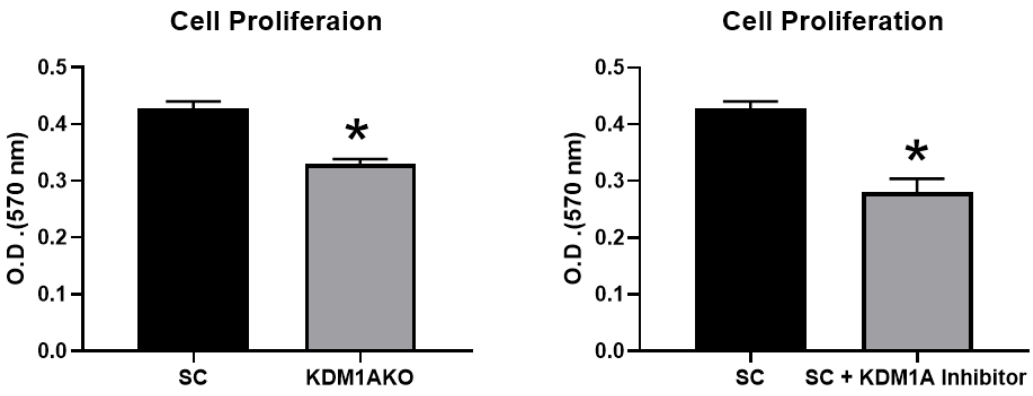

Figure 35. Cell proliferation assay for SC ACH-3P cells, KDM1A KO cells, and SC cells treated with KDM1A inhibitor. (n=4/treatment). *P<0.05 *vs.* control.

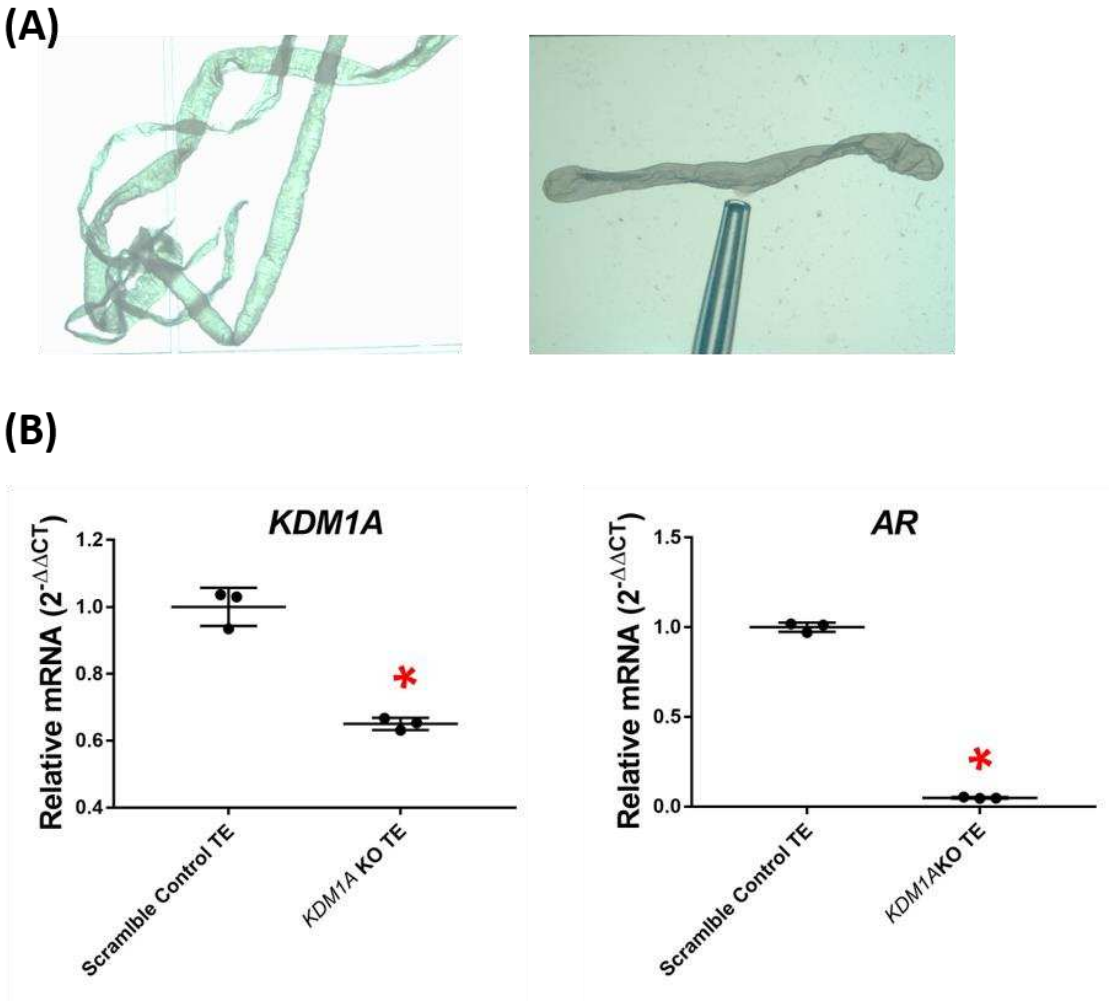

Figure 36. KDM1A knockout in sheep TE (A) Representative SC (n=5) and KDM1A KO (n=4) conceptuses (B) KDM1A and AR mRNA in KDM1A KO conceptuses compared to SC. *P<0.05 *vs.* control.

Table 10. *CRISPR-Cas9 oligos*

KDM1A (Human-1)	Forward oligo	5’ CACCGCGGCTCCGAGAACGGGTCTG 3’
	Reverse oligo	5’ AAACCAGACCCGTTCTCGGAGCCGC 3’
KDM1A (Human-2)	Forward oligo	5’ CACCGCCGCAAGAAAGAGCCTCCGC 3’
	Reverse oligo	5’ AAACGCGGAGGCTCTTTCTTGCGGC 3’
KDM1A (Sheep)	Forward oligo	5’ CACCGAGAGTAGACTTCCTCATGAC 3’
	Reverse oligo	5’ AAACGTCATGAGGAAGTCTACTCTC 3’
Scramble	Forward oligo	5’ CACCGGCTGATCTATCGCGGTCGTC 3’
	Reverse oligo	5’ AAACGACGACCGCGATAGATCAGCC 3’

Table 11. Real-time RT-PCR primers

LIN28A	Forward primer	5’ CTTTAAGAAGTCAGCCAAGGG 3’
	Reverse primer	5’ TGGCATGATGATCTAGACCTC 3’
LIN28B	Forward primer	5’ TAGGAAGTGAAAGAAGACCCA 3’
	Reverse primer	5’ ATGATGCTCTGACAGTAATGG 3’
KDM1A	Forward primer	5’ CTCTTCTGGAACCTCTATAAAGC 3’
	Reverse primer	5’ CATTTCCAGATGATCCTGCAGCAA 3’
AR	Forward primer	5’ TGTCCATCTTGTCGTCTTC 3’
	Reverse primer	5’ CCTCTCCTTCCTCCTGTAG 3’
RPS15 (Sheep)	Forward primer	5’ ATCATTCTGCCCGAGATGGTG 3’
	Reverse primer	5’ TGCTTGACGGGCTTGTAGGTG 3’
AR (Sheep)	Forward Primer	5’ TCCTGGATGGGGCTTATGGT 3’
	Reverse Primer	5’ GCCTCATTCGGACACACTGG 3’
KDM1A (Sheep)	Forward primer	5’ ACATTGCAGTTGTGGTTGGA 3’
	Reverse primer	5’ GACCCCAGAGCCTATGATGA 3’
HMGA1	Forward primer	5’ AGGAAAAGGACGGCACTGAGAA 3’
	Reverse primer	5’ CCCCGAGGTCTCTTAGGTGTTGG 3’
cMYC	Forward primer	5’ CTGGTGCTCCATGAGGAGA 3’
	Reverse primer	5’ CCTGCCTCTTTTCCACAGAA 3’
VEGF-A	Forward primer	5’ CCGGAGAGGGAGCGCGAGCCGCGCC 3’
	Reverse primer	5’ GATGTCCACCAGGGTCTCGATTG 3’
GAPDH	Forward primer	5’ AAGGTCGGAGTCAACGGATTTG 3’
	Reverse primer	5’ CCATGGGTGGAATCATATTGGAA 3’

Table 12. Antibodies

Protein	Vendor	Catalog #	Host Species	Dilution	Band size
KDM1A	Abcam	ab17721	Rabbit	1:1000	95 kDa
AR	Abcam	ab3509	Rabbit	1:1000	100 kDa
LIN28A	Abcam	ab63740	Rabbit	1:1000	30 kDa
LIN28B	Bethyl Labs	A303-588A	Rabbit	1:2000	35 kDa
cMYC	Abcam	ab32	Mouse	1:1000	45 kDa
HMGA1	Abcam	ab226850	Rabbit	1:1000	20 kDa
VEGF-A	SCBT	sc-7269	Mouse	1:500	30 kDa
GAPDH	Abcam	ab9485	Rabbit	1:3000	37 kDa
α-tubulin	Abcam	ab4074	Rabbit	1:3000	50 kDa
Goat anti-rabbit (HRP)	Abcam	ab97051	Goat	1:3000	Secondary (HRP)
Goat anti-mouse (HRP)	Abcam	ab97023	Goat	1:3000	Secondary (HRP)

Table 13. Chip assay primers

AR Primer 1	Forward primer	AGATCTTGTCCACCGTGTGT
	Reverse primer	GGAAGCTCCAGAGAAGGAAA
AR Primer 2	Forward primer	AGACAGACTGTGAGCCTAGCA
	Reverse primer	TTCAACAGGCTGTGATGATG
AR Primer 3	Forward primer	CTCAGTCGGCTACTCTCAGC
	Reverse primer	AGAGCCTTCTTTGCAATGTG
AR Primer 4	Forward primer	CTCAGTCGGCTACTCTCAGC
	Reverse primer	AAGGGAGTTACCTCTCTGCAA
AR Primer 5	Forward primer	GCGACAGAGGGAAAAAGG
	Reverse primer	AGTCCTACCAGGCACTTTCC

REFERENCES

1. Redman, C.W.G.; Staff, A.C. Preeclampsia, biomarkers, syncytiotrophoblast stress, and placental capacity. Am. J. Obstet. Gynecol. 2015, 213, S9.e1-S9.e4.
2. Morisaki, N.; Togoobaatar, G.; Vogel, J.P.; Souza, J.P.; Hogue, C.R.; Jayaratne, K.; Ota, E.; Mori, R. Risk factors for spontaneous and provider-initiated preterm delivery in high and low Human Development Index countries: a secondary analysis of the World Health Organization Multicountry Survey on Maternal and Newborn Health. *BJOG Int. J. Obstet. Gynaecol.* **2014**, *121*, 101–109.
3. Bazer, F.W.; Spencer, T.E.; Johnson, G.A.; Burghardt, R.C.; Wu, G. Comparative aspects of implantation. *Reprod. Camb. Engl.* **2009**, *138*, 195–209.
4. Mclaren, A. Embryo research Available online: https://www.nature.com/articles/320570b0 (accessed on Apr 6, 2018).
5. Huppertz, B.; Frank, H.G.; Reister, F.; Kingdom, J.; Korr, H.; Kaufmann, P. Apoptosis cascade progresses during turnover of human trophoblast: analysis of villous cytotrophoblast and syncytial fragments in vitro. *Lab. Investig. J. Tech. Methods Pathol.* **1999**, *79*, 1687–1702.
6. Kouzarides, T. Chromatin modifications and their function. *Cell* **2007**, *128*, 693–705.
7. Shi, Y.; Lan, F.; Matson, C.; Mulligan, P.; Whetstine, J.R.; Cole, P.A.; Casero, R.A.; Shi, Y. Histone demethylation mediated by the nuclear amine oxidase homolog LSD1. *Cell* **2004**, *119*, 941–953.

8. Metzger, E.; Wissmann, M.; Yin, N.; Müller, J.M.; Schneider, R.; Peters, A.H.F.M.; Günther, T.; Buettner, R.; Schüle, R. LSD1 demethylates repressive histone marks to promote androgen-receptor-dependent transcription. *Nature* **2005**, *437*, 436–439.

9. Laurent, B.; Ruitu, L.; Murn, J.; Hempel, K.; Ferrao, R.; Xiang, Y.; Liu, S.; Garcia, B.A.; Wu, H.; Wu, F.; et al. A specific LSD1/KDM1A isoform regulates neuronal differentiation through H3K9 demethylation. *Mol. Cell* **2015**, *57*, 957–970.

10. Wang, J.; Hevi, S.; Kurash, J.K.; Lei, H.; Gay, F.; Bajko, J.; Su, H.; Sun, W.; Chang, H.; Xu, G.; et al. The lysine demethylase LSD1 (KDM1) is required for maintenance of global DNA methylation. *Nat. Genet.* **2009**, *41*, 125–129.

11. Wang, J.; Scully, K.; Zhu, X.; Cai, L.; Zhang, J.; Prefontaine, G.G.; Krones, A.; Ohgi, K.A.; Zhu, P.; Garcia-Bassets, I.; et al. Opposing LSD1 complexes function in developmental gene activation and repression programmes. *Nature* **2007**, *446*, 882–887.

12. Adamo, A.; Sesé, B.; Boue, S.; Castaño, J.; Paramonov, I.; Barrero, M.J.; Izpisua Belmonte, J.C. LSD1 regulates the balance between self-renewal and differentiation in human embryonic stem cells. *Nat. Cell Biol.* **2011**, *13*, 652–659.

13. Zhao, Z.-K.; Dong, P.; Gu, J.; Chen, L.; Zhuang, M.; Lu, W.-J.; Wang, D.-R.; Liu, Y.-B. Overexpression of LSD1 in hepatocellular carcinoma: a latent target for the diagnosis and therapy of hepatoma. *Tumour Biol. J. Int. Soc. Oncodevelopmental Biol. Med.* **2013**, *34*, 173–180.

14. Lv, T.; Yuan, D.; Miao, X.; Lv, Y.; Zhan, P.; Shen, X.; Song, Y. Over-expression of LSD1 promotes proliferation, migration and invasion in non-small cell lung cancer. *PloS One* **2012**, *7*, e35065.

15. Schulte, J.H.; Lim, S.; Schramm, A.; Friedrichs, N.; Koster, J.; Versteeg, R.; Ora, I.; Pajtler, K.; Klein-Hitpass, L.; Kuhfittig-Kulle, S.; et al. Lysine-specific demethylase 1 is strongly expressed in poorly differentiated neuroblastoma: implications for therapy. *Cancer Res.* **2009**, *69*, 2065–2071.

16. Kauffman, E.C.; Robinson, B.D.; Downes, M.J.; Powell, L.G.; Lee, M.M.; Scherr, D.S.; Gudas, L.J.; Mongan, N.P. Role of androgen receptor and associated lysine-demethylase coregulators, LSD1 and JMJD2A, in localized and advanced human bladder cancer. *Mol. Carcinog.* **2011**, *50*, 931–944.

17. Kahl, P.; Gullotti, L.; Heukamp, L.C.; Wolf, S.; Friedrichs, N.; Vorreuther, R.; Solleder, G.; Bastian, P.J.; Ellinger, J.; Metzger, E.; et al. Androgen Receptor Coactivators Lysine-Specific Histone Demethylase 1 and Four and a Half LIM Domain Protein 2 Predict Risk of Prostate Cancer Recurrence. *Cancer Res.* **2006**, *66*, 11341–11347.

18. Hayami, S.; Kelly, J.D.; Cho, H.-S.; Yoshimatsu, M.; Unoki, M.; Tsunoda, T.; Field, H.I.; Neal, D.E.; Yamaue, H.; Ponder, B.A.J.; et al. Overexpression of LSD1 contributes to human carcinogenesis through chromatin regulation in various cancers. *Int. J. Cancer* **2011**, *128*, 574–586.

19. Gene Set - KDM1A Available online: http://amp.pharm.mssm.edu/Harmonizome/gene_set/KDM1A/ENCODE+Transcription+Factor+Targets (accessed on Feb 13, 2020).

20. Lehmann, B.D.; Bauer, J.A.; Chen, X.; Sanders, M.E.; Chakravarthy, A.B.; Shyr, Y.; Pietenpol, J.A. Identification of human triple-negative breast cancer subtypes and preclinical models for selection of targeted therapies. *J. Clin. Invest.* **2011**, *121*, 2750–2767.

21. Robinson, J.L.L.; MacArthur, S.; Ross-Innes, C.S.; Tilley, W.D.; Neal, D.E.; Mills, I.G.; Carroll, J.S. Androgen receptor driven transcription in molecular apocrine breast cancer is mediated by FoxA1. *EMBO J.* **2012**, *31*, 1617.

22. Feng, J.; Li, L.; Zhang, N.; Liu, J.; Zhang, L.; Gao, H.; Wang, G.; Li, Y.; Zhang, Y.; Li, X.; et al. Androgen and AR contribute to breast cancer development and metastasis: an insight of mechanisms. *Oncogene* **2017**, *36*, 2775–2790.

23. Nadiminty, N.; Tummala, R.; Lou, W.; Zhu, Y.; Zhang, J.; Chen, X.; eVere White, R.W.; Kung, H.-J.; Evans, C.P.; Gao, A.C. MicroRNA let-7c suppresses androgen receptor expression and activity via regulation of Myc expression in prostate cancer cells. *J. Biol. Chem.* **2012**, *287*, 1527–1537.

24. McWhorter, E.S.; West, R.C.; Russ, J.E.; Ali, A.; Winger, Q.A.; Bouma, G.J. LIN28B regulates androgen receptor in human trophoblast cells through Let-7c. *Mol. Reprod. Dev.* **2019**, *86*, 1086–1093.

25. Jia, J.; Zhang, H.; Zhang, H.; Du, H.; Liu, W.; Shu, M. Activated androgen receptor accelerates angiogenesis in cutaneous neurofibroma by regulating VEGFA transcription. *Int. J. Oncol.* **2019**, *55*, 157–166.

26. Kashyap, V.; Ahmad, S.; Nilsson, E.M.; Helczynski, L.; Kenna, S.; Persson, J.L.; Gudas, L.J.; Mongan, N.P. The lysine specific demethylase-1 (LSD1/KDM1A) regulates VEGF-A expression in prostate cancer. *Mol. Oncol.* **2013**, *7*, 555–566.

27. Hiden, U.; Wadsack, C.; Prutsch, N.; Gauster, M.; Weiss, U.; Frank, H.-G.; Schmitz, U.; Fast-Hirsch, C.; Hengstschläger, M.; Pötgens, A.; et al. The first trimester human trophoblast cell line ACH-3P: a novel tool to study autocrine/paracrine regulatory loops of

human trophoblast subpopulations--TNF-alpha stimulates MMP15 expression. *BMC Dev. Biol.* **2007**, *7*, 137.

28. Bae, S.; Park, J.; Kim, J.-S. Cas-OFFinder: a fast and versatile algorithm that searches for potential off-target sites of Cas9 RNA-guided endonucleases. *Bioinformatics* **2014**, *30*, 1473–1475.

29. Park, J.; Bae, S.; Kim, J.-S. Cas-Designer: a web-based tool for choice of CRISPR-Cas9 target sites. *Bioinformatics* **2015**, *31*, 4014–4016.

30. Ali, A.; Anthony, R.V.; Bouma, G.J.; Winger, Q.A. LIN28-let-7 axis regulates genes in immortalized human trophoblast cells by targeting the ARID3B-complex. *FASEB J. Off. Publ. Fed. Am. Soc. Exp. Biol.* **2019**, *33*, 12348–12363.

31. Baker, C.M.; Goetzmann, L.N.; Cantlon, J.D.; Jeckel, K.M.; Winger, Q.A.; Anthony, R.V. Development of ovine chorionic somatomammotropin hormone-deficient pregnancies. *Am. J. Physiol. - Regul. Integr. Comp. Physiol.* **2016**, *310*, R837–R846.

32. Wissmann, M.; Yin, N.; Müller, J.M.; Greschik, H.; Fodor, B.D.; Jenuwein, T.; Vogler, C.; Schneider, R.; Günther, T.; Buettner, R.; et al. Cooperative demethylation by JMJD2C and LSD1 promotes androgen receptor-dependent gene expression. *Nat. Cell Biol.* **2007**, *9*, 347–353.

33. Kong, L.; Zhang, P.; Li, W.; Yang, Y.; Tian, Y.; Wang, X.; Chen, S.; Yang, Y.; Huang, T.; Zhao, T.; et al. KDM1A promotes tumor cell invasion by silencing TIMP3 in non-small cell lung cancer cells. *Oncotarget* **2016**, *7*, 27959–27974.

34. Zhang, W.; Sun, W.; Qin, Y.; Wu, C.; He, L.; Zhang, T.; Shao, L.; Zhang, H.; Zhang, P. Knockdown of KDM1A suppresses tumour migration and invasion by epigenetically

regulating the TIMP1/MMP9 pathway in papillary thyroid cancer. *J. Cell. Mol. Med.* **2019**, *23*, 4933–4944.

35. Pajtler, K.W.; Weingarten, C.; Thor, T.; Künkele, A.; Heukamp, L.C.; Büttner, R.; Suzuki, T.; Miyata, N.; Grotzer, M.; Rieb, A.; et al. The KDM1A histone demethylase is a promising new target for the epigenetic therapy of medulloblastoma. *Acta Neuropathol. Commun.* **2013**, *1*, 19.

36. Huang, Y.; Zou, Y.; Lin, L.; Ma, X.; Zheng, R. miR-101 regulates cell proliferation and apoptosis by targeting KDM1A in diffuse large B cell lymphoma. *Cancer Manag. Res.* **2019**, *11*, 2739–2746.

37. Uchikura, Y.; Matsubara, K.; Matsubara, Y.; Mori, M. P34. Role of high-mobility group A1 protein in trophoblast invasion. *Pregnancy Hypertens. Int. J. Womens Cardiovasc. Health* **2015**, *5*, 243.

38. Uchikura, Y.; Matsubara, K.; Muto, Y.; Matsubara, Y.; Fujioka, T.; Matsumoto, T.; Sugiyama, T. Extranuclear Translocation of High-Mobility Group A1 Reduces the Invasion of Extravillous Trophoblasts Involved in the Pathogenesis of Preeclampsia: New Aspect of High-Mobility Group A1. *Reprod. Sci. Thousand Oaks Calif* **2017**, *24*, 1630–1638.

39. Kumar, P.; Luo, Y.; Tudela, C.; Alexander, J.M.; Mendelson, C.R. The c-Myc-regulated microRNA-17~92 (miR-17~92) and miR-106a~363 clusters target hCYP19A1 and hGCM1 to inhibit human trophoblast differentiation. *Mol. Cell. Biol.* **2013**, *33*, 1782–1796.

40. Li, Y.; Zhu, H.; Klausen, C.; Peng, B.; Leung, P.C.K. Vascular Endothelial Growth Factor-A (VEGF-A) Mediates Activin A-Induced Human Trophoblast Endothelial-Like Tube Formation. *Endocrinology* **2015**, *156*, 4257–4268.

41. Cleys, E.R.; Halleran, J.L.; Enriquez, V.A.; da Silveira, J.C.; West, R.C.; Winger, Q.A.; Anthony, R.V.; Bruemmer, J.E.; Clay, C.M.; Bouma, G.J. Androgen Receptor and Histone Lysine Demethylases in Ovine Placenta. *PLoS ONE* **2015**, *10*.

CHAPTER V: SUMMARY

More than half a million women die every year because of pregnancy-associated conditions. Abnormal placental structure and function is the most common cause of pregnancy complications. The growing fetus is dependent on placenta for nutrients, gaseous exchange and waste removal. Therefore, a malformed placenta can have short-term and long-term consequences on both maternal and fetal health. Placental development begins as blastocyst interacts with uterus. The progenitor cytotrophoblast cells undergo rapid proliferation and differentiate into syncytiotrophoblast and extravillous trophoblast cells. The syncytiotrophoblast helps the blastocyst to make its way into the decidualized uterine stroma whereas extravillous trophoblast cells invade deep in the uterine wall and transform the spiral arteries. The hemochorial human placenta is fully established and functional by week 12 of pregnancy but continues to grow throughout the gestation. Unlike tumor cells, proliferation of trophoblast cells is a controlled process which is regulated by complex genetic pathways. Reduced proliferation of CTBs can cause placental insufficiency whereas excessive proliferation can lead to trophoblastic disease. The aim of this study was to explore genetic pathways involved in proliferation of trophoblast cells during early placental development.

We investigated the role LIN28-*let7* miRNA axis in regulation of proliferation-associated genes in trophoblast cells. The pluripotency factor LIN28 is an RNA binding protein with two paralogues, LIN28A and LIN28B. One of the main functions of LIN28 is to bind pre-*let-7* and pri-*let-7* miRNAs and inhibit the biogenesis of mature *let-7* miRNAs. The mature *let-7* miRNAs bind the mRNA of several target genes and reduce their expression. Many *let-7* miRNA target genes have been associated with cell proliferation and maintaining pluripotency of cells. *HMGA1, c-*

MYC, VEGF-A, WNT1, ARID3A and *ARID3B* are examples of such genes. We saw that in term human placentas from IUGR pregnancies, LIN28 was significantly reduced, *let-7* miRNAs were significantly increased and ARID3A and ARID3B were significantly reduced.

Many proliferation factors in the cells are regulated by the ARID3B-complex which comprises of ARID3A, ARID3B and KDM4C. The ARID3B-complex bind in the promoter areas of genes and activate their transcription through histone demethylation caused by KDM4C. The three members of the ARID3B-complex are also known targets of *let-7* miRNAs. Hence, there are two possible pathways of gene regulation by *let-7* miRNAs. Either the *let-7* miRNAs directly bind the mRNAs of target genes to degrade them or inhibit their translation, or they operate by targeting the ARID3B-complex. This led us to the idea of existence of LIN28-*let-7*-ARID3B pathway in human trophoblast cells.

We used two first trimester human trophoblast cell lines, ACH-3P and Sw.71, which have contrasting expression of LIN28. ACH-3P cells have higher LIN28 and low *let-7* miRNAs whereas Sw.71 cells have low LIN28 and high *let-7* miRNAs. Knockout of LIN28 in ACH-3P cells resulted in increased *let-7* miRNAs and reduced expression of ARID3A, ARID3B and KDM4C. Moreover, LIN28 knockout lead to reduction in HMGA1, c-MYC, VEGF-A and WNT1 expression. In Sw.71 cells, overexpression of LIN28 lead to reduced *let-7* miRNAs and increased expression of proliferation associated genes. We further found that the ARID3B-complex binds the promoter regions of *HMGA1, c-MYC, VEGF-A* and *WNT1*. Knockout of ARID3B in ACH-3P cells lead to reduced expression of HMGA1, c-MYC, VEGF-A and WNT1. Additionally, knockout of LIN28 and ARID3B lead to reduced proliferation of ACH-3P cells. From these findings, we interpret that *let-7* miRNAs play crucial role in trophoblast cell proliferation either by direct targeting the

proliferation factors or by regulation of proliferation-associated genes through the ARID3B-complex.

Our *n vitro* findings led us to further investigate the role of LIN28-*let-7* axis *in vivo.* Day 9 hatched sheep blastocyst is structurally similar to day 5-6 hatched human blastocyst. A hatched blastocyst has single layer of trophectoderm, a blastocoel and an inner cell mass. If incubated with lentiviral particles for gene knockout or RNAi, only the trophectoderm is infected with the virus while other cells including inner cell mass are spared of lentiviral infection. In both human and sheep, rapid proliferation of trophoblast cells is required for successful placental development and establishment of pregnancy. Sheep blastocyst elongates from day 10-16 due to rapid proliferation of trophoblast cells. By day 16, the conceptus is elongated but still not attached to the endometrium which can be easily collected by uterine flush. The above-mentioned factors make sheep a prefect model to investigate genetic pathways involved in proliferation of trophoblast cells.

We infected day 9 sheep blastocysts with shRNA expressing lentiviral particles to knockdown LIN28A or LIN28B or scramble control and transferred them to synchronized ewes at day 9 of cycle. When collected at day 16, the conceptuses with LIN28A or LIN28B knockdown specifically in trophectoderm were smaller compared to SC. This indicated that LIN28 knockdown in trophoblast cells *in vivo* led to reduced cell proliferation. TE with LIN28 knockdown had increased *let-7* miRNAs and reduced expression of proliferation factors including *IGF2BP1, IGF2BP2, IGF2BP3*, *HMGA1*, *ARID3B* and *c-MYC*. From these results we interpret that reduced elongation of LIN28 knockdown conceptuses is due to reduced expression of proliferation factors in trophoblast cells. The ovine trophoblast cells (OTR) generated from day 16 TE represent a completely different phenotype of cells compared to day 16 TE. We saw depletion of LIN28 and increase in *let-7* miRNAs in OTR cells compared to day 16 TE and these cells senesced after only

few passages. OTR cells also had significantly reduced expression of *IGF2BP1, IGF2BP2, IGF2BP3*, *HMGA1*, *ARID3B* and *c-MYC*.

Due to senesce of OTR cells, we immortalized them and overexpressed LIN28 to generate a cell line that resembles more to day 16 TE. Overexpression of LIN28 led to reduced level *let-7* miRNAs and increased the expression of *IGF2BP1, IGF2BP2, IGF2BP3*, *HMGA1*, *ARID3B* and *c-MYC*. Both iOTR cells and Sw.71 cell have depleted LIN28A and LIN28B and high *let-7* miRNAs. These cells are not a good representative of human or sheep trophoblast cells *in vivo* because they have higher LIN28 expression. However, LIN28 overexpressing iOTR and Sw.71 cells generated in this study are a better *in vitro* model to study gene regulation in placenta.

Next, we investigated if epigenetic pathways play role in gene regulation in placental development. KDM1A is a lysine demethylase which catalyzes the demethylation at H3K9me1/2 causes transcriptional activation. KDM1A can bind to promoter regions of more than 7000 genes, and interestingly LIN28 is one of them. Knockout of KDM1A in ACH-3P cells leads to reduced expression of LIN28 and increased *let-7* miRNAs. Additionally, KDM1A knockout ACH-3P cells had reduced expression of AR, VEGF-A, HMGA1 and cMYC and the cell proliferation was also significantly reduced. Interestingly, AR, VEGF-A, HMGA1 and cMYC are also known targets of *let-7* miRNAs. Either KDM1A knockout is the direct cause of downregulation of these genes, or it operate indirectly through LIN28-*let-7* axis is still unknown. TE specific knockout of KDM1A led to reduced elongation of sheep conceptus at day 16, indicating importance of KDM1A for conceptus elongation and trophoblast proliferation *in vivo.*

In sum, these results show that LIN28-*let-7*-ARID3B pathway is involved in trophoblast cell proliferation both *in vitro* and *in vivo.* The main highlight of this study is the macro role of *let-7* miRNAs in gene regulation in trophoblast cells. Several studies have shown that miRNAs can

be used as biomarkers to indicate or predict a pathological condition in the body. MiRNAs can be easily measured in peripheral blood, cerebrospinal fluid, tissue biopsies, saliva, urine and other biological samples. In this study, *let-7* miRNAs were high in term human placentas from IUGR pregnancies. It would be interesting to find out if the difference in *let-7* miRNAs can be detected in blood samples or placental biopsy at early stages of pregnancy and if it can be used as an indicator of placental pathology. Use of small RNAs in therapy has been a very exciting development in clinical research and first approval to use siRNA as drug was approved by FDA in 2018. Until today, miRNAs are not approved by FDA to be used in medical intervention. However, there are many companies focused exclusively on use of miRNAs in diagnosis and therapeutics.